芝浦工業大學
SHIBAURA INSTITUTE OF TECHNOLOGY

# ISLANDING DETECTION AND POWER QUALITY ANALYSIS IN MICROGRID

a Dissertation Submitted to the
GRADUATE SCHOOL OF ENGINEERING AND SCIENCE OF
SHIBAURA INSTITUTE OF TECHNOLOGY

by

**TRAN THANH SON**

IN PARTIAL FULFILLMENT OF THE REQUIREMENTS
FOR THE DEGREE OF

**DOCTOR OF PHILOSOPHY**

SEPTEMBER 2019

# Acknowledgments

First of all, I would like to express my endless thanks to my supervisor, Professor Goro FUJITA for his kindness, encouragements, enthusiastic guidance, helpful advice and technical supports throughout my research. Without his motivation and instructions, the thesis would have been impossible to be done effectively.

I would also like to thank Hybrid Twinning Program of Shibaura Institute of Technology and Japanese Government scholarship (MEXT) for providing the fund for me to study Ph.D. in Japan.

From the deepest of my heart, I would like to thank my family members. Without their support and encouragement, I would never have the strength to finish my Ph.D. course.

Finally, I would like to thank my professors, my collages, my laboratory members and all my friends to be a part of my life in Japan.

Tokyo, September 2019

TRAN THANH SON

# Abstract

The microgrid (MG) has been developed based on the important concept of distributed generation (DG) with high penetration of renewable energy integrated with energy storage systems (ESSs). MGs can operate in both grid-connected and islanding mode. Therefore, this thesis focuses on autonomous multi-islanded entities and the seamless reconnection to the main grid as the self-healing ability of the future power system. The minimization of power quality issues (mainly that of voltage, frequency, and harmonics) in such entities based on controllers, with or without intercommunication, is also an important part of this thesis. The future power system, with the significant penetration of distributed generations (DGs), can rapidly respond to any problem occurring within it by separating into autonomous islanded entities to prevent the disconnection of DGs. As a result, high-quality and continuous power is supplied to consumers. The future research that is necessary for the realization of the future power system is discussed.

Besides, the emergence of Distributed Generation (DG) in the electric system has brought about the appearance of the islanding phenomenon. In AC networks, there are a lot of Islanding Detection Methods (IDMs) have been studied. However, not too much IDMs in DC networks have been published because of the absence of frequency and reactive power. The active IDM based on injected perturbation signal and rate of change of power output is proposed. This IDM can detect islanding condition not only in the worst case (the power of the load and PV are equal) but also in another case (the power of load is greater than the power of PV). It can be applied to both single

and multi-PV operation scenarios. Also, the cancellation problem is analyzed and the solution is proposed to solve this problem. Besides, the effectiveness of the proposed method, the cancellation problem, and the solution are verified by simulation in Matlab/Simulink.

# Contents

# List of Figures

# List of Tables

# List of Abbreviations

## Acronyms

| Symbol | Description |
|---|---|
| AC | Alternative Current |
| APF | Active Power Filters |
| BESSs | Battery Energy Storage Systems |
| CAES | Compressed Air Energy Storage |
| CC-VSIs | Current Controlled-Voltage Source Inverters |
| CHP | Combined Heat and Power |
| CVFs | Constraint Violation Functions |
| DC | Direct Current |
| DERs | Distributed Energy Resources |
| DFIGs | Doubly Fed Induction Generators |
| DG | Distributed Generation |
| DVRs | Dynamic Voltage Restorers |
| DVS | Droop-controlled Voltage Source |
| ECES | Electrochemical Capacitor Energy Storage |

| | |
|---|---|
| EI | Energy Internet |
| EMS | Energy Management System |
| EPS | Electric Power System |
| ESAs | Energy Storage Agents |
| ESSs | Energy Storage Systems |
| ETFs | Event-Triggered Functions |
| FES | Flywheel Energy Storage |
| IBS | Intelligent Bypass Switch |
| ICT | Information and Communication Technology |
| IDM | Islanding Detection Method |
| IED | Intelligent Electronic Device |
| IGs | Initial Groups |
| IHD | Individual Harmonic Distortion |
| IoT | Internet of Think |
| IP | Internet Protocol |
| LA | Load Agent |
| MAS | Multi-Agent System |
| MFI | Multi-Functional Inverter |
| MG | Microgrid |
| MGA | Microgrid Agent |
| MPP | Maximum Power Point |
| MPPT | Maximum Power Point Tracking |

| | |
|---|---|
| NDZ | Non-Detection Zone |
| OV/UV | Over Voltage/Under Voltage |
| PCC | Point of Common Coupling |
| PEI | Power Electronic Interface |
| PLL | Phase Lock Loop |
| PMU | Phasor Measurement Unit |
| PQDC | P/Q Droop Control |
| PREA | Primary Renewable Energy Agents |
| PV | Photovoltaic |
| RE | Renewable Energy |
| REAs | Reweable Energy Agents |
| ROCOF | Rate Of Change Of Frequency |
| ROCOP | Rate Of Change Of output Power |
| SCADA | Supervisory Control And Data Acquisition |
| SG | Smart Grid |
| SMES | Superconducting Magnetic Energy Storage |
| SOC | State Of Charge |
| SREA | Secondary Renewable Energy Agents |
| SSTS | Solid-State Transfer Switch |
| STATCOM | Static Synchronous Compensators |
| THD | Total Harmonic Distortion |
| UF | Unbalance Factor |

| | |
|---|---|
| UPQCs | Unified Power Quality Conditioners |
| VC-VSIs | Voltage Controlle-Voltage Source Inverter |
| VFDC | V/f Droop Control |
| VSC | Voltage Source Converter |
| VUF | Voltage Unbalanced Factor |
| WTs | Wind Turbines |

## Subscripts

| **Symbol** | **Description** |
|---|---|
| $\Delta P$ | Change of active power |
| $\Delta V$ | Voltage deviation |
| $C$ | DC/DC converter output capacitance |
| $D$ | Duty cycle |
| $dP$ | Rate of change of output power |
| $Eps$ | Abnormal event value |
| $I_{pv}$ | Photovoltaic current |
| $n_k$ | Perturbation factor at step $k$ |
| $R$ | DC load (resistance) |
| $t$ | Time |
| $V_{dcmin}$ | Under voltage threshold |
| $V_{dc}$ | DC bus voltage in normal condition |
| $V_{in}$ | DC/DC converter input voltage |
| $V_{mpm}$ | PV array voltage measurement at maximum power point |

| | |
|---|---|
| $V_{mpref_{module}}$ | Manufacture PV module voltage reference at maximum power point |
| $V_{mpref}$ | Manufacture PV array voltage reference at maximum power point |
| $V_{out}$ | DC/DC converter output voltage |
| $V_{pv}$ | Photovoltaic voltage |
| $V_{ref}$ | DC bus voltage reference (500V) |
| $i_C(t)$ | DC/DC converter output capacitance current |
| $i_R(t)$ | DC load current |
| $i_{conv}(t)$ | DC/DC converter output current |
| $i_{pv}(t)$ | Current of PV module |
| $N_k$ | DC/DC output current perturbation factor at step $k$ |
| $P_{pv}$ | Photovoltaic maximum power |
| $v_0$ | DC/DC converter output current |
| $v_{dc}(t)$ | DC bus voltage |

# Chapter 1

# Introduction

The content in this thesis relates to the analysis of power quality issues on islanding operation in micro-grid and islanding detection method which is proposed to detect islanding phenomenon. The background and motivation for the research are provided in the following sections

## 1.1 Outline of the thesis

The thesis includes the following chapters:

*Chapter 1 Introduction:* First of all, the background of the micro-grid and islanding phenomenon are presented. Thereafter, each problem is described to show the motivation of each research.

*Chapter 2 The analysis of the technical trend in islanding operation and power quality of islanded entities.* This chapter discusses the islanding phenomenon and subsequent actions to maintain the power supply with a high penetration of RE. The self-controlling for DG unit and central controlling using a hierarchical scheme are explained explicitly. The capability to operate in conventional grid-connected mode or islanded mode and the smoothy transient between two based on the advanced controller is pointed out. To make the smart and resilient operation of the coming power system, many research directions need to be investigated

such as robust hierarchical controller, advanced droop control, active/reactive power-sharing, harmonic mitigation inside the islanded entity, high-performance ESS and its proper controller, reliable communication system, etc.

*Chapter 3 Active islanding detection method in DC grid-connected photovoltaic system.* The main contribution of this chapter is proposed IDM can detect islanding phenomenon in DC network faster than the others IDMs and without IDM. Besides, it is capable of detecting not only in hardest but also another islanding condition.

*Chapter 4 Injected Signals Cancellation Analysis and Solution in Multi-PV System.* In this chapter, this issue was analyzed by injecting perturbation signal in the multi-photovoltaic system. Furthermore, the promising solution to eliminate injected signal cancellation was proposed in this chapter. The solution was validated through mathematical explanations and simulation results.

*Chapter 5 Conclusions and future works:* summarize and conclude on the obtained results and future works.

*List of publications:* lists all journals and conferences paper published during the Ph.D. course.

## 1.2 Microgrid

### 1.2.1 Definition

In recent years, energy issues such as serious environmental pollution, the lack of traditional energies have become significant increasingly. Therefore, using distributed energy resources (DERs) is a potential solution to solve those problems. With the penetration of DERs increasing the concept of microgrid (MG) has been proposed to coordinate between traditional grid and DERs and optimize the advantages of DERs in environment, energy, and economy. The position of MG in Power System are shown in Figure1.1.

There are some definitions of a microgrid in the world. Following the U.S.

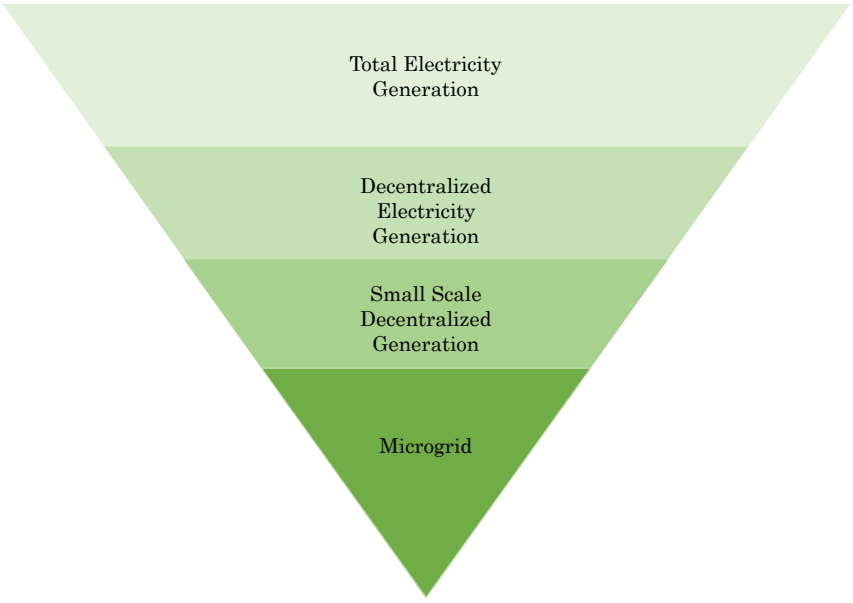


Figure 1.1: The position of MG in power system.

Department of Energy, MGs are a group of interconnected loads and distributed energy resources within clearly defined electrical boundaries that acts as a single controllable entity with respect to the grid and that connects and disconnects from such grid to enable it to operate in both grid-connected or island mode.

Accordingly the CIGRE C6.22, microgrids are electricity distribution systems containing loads and distributed energy resources, (such as distributed generators, storage devices, or controllable loads) that can be operated in a controlled, coordinated way either while connected to the main power network or while is landed.

From the CORDIS Europe point of view, a microgrid is defined as a series of electrical loads, elements of generated power supply and storage elements that, connected to the electric grid by means of a single point of connection, are all linked through a strategy that manages both the flow of energy within the grid as well as the interchange of power with the main supply grid.

Basically, an MG is a small-scale power grid that can operate either grid-connected mode or autonomous (islanded mode). In the grid-connected mode,

it has exchangeability energy between MG and utility. Besides, in the islanded mode, it has self-controlled and self-managed. MG includes distributed generations (DGs), storage, control devices and loads.

### 1.2.2 Characteristics of Microgrid

MG has some characteristics as below:

**(1) Independence**: MG can operate in islanded mode. In autonomous operation, MG is capable of balancing generation and load. Besides, It can keep system voltage and frequency in defined limits with adequate controls.

**(2) Flexibility**: The expansion and growth rate of MGs do not need to follow any precise forecasts. According to operation modes, MGs can operate in different modes. Connecting to the main grid is optional.

**(3) Stability**: MG can operate stably during nominal operating modes and transient events, no matter whether the larger grid is up or down (Additional research is required).

**(4) Interactivity**: MGs are compatible with the main grid. They can support the main grid if it is necessary and the main grid can also supply for MGs.

**(5) Expanse**: MGs can grow easily by adding more DERs and loads. It is easier than expand the traditional grid.

**(6) Efficiency**: The utilization of DERs optimization and manage loads by using centralized as well as distributed MG controller is the way to make energy management goals optimization.

**(8) Economic**: The utilization of DERs is the key to reduce fuel cost and $CO_2$ emissions.

### 1.2.3 Types of Microgrid

There are several types of MGs for different applications. As markets, technology, and regulation changes, the types of MGs will continue to evolve.

**(1) Customer MGs or true MGs**: They are self-governed grids, consisting of a certain number of buildings in a limited geographical location, and always downstream of a point of common coupling (PCC). The power quality requirements differ, depending on the type of customer.

**(2) Utility or community MGs or milligrids**: This grid mainly contains private end-user in principally residential locations, and sometimes industrial and commercial users as well. Such MGs can supply power to urban or rural communities that are connected to the main grid.

**(3) Virtual MGs**: Virtual MGs include DERs at multiple positions and they are coordinated such that they can be represented as a single controlled entity. There are few virtual grids have been proposed in the literature. The virtual grids system must be able to operate as a controlled island or coordinated multiple islands.

**(4) Island and Remote MGs**: Island and Remote MGs operate as an autonomous grid, and they usually look like microgrids. The main difference is that in most cases there will be no connection to the main grid. These grids are built to remain autonomous to maintain energy independence.

### 1.2.4 Advantages and Disadvantages of MGs

MGs benefit its customers and society in many ways.

**(1) Advantages of Microgrids**:

- Energy efficiency.
- Minimization of overall energy consumption.
- More environmentally friendly.
- More flexible.
- Less vulnerable.
- More modular.

- Improvement of energy system reliability.
- Immune to issues occurring elsewhere.
- Cost-efficient electricity infrastructure replacement.
- MGs can be integrated into existing systems without having to interrupt the load.
- MGs allow for combined heat and power (CHP) generation.

However, there are some disadvantages of MGs.

**(2) Disadvantages of Microgrids**:

- Voltage, frequency, and power quality should be at acceptable limits.
- Requires battery tanks to store which requires space and maintenance.
- Resynchronization to the utility grid is difficult.
- Protection is difficult.

### 1.2.5 Microgrid structure

There are three types of microgrid structure as below

#### 1.2.5.1 AC Microgrid

The structure of AC microgrid shows in Fig. 1.2. In an AC microgrid, DERs are connected to an AC bus through power electronic devices and supply power for the loads.

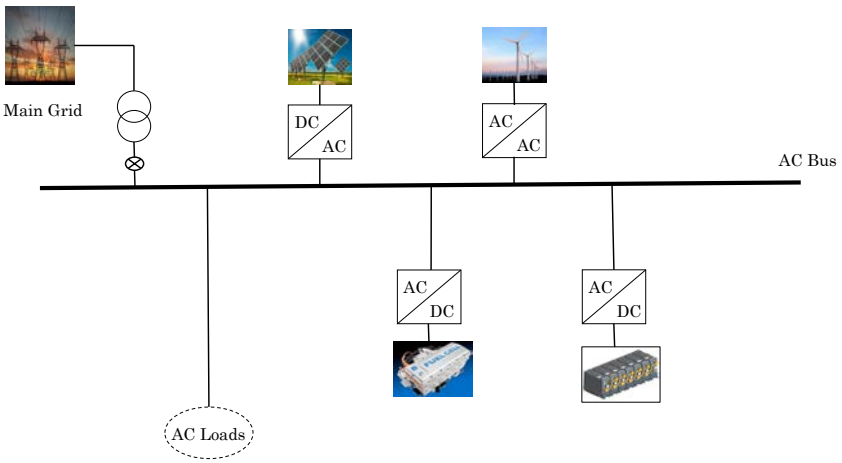


Figure 1.2: Typical structure of an AC microgrid.

#### 1.2.5.2 DC Microgrid

In DC microgrid, DERs and loads are connected to DC bus through power electronic devices. Besides, DC microgrid is connected to the main grid through an inverter, as shown in Fig. 1.3. DC microgrid includes DC power sources and loads is more economical.

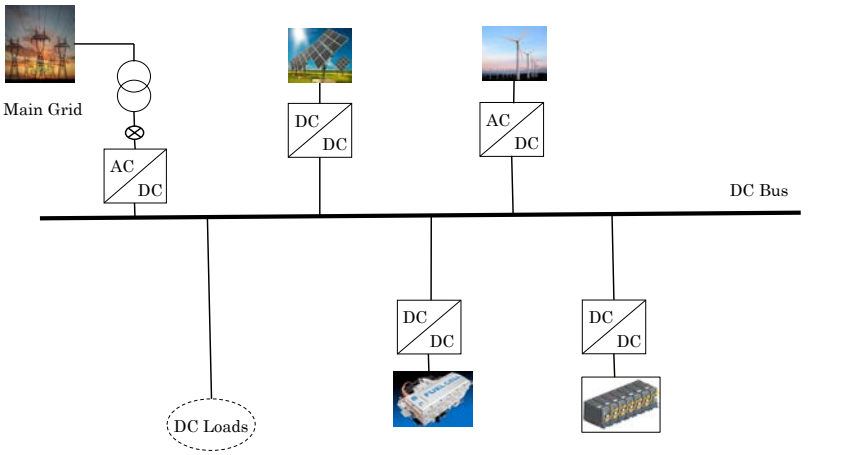


Figure 1.3: Typical structure of a DC microgrid.

#### 1.2.5.3 Hybrid AC/DC Microgrid

The hybrid AC/DC microgrid shown in Fig. 1.4 is included of an AC and DC bus to supply both AC and DC loads. A hybrid AC/DC microgrid combines the characteristics of both AC and DC microgrids.

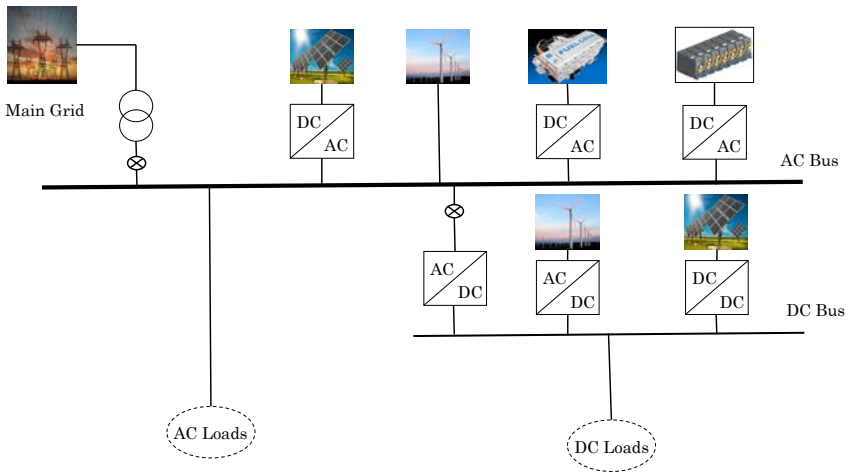


Figure 1.4: Typical of a Hybrid microgrid.

## 1.3 Islanding Phenomenon

Due to the significant penetration of DG in the power system, one severe phenomenon frequently occurs in the microgrid is islanding phenomenon.

### 1.3.1 Definition

According to the IEEE 1547 Std (IEEE Standard for Interconnecting Distributed Resources with Electric Power Systems), "Islanding is a condition in which a portion of an Area EPS (Electrical Power System) is energized solely by one or more Local EPSs through the associated PCCs (Point of Common Couplings) while that portion of the Area EPS is electrically separated from the rest of the Area EPS."

### 1.3.2 Islanding Classification

There are two types of islanding

(.) **Intentional islanding**: is the purposeful sectionalization of the main grid to create the power islands or the planned islands. The DERs of islands can supply the load power demand of the islands until the islands reconnect the main system.

(.) **Unintentional islanding**: occurs without customers intervention or planning.

### 1.3.3 Islanding detection

Unintentional islanding causes many problems because it is unplanned island such as safety concern, damage to customer's appliances, inverter damage, delay of restoration. For those reasons, the islanding problem must be detected by using the islanding detection methods. Consequently, the islanding phenomenon must be detected and cease to supply the area electrical power system within two seconds of the formation of an island based on IEEE standard 929-2000. According to the islanding detection methods, there are 3 types of IDMs depend on the parameters which use to detect islanding problem.

(.) **Passive method**: Depend on the changes in voltage, frequency, harmonics. This method does not give rise to power quality problems. But it has long-time detection and large non-detection zone.

(.) **Active method**: Depend on inject disturbance in the frequency, voltage or current signals, and then detecting whether or not the signals changes. This method affects the system but it has some advantages such as short detection time and small non-detection zone.

(.) **Remote method**: Depend on the communication signals between DERs and substations. It has short time detection, no non-detection zone, and no affect the system. But it is expensive and complicates.

To summarize, the microgrid (MG) has been developed based on the important concept of distributed generation (DG) with high penetration of renewable energy integrated with energy storage systems (ESSs). In MGs, consumers forming parts of the grid invested in DG can generate, store, control, and manage a portion of the energy that they consume, resulting in a cheaper and more efficient energy supply solution [1]. To improve power system security, the distribution network can separate from the main power system and operate autonomously as an island during any unusual phenomena and then reconnect to the main grid if needed. Although the incorporation of technological advancements in digital control into modern communications has facilitated the islanding scheme, it presents challenges related to power quality, protection, out-of-synchronism reclosure, and earthing [2]. The IEEE standard 1547.4 enumerates the benefits of the islanded operation of MGs: (i) improving reliability for customers, (ii) relieving electric power system overload problems, (iii) resolving power quality issues, and (iv) allowing for the maintenance of power system components without interrupting service to customers [3]. Therefore, autonomous operation after islanding will be very important in future grids with high DG penetration. Thus, advanced DGs with "plug and play" characteristics should be integrated with distribution systems. These DGs can operate seamlessly in grid-connected mode, islanding mode during the transient-to-islanded mode, and islanded operation, which reduces the chance of a load being unnecessarily excluded from the island and permits maximum flexibility of the multi-islanded system. The future power system can robustly respond to any fault occurring within by dividing itself into several islanded entities without stopping the DG operation. Chapter 2 will discuss such separated multi-islanded entities and their seamless reconnection as a self-healing ability of the future power system. Controllers with/without intercommunication mitigate power quality problems in these entities, and, eventually, the consumers will receive continuous power of high quality.

## 1.4 Motivation of research on DC microgrid

Nowadays, energy faces some serious problems, such as it is one of the reasons causing environmental pollution and the lack of energy when the traditional energies are going exhausted. Therefore, distributed energy resources (the wind, solar, ocean wave, fuel-cell, etc.) and some of them are natively DC which become considerably penetration in the power system as a potential solution. Distributed Generations (DGs) have much lower energy density than fossil fuels, and so the generators are smaller and geographically widely spread. All types of power sources connected to the distribution system at a voltage level from 120/230 V to 150 kV [56] are DGs, for example in Figure 1.5: PV, Wind turbine, fuel-cell, and battery are the DGs. All DGs connect with DC bus and supply to DC loads such as data center, electric vehicles, and other DC loads. Besides, the development of fullness DC as storage technologies (batteries, ultra-capacitors, etc.) and DC loads (Data centers, electronic-based office, home appliances, plug-in electric vehicles, variable speed drives, and DC electric arc furnaces) are significantly increased [57]. In addition, DC networks in Figure 1.5 have some advantages compared with AC networks: (1) Simpler system (easier integration of DC DGs to the common bus, eliminating the need for synchronizing generators); (2) Higher system efficiency, lower losses and voltage drops in lines because of reduction of conversion loss by reducing inverters; (3) More efficient supply of DC loads (Data centers, electric vehicles,electronic-based office, etc.) [58, 59, 60, 61]. For those reasons, the DC grid has been increasing significantly in the power system.

### 1.4.1 Need to research on islanding phenomenon in DC microgrid

One severe phenomenon frequently occurs in the DG grid is islanding. In Figure 1.5, when AC grid disconnects, all load are fed by only DGs, so islanding problem occurs.

This issue causes some problems such as:

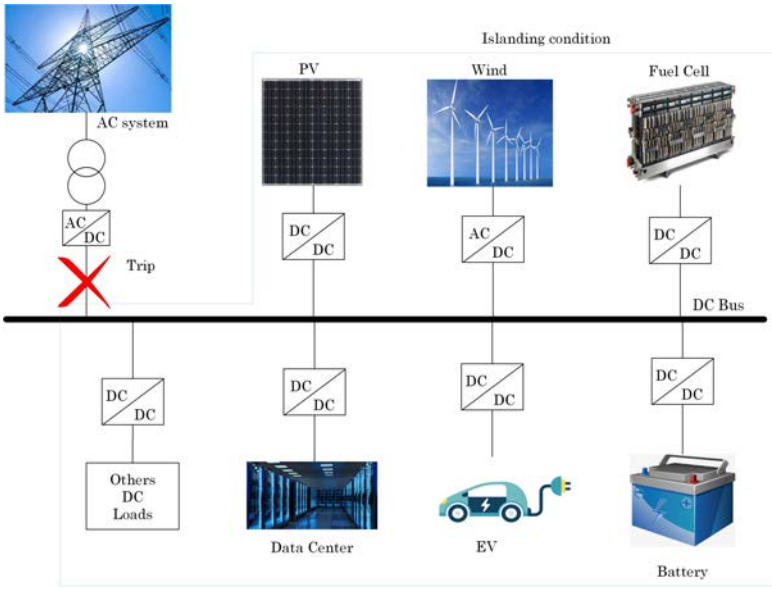


Figure 1.5: General DC system diagram.

(.) **Safety**: This may confuse the utility workers and expose them to hazards such as electric shocks.

(.) **Damage to load**: This may cause severe damage to electrical equipment, appliances, and devices. Some devices are more sensitive to voltage fluctuations than others.

(.) **Inverter confusion**: Reclosing onto an active island may confuse the operation of inverters.

(.) **Delay of restoration**: If the islanding phenomenon repeatedly occurs in the power system, the restoration of the power system from the failure will be delayed because of asynchronous closing.

Due to the absence of the frequency in the DC system, the islanding detection methods in the DC grid are more complicated than that in AC networks. Together with the development of DGs in the power system, DG interconnection protection is becoming more important. In Figure 1.5, islanding problem occurs when the AC system disconnects, DC grid will operate in islanded operation. Therefore, islanding phenomenon becomes one important issue should be solved not only in AC system but also in DC networks. According to the IEEE standard 929–2000,

this network must detect the condition issue and disconnect within 2 s at maximum [62]. This standard is necessary to prevent damage to electrical equipment and safety for maintenance staffs. Moreover, with the quick development of DC networks including renewable energy resources, information technology, power electronic technology, semiconductor technology and the requirement of higher power quality, reliability, and economy, the islanding detection schemes in DC grid increasingly become necessary.

## 1.5 Islanding Detection in AC and DC System

### 1.5.1 AC System

Islanding detection in the AC network has been studied in many published papers. They can be classified into three groups: Passive, Active and Remote Detection IDMs are shown in Table 1.1 [69, 70, 71, 72, 73].

Table 1.1: Islanding detection methods classification.

| **Islanding Detection Techniques** | | |
|---|---|---|
| **Passive** | **Active** | **Remote** |
| Under/Over Voltage | Impedance measurement | Power line carrier |
| Under/Over Frequency | Reactive power fluctuation | Disconnect signal |
| Voltage harmonics | QC-mode frequency shift | SCADA |
| Voltage phase shift | Reactive power compensation | PMU |
| Voltage unbalance | Load fluctuation | Comparison of ROCOF |
| Total harmonic distortion | Inter-harmonic injection | |
| ROCOP | Sandia frequency shift | |
| ROCOF | Sandia voltage shift | |
| | Frequency bias | |

A structure of the AC grid in normal and islanding condition is shown in Figure 1.6. In normal condition, the breaker closes, RLC load is supplied by both DG and AC grid. When the breaker opens, only DG supplies power with the

RLC load grid. Assuming the resonant frequency of the RLC load is the same as the grid frequency.

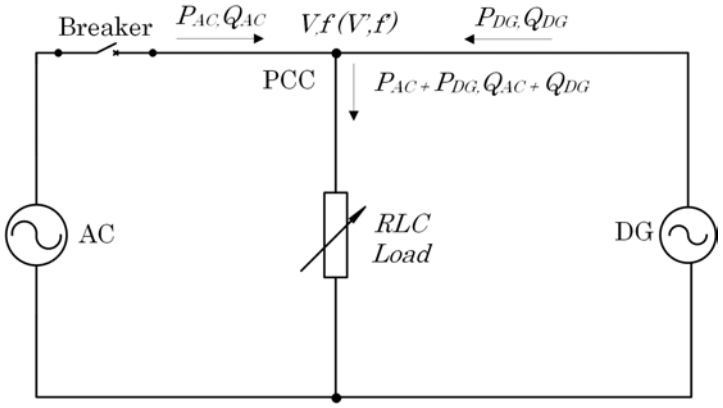


Figure 1.6: AC grid in normal and islanding condition.

Mathematically, the voltage and frequency at point of common coupling (PCC) can be represented as

$$V = \sqrt{P \cdot R} \tag{1.1}$$

$$f = \frac{1}{2\pi\sqrt{LC}} \tag{1.2}$$

where *V, f, P, R, C, L* are the PCC voltage, PCC frequency, active power, load resistance, load capacitance and load inductance.

In normal condition, load is supplied by both AC grid and DG.

$$P_{Load} = P_{AC} + P_{DG} \tag{1.3}$$

$$Q_{Load} = Q_{AC} + Q_{DG} \tag{1.4}$$

In islanding condition, AC grid is disconnected, only DG supplies the load.

$$P_{Load} = P_{DG} \tag{1.5}$$

$$Q_{Load} = Q_{DG} \tag{1.6}$$

where

- $P_{Load}$ is the active power of the load.
- $P_{AC}$ is the active power supplied by the AC grid.
- $P_{DG}$ is the active DG power.
- $Q_{Load}$ is the reactive power of the load.
- $Q_{AC}$ is the reactive power supplied by the AC grid.
- $Q_{DG}$ is the reactive DG power.

Based on Equations (2.1)–(1.6), when islanding occurs, due to the appearance of the frequency, many signals will be forced to the new values. They can be used to detect islanding condition, such as voltage magnitude, frequency, harmonic signal, reactive power, etc.

### 1.5.2 DC System

The DC grid model in normal and islanding condition are shown in Figure 1.7. When the breaker closes, the figure shows normal condition, DC load receives power from both the DC and AC system. When islanding occurs, the breaker opens, DC load is supplied by only the DC grid.

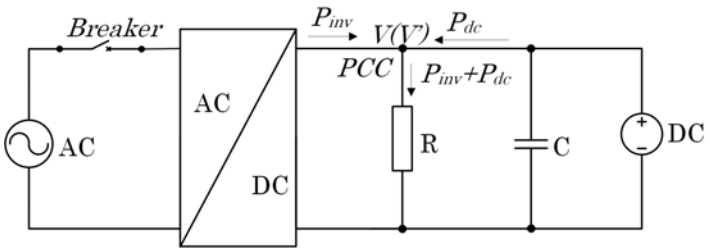


Figure 1.7: DC grid in normal and islanding condition.

In normal condition, the load is supplied by both AC and DC grid.

$$P_{Load} = P_{inv} + P_{dc} \tag{1.7}$$

$$V = \sqrt{(P_{inv} + P_{dc})\, R} \tag{1.8}$$

In islanding condition, AC grid is disconnected is:

$$P_{Load} = P_{dc} \tag{1.9}$$

$$V' = \sqrt{P_{dc} R} \tag{1.10}$$

where

- $P_{Load}$ is the active power of DC load.
- $P_{dc}$ is the active power of DC grid.
- $P_{inv}$ is the active power supplied by AC system.
- $V$ is the DC bus voltage in normal condition.
- $V'$ is the DC bus voltage in islanding condition.
- $R$ is the DC load resistance.

Due to Equations (1.7)–(1.10), in practical conditions, there is always unbalance power because of some power mismatch between the DG and load. Before the islanding, the power mismatch will be supplied by the main grid. After AC grid is disconnected, the power of DC load will be compensated by the DC grid. Different from the AC system, only the voltage signal can be used to detect islanding condition due to the absence of the frequency in the DC system when the grid is disconnected. Therefore, almost IDMs in the AC grid cannot be used to detect islanding condition in the DC system.

Consequently, chapter 3 proposes an active islanding detection method to detect islanding phenomenon in the DC grid-connected photovoltaic system.

Besides, the injected signal cancellation caused by the proposed IDM also analyses and a potential solution to solve this problem has been proposed in chapter 4.

## 1.6 Structure of the thesis

To this end, the remaining of the thesis is organized as follows:

The analysis of the technical trend in islanding operation and power quality of islanded entities is represented in chapter 2

Chapter 3 presents the active islanding detection method based on injecting perturbation signal and rate of change of output power in DC grid-connected photovoltaic system.

Chapter 4 The cancellation problem is analyzed and the solution is proposed to solve this problem.

The thesis ends with conclusions and future works in Chapter 5.

# Chapter 2

# The analysis of the technical trend in islanding operation and power quality of islanded entities.

## 2.1 Flexible Operation of the Future Power System

Renewable energy (RE) has received attention worldwide due to its fantastic advantages: it is a cheap/free fundamental fuel with no emissions. In particular, the 2011 Fukushima nuclear disaster necessitated the use of RE to compensate for the lack of power after shutting down Japan's nuclear reactors and the sudden increases in $CO_2$ emissions. With the high DG penetration of the distribution power system, cost and reliability constraints may motivate a multi-functional power electronic interface (PEI) for DG, where a single DG unit can perform many tasks, such as identifying and preventing potential trends, islanding detection, synchronizing to the main grid, and black start operation. Also, it is characterized by voltage ride-through capability, self-adaptive control, the power quality of islanded entities, the flexibility to integrate DG by management and control, etc. Therefore, a reliable islanding detection method and a powerful PEI of DG will contribute to boosting the "proactive DG grids" concept.

### 2.1.1 Multi-Agent System for the Energy Internet

As stated in [4], the concept of the "Energy Internet", as in Figure 2.1, has been recently proposed. The components of the Energy Internet consist primarily of RE, ESSs, and other parts of generations, which are not mentioned here. The Energy Internet has the ability to operate in either the grid-connected or islanded mode. High RE penetration will inevitably change the way power flows, transitioning from passive to active generation. In Figure 2.1, the Energy Internet is isolated and cut off from the power supply due to a fault that occurred on a feeder which resulted in the opening of solid-state transfer switch (SSTS). The isolated entity can be reconnected with the utility once any RE is closed during the isolated period running as in autonomous operation. The critical design and control objectives of the Energy Internet during this mode are: (i) maintaining flexible and proportional power-sharing among REs; (ii) maintaining the system's continuous synchronization with the utility in the presence of load variations; (iii) minimizing circulating currents between DGs; and (iv) achieving seamless energy transitions between the Energy Internet and the utility if necessary. The conventional power system uses the supervisory control and data acquisition (SCADA) system to exchange status and control signals of components. This centralized SCADA system was originally designed for traditional passive networks; it thus may be inadequate to cope with complex control decisions because it lacks flexibility and extensibility [5]. The designation of the controller structure used in an Energy Internet is based on the "multi-agent system" (MAS) structure, wherein a different agent controls each component. The MAS helps monitor and control the new complex power system. In the MAS, one centralized control is separated into simpler single entities that work in collaboration pursuing assigned tasks to achieve the overall goal of the system. It is a system based on the advantages of the agents' properties: flexibility, scalability, autonomy, sociality, reactivity, proactivity, and reduced complexity. Under the control of the MAS scheme, the power system performs demand-side management to secure critical loads, shedding low-priority loads in severe cases. Various RE units and other components of the grid communicate with the islanded entity through the IP-based local control model (IP = Internet Protocol). The entity disconnects itself from the utility

and operates autonomously to maintain the integrity of the system. Figure 2.1

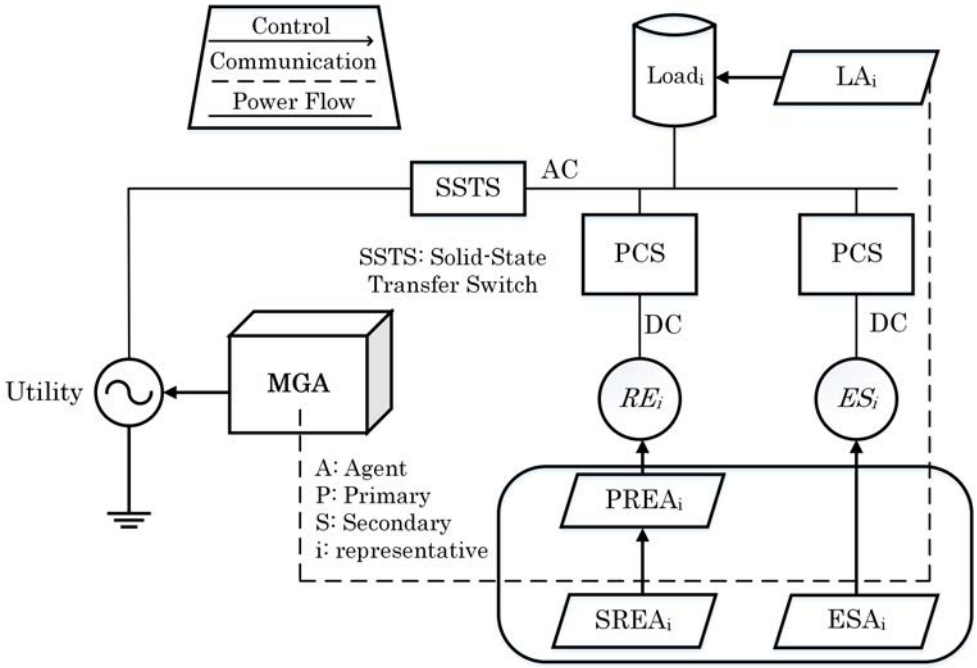


Figure 2.1: Architecture of the Energy Internet.

shows three different agents designed for the distributed coordinated controller, including the upper-level coordinated control strategies, MG agent (MGA), and the RE agents (REAs). An REA, comprising a primary REA (PREA), secondary REA (SREA), and energy storage agents (ESAs), implements local decentralized continuous control. The MGA executes its functions according to information provided by all agents, and tasks are implemented by sending logic control commands to the unit control agents through a master/slave communication mode. The MGA is also called the energy router and is used to regulate the power flow between the Energy Internet and the utility. The ESA and SREA together are called the energy switcher, which is used to regulate the power flow within the Energy Internet. Also, to improve the Energy Internet management, load agents (LAs) should also be considered. The Energy Internet operates under two modes: (i) the utility-connected mode, in which the stiff utility compensates for power unbalance within the Energy Internet; (ii) the isolated mode, in which one of the DGs or REs should be chosen as the control master. Advanced droop control is

distributed to implement proportional power-sharing among DGs in the Energy Internet as a primary control. Then, a secondary control via a centralized or distributed method is added to restore the voltage and frequency to nominal values. The centralized control, which requires proper communication systems to realize the control goals, sometimes presents a single point failure. In such a scenario, the MAS acts as a kind of distributed control structure to make control decisions for each DG according to it's neighbors information, demonstrating its flexibility for faster and computational efficiency.

Another approach is presented in Figure 2.2, which shows the architecture of a MAS. The MAS comprises four types of agent, namely, a control agent, a DER agent, an additional user agent, and a database agent. Each agent has a unique objective and responsibility, as defined explicitly as in [6]. The principle of agent structure is presented in Figure 2.3 [7]. According to information which is external to the agent, the agent management creates a database, processes these data, and then outputs a control signal to its components regarding the response from the other agents.

An event-triggered hybrid control for the Energy Internet was proposed in [8]. In this paper, by developing a MAS-based event-triggered hybrid control scheme, the Energy Internet could comprehensively use the RERs when encountering load demand with high security. The MAS could be used to implement hierarchical hybrid control in a coordinated way based on four types of control strategies, such as hierarchical load shedding and the hierarchical switching control of RERs, designed as event-triggered functions (ETFs), or local switching control and distributed dynamical control, designed as constraint violation functions (CVFs), which are completely dependent on the logical resource-grid-load-storage relationship.

### 2.1.2 Flexible Operation

With the general theme "Flexible islanded operation of proactive DG grids", the DG unit can operate seamlessly in the grid-connected mode (by current control), islanding mode during the transient-to-islanded mode (by energy storage), and

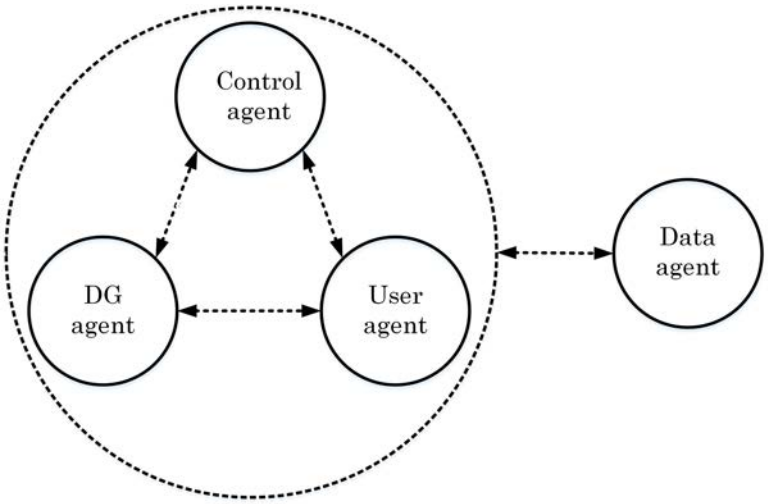


Figure 2.2: The microgrid (MG) multi-agent architecture.

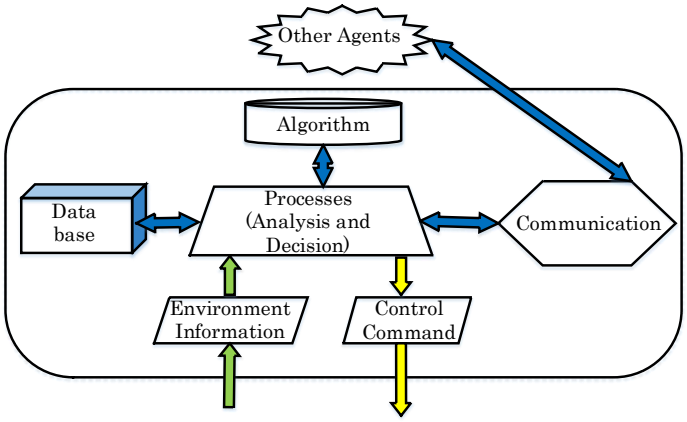


Figure 2.3: Agent structure.

islanded operation (by droop control) [9, 10, 11]. Autonomous operation subsequent to islanding will be very important in future DG grids [12, 13, 14, 15, 16, 17]. The desired PEI-DGs with "plug and play" characteristics should be integrated into distribution systems. As a result, the whole power system can robustly respond to any fault occurring within by dividing itself into several islanded entities without stopping the DG operation. With DGs, in order to fulfill these goals,

the PEI plays the main role in control. Power electronic equipment reacts very quickly, which can overcome severe transient events. Thus, besides interfacing with utility grids, PEIs have the potential to mitigate power quality problems (such mitigation includes active filtering, voltage unbalance compensation, grid support, and ride-through control under voltage dips, among other functions) and carry out other duties, such as identifying and preventing potential trends.

Recent approaches focus on separated multi-islanded entities and seamless reconnection to continuously supply power of high quality. It is not only self-control conducted without intercommunication [18, 19]; some PEI-DGs of the DG grid are to be managed using a central controller linked by communicated signals [2, 20, 21]. Then, the power system operating with DG should emerge as a convergence of electrical, information, and technological engineering. Three operation modes of the DG grid are discussed herein, as follows:

(.) **Grid-connected mode**: To a large extent, grid-connected mode system dynamics are fixed by the utility because of the small size of the DG units. MGs aim to satisfy demand by local DGs. Excess or deficient active and reactive power in an MG can be absorbed or supplied by the utility grid, respectively.

(.) **Autonomous/islanded operation mode**: The disconnected scenarios include intentional (e.g., maintenance or detection of a permanent fault) and unintentional disconnection (e.g., blackout due to disconnection from the utility). In this mode, the system dynamics are depicted by its own DG units. The power balance within the islanded entity between generation and demand must be observed to maintain system frequency and voltage within acceptable limits and ensure stability. Reactive power compensation and harmonic current are shared within an islanded entity by applying droop control to DGs. The virtual impedance method as an advanced technique is further used to reduce active power control errors, enhance fast dynamic control during the transient, and minimize the circulating power among controllers, as seen in Figure 2.4.

(.) **Transient mode: into-islanded and back into-utility**: Power balance should be provided by power storage systems, such as batteries, supercapacitors, or flywheels. An intelligent bypass switch (IBS) [12] continuously supervises

both grid-connected and islanded modes. When the IBS detects that maintenance is needed or a fault is present at the utility side, the islanded entity must be disconnected, and then a restoration process is activated to ensure high reliability. The IBS can detect the main grid's fault-free stability and synchronize voltage amplitude, phase, and frequency, which are utilized for the reconnecting procedure. In the event that islanded mode is forced to run for a long time, synchronization of voltage, frequency, and phase between islanded entities and the utility is implemented to seamlessly reconnect after an approximate zero-point reclosing of smooth and soft synchronization.

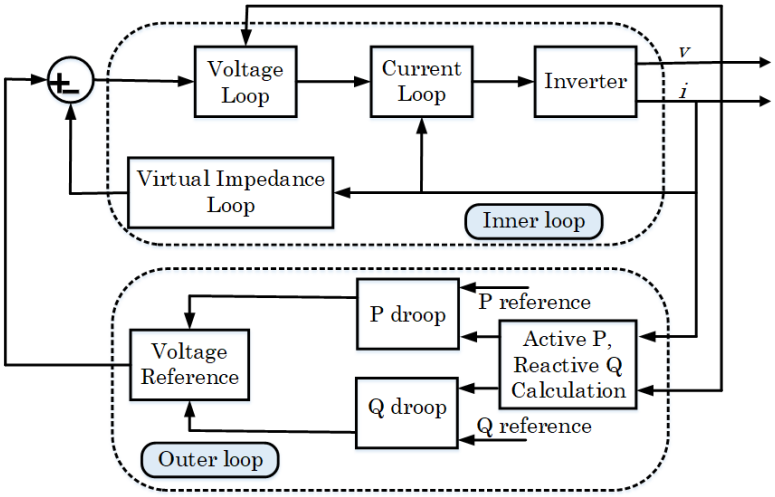


Figure 2.4: Multi-loop control droop strategy with the virtual output impedance approach.

### 2.1.3 Hierarchical Control

Hierarchical control of islanded entities basically includes three main levels [12, 22]. Primary control is the droop control used to share loads between PEI-DGs in order to adjust the islanded frequency or amplitude output voltage, as seen in Figure 2.5 hereafter. Local controllers in DG are operated primarily for speed and reliability. Secondary control is responsible for removing any steady-state errors imposed by the primary control to guarantee the stabilization of voltage and frequency for loads. It links all of the DG's controllers to let the system

respond consistently in wider areas. Power flow modeling of droop-controlled distributed generation units with secondary frequency and voltage restoration control for hierarchically controlled islanded microgrids was introduced in [23]. Tertiary control, which involves more global responsibilities, determines the import or export of energy among islanded entities to compensate for voltage harmonics in the point of common coupling (PCC) and generates synchronization loops to transfer from islanded mode back to grid-connected mode. A simple illustration of the three-level hierarchical control is in Figure 2.5. All DGs in the hierarchy respond to disturbances as one set or, in the most appropriate manner, all DGs respond to a disturbance, and there will be a speedier return to a stable synchronous islanded operation. However, the whole control system must be resilient to a telecommunication delay and be robust to temporary communication outages. The communication bandwidth chosen for the entity is a compromise between the amount of data that is transferred along with the network infrastructure and the transient response that is required from the secondary control loops. A high data bandwidth implies a fast transient response for the secondary control loops while providing a high data transfer rate along with the network. Since the restoration of the voltage and frequency of the MG are noncritical, bandwidth communications of as low as 1 Hz can be used to achieve the required functionality.

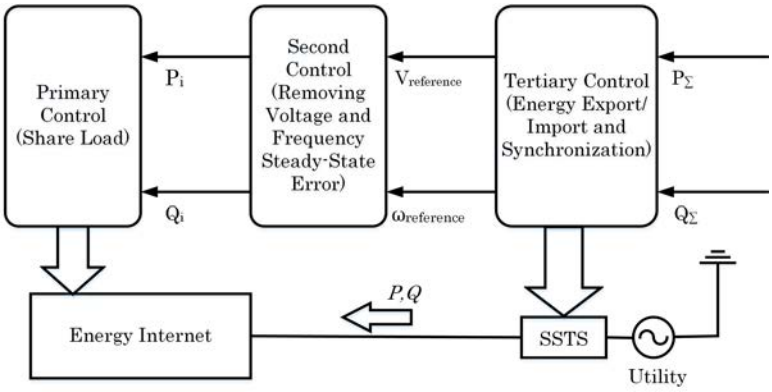


Figure 2.5: Three-level hierarchical control strategy for the Energy Internet.

### 2.1.4 Load Sharing without Communication—Droop Control

As one level of the hierarchical mechanism, droop control concepts have been widely adopted to provide decentralized power-sharing control between DGs without relying on communications. Assuming the line is mainly inductive, the *P-f* and *Q-V* droop strategies provide stable active and reactive power-sharing. However, in a low-voltage distribution system, where the X/R ratio is small, especially for transformer-less inverters that have very small output inductance, droop control is subject to real and reactive power coupling and steady-state reactive power sharing errors. Additional compensation schemes for the traditional droop control, such as opposite droop, virtual inductance, average power control, or virtual impedance compensation, have been proposed for accurate power control [20]. Moreover, in addition to droop control, communication can be used as a non-critical element in a higher control layer, such as the secondary control of the hierarchical structure, to enhance the performance of the islanded entities without reducing system reliability. Therefore, each DG unit should have the ability to exchange information with the central energy management system (EMS) to receive the reference values through a communication link.

Although the *P-f* droop technique can achieve accurate real power-sharing, voltage droop control *Q-V* commonly results in poor reactive power-sharing. This is due to the mismatch in the voltage drops across the DG unit feeders, which is induced by the mismatch in the feeder impedances (virtual output impedances of the closed-loop voltage controller of the DG units or feeder physical impedances, including the transformers, cables, and interface reactors, or even the variation of droop slope $k_Q$) and even the differences in the power ratings of the units. The time delays in communications may also significantly reduce the reactive power-sharing accuracy, which can also be affected by lost communication [24]. A complex configuration of an entity (looped or mesh networks) will also make reactive power-sharing more challenging and often degrade not only the voltage but also frequency quality due to a harmonic injection. In one study aiming to solve the reactive power-sharing problem [19], small real-reactive power coupling

disturbances (the real and reactive power are coupled together for frequency and voltage droop control) were injected to obtain accurate reactive power sharing before automatically switching back to conventional droop control. This method is effective for all types of configurations, and detailed structural information of these entities is not needed to achieve the "plug and play" operation of DGs and loads.

Two new problems need to be solved immediately in a cascade-type microgrid: the synchronization and power balance of distributed generators. A *f-P/Q* droop control strategy is proposed in [25] solve this problem. This proposed droop control can achieve power balance under both resistive-inductive and resistive-capacitive loads autonomously. It has a clear advantage in extending the scope of application compared with the inverse power factor droop control.

#### 2.1.4.1 Conventional Droop Control

In the grid-connected mode, the supply-demand balance of an MG is less restrictive since the grid behaves like a large energy reservoir for buffering any mismatches between the power supply and load demand. The buffering effect is, however, not available in the islanded operation mode, which requires a stricter supply-demand balance. Also, a load-sharing function among the DGs is needed to avoid stressing a particular DG. As a result, the control of DGs needs a decentralized technique (i.e., droop control), which is tuned according to the individual DG rating. The operation of DGs relies only on locally measured quantities and, hence, does not require communication links [26].

Figure 2.6 shows the typical configuration of an MG which consists of a number of REs or DGs and loads. Each DG is interfaced to an MG with a power conditioner system (PCS) consisting of an inverter, which then connects to a common AC bus by its own feeder. A central controller monitors the status of all components inside this MG to decide whether to operate in grid-connected mode or islanding mode by controlling the SSTS at PCC. While in the grid-connected mode, real and reactive power references are normally assigned by the central controller, and conventional droop control can be used for power tracking.

The deficient or excess power can be easily compensated for by the utility. Then, typically, DG will generate its maximum power, and power-sharing is not a concern in this mode. In the islanding mode, the total load demand must be properly shared by the DG units within the islanded entity by applying two well-known mechanism-based equations, as seen in Figure 2.7:

$$\omega = \omega_0 - k_P P \tag{2.1}$$

$$E = E_0 - k_Q Q \tag{2.2}$$

where $\omega_0$ and $E_0$ are the nominal values of DG angular frequency and DG voltage magnitude; $P$ and $Q$ are the measured real and reactive powers; $k_P$ and $k_Q$ are the real and reactive power droop slopes.

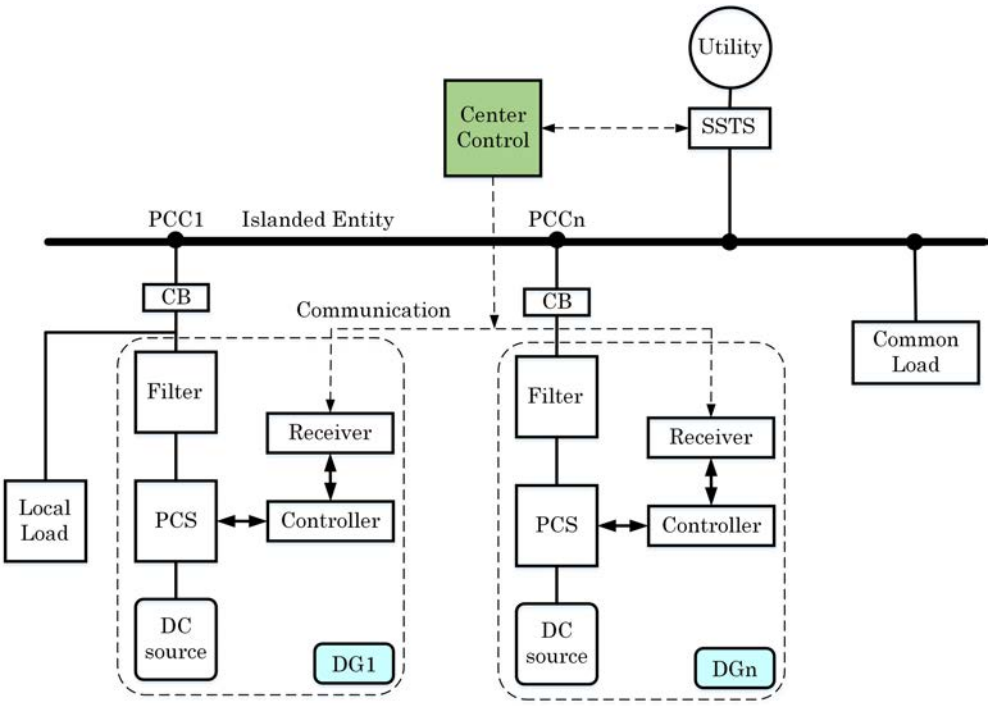


Figure 2.6: Phase angle difference estimation.

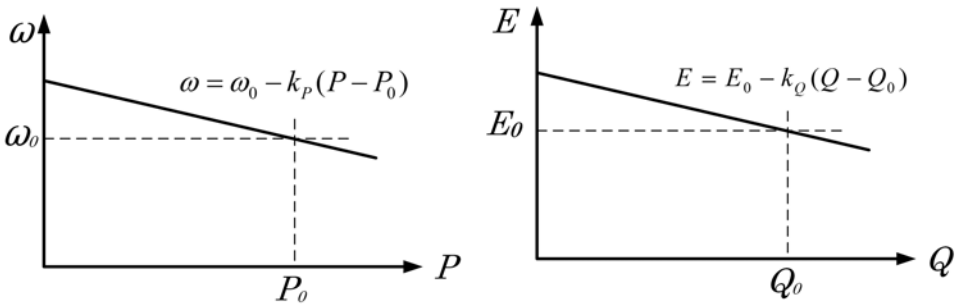


Figure 2.7: Conventional droop control.

#### 2.1.4.2 Advanced Droop Control

Since conventional droop control faces several drawbacks in term of sharing accuracy, improved droop techniques have been proposed by many papers, year after year. In [18], a three-layer control scheme was proposed for inverters operating in parallel without intercommunication. In [7], the droop control method is proposed as a good solution to the outer loop power controller in an MG. However, the method itself is not suitable for the upcoming flexible MG. The inner loop controller (PI controller, robust controller, prescribed performance) ensures that frequency and voltage deviations are regulated robustly toward zero after every change in load or generation inside the MG. When nonlinear loads exist, besides balancing active and reactive power, controlling that load sharing is a challenge. Thus, harmonic-current-sharing techniques have been proposed recently to avoid the circulating distortion power that occurs when sharing nonlinear loads. Novel control loops that adjust the output impedance of the units by adding output virtual reactors or resistors have been included in the droop method with the purpose of sharing the harmonic-current content properly [1]. Further, by using the droop method, power-sharing is affected by the output impedance of the units and the line impedances. Hence, these virtual output-impedance loops can also solve this problem. In this sense, the output impedance can be seen as another control variable [1]. In case of paralleling DC power converters, the droop method consists of subtracting a proportional part of the output current from the output voltage reference of each module. Thus, a virtual output resistance can

be implemented through this control loop. This loop, also called the adaptive voltage position, has been applied to improve the transient response of the voltage regulation modules in low-voltage high-current applications. In addition, the droop method has an inherent trade-off between voltage regulation and current sharing between the converters. To cope with this problem, an external control loop, named secondary control, has been proposed to restore the nominal values of the voltage inside the MG. Further, additional tertiary control can be used to bidirectionally control the power flow when the MG is connected to a stiff utility (in the case of AC MGs) [1].

### 2.1.5 Intelligent Controlled Islanding Scheme

During stressed conditions of power systems, such as peak load periods, a fault can cause cascading problems that lead to grid collapse. To prevent a blackout, a power system can be intentionally split into separated self-healing islanded entities that await a reconnection condition. However, to establish an effective islanding scheme, many obstacles need to be overcome. Islanding locations, time of disconnection, and the moment to reclose based on the network's operating topology or local relays are determined coordinately. The aim is to stabilize each islanding at the highest power balance, considering generator coherency. This configuration, where the number of islanding entities is known ahead of time, could facilitate autonomous operation within each entity. In a study by [27], one islanding execution algorithm and topology was performed. The procedure for determining the time of islanding is performed at three different points: offline, online, and in real-time. The number of stable islands with appropriate security levels is pre-determined by monitoring the dominant inter-area oscillations between the initial groups (IGs), as depicted in Figure 2.8. For the MAS, to exchange information and to coordinate control, the entities are connected tightly in a cyber-communication network [28]. In the autonomous operation mode, each entity operates independently by controlling DGs, ESSs, and loads for economic and self-adequate objectives. Ideally, no information exchange or power flow exchange is needed among MGs. When a fault occurs in an entity, it receives power support from another entity in the self-healing mode. There are

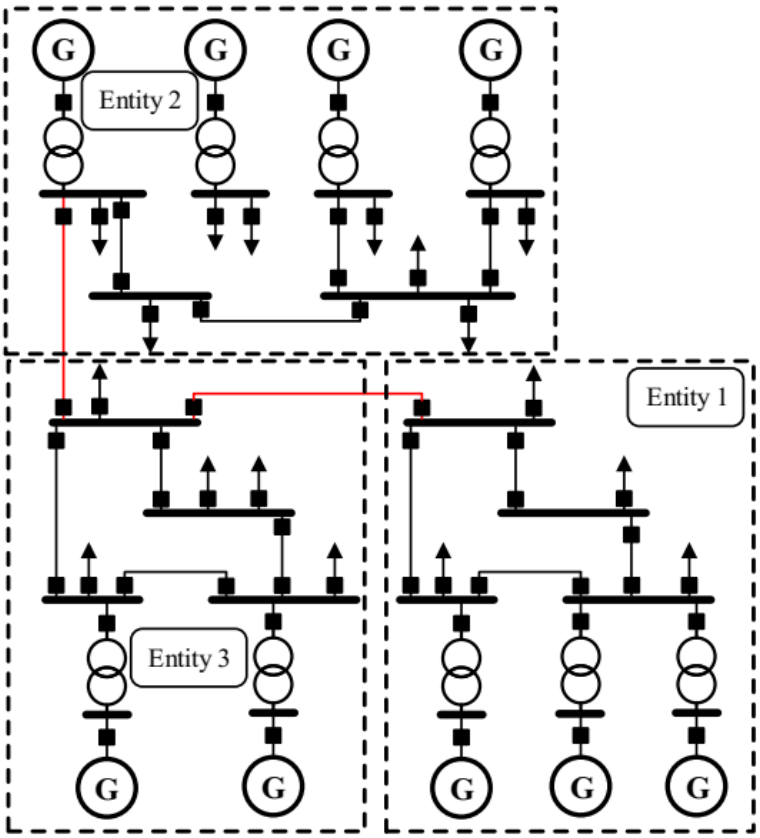


Figure 2.8: Determined initial groups (IGs) and islands boundaries in advance.

two layers in the cyber-communication and control network. The lower layer is in the entities to control DGs, ESSs, and loads locally, while the upper layer communicates with neighboring counterparts by broadcasting its power support request or response to other requests to obtain actual aggregated support until the fault is cleared to achieve overall reliability. Figure 2.9 shows autonomous networked MGs. The network consists of both strong cyber-links for communication and physical connections via a common point for power exchange. The connection could be a DC line to separate each MG completely.

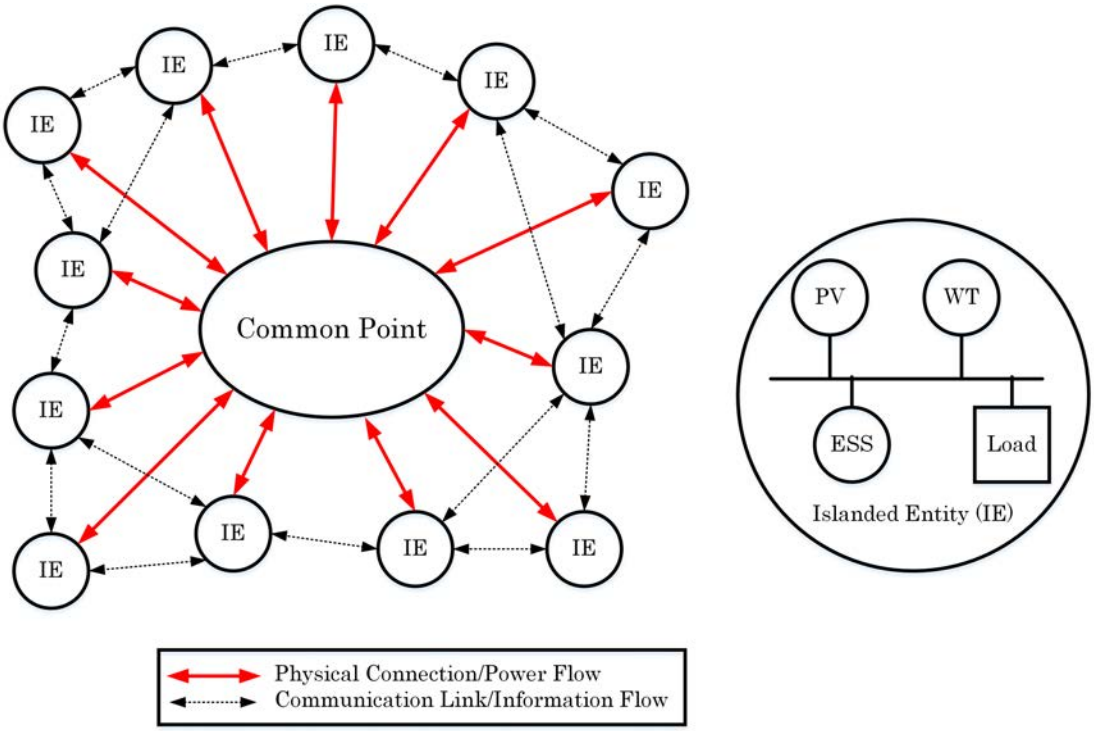


Figure 2.9: Concept of networked MGs.

### 2.1.6 Role of ESS in Islanded Entities

Technically, controlling autonomous islanded entities is complicated. Due to its small physical inertia, even a small interruption, such as the output power fluctuations of photovoltaics (PVs) or wind turbines (WTs) and switching in/out of loads, may lead to voltage and frequency problems or MG instability. With the crucial presence of an ESS, the frequency and voltage of an entity can be maintained stably through an appropriate ESS controller by flexibly releasing or absorbing active/reactive power. For a small entity, one ESS as a constant voltage/frequency source can manage MG operation. With the larger entity, where many ESSs exist, coordinated control is relatively complex. Droop control for an ESS has been considered a solution in recent studies. The voltage angle and amplitude of each ESS are regulated according to their output active and reactive power, respectively. Therefore, the active/reactive power can be shared according to a preset droop coefficient among the parallel ESSs. Unfortunately, since the

real and reactive power coupling among ESSs is due to a predominant resistive MG, the control scheme is more difficult. As mentioned, advanced virtual output impedance methods could enhance load sharing, but it reduces the control bandwidth, resulting in deterioration of the system dynamic stability. Also, combining the traditional $V/f$ droop control (VFDC) with $P/Q$ droop control (PQDC) to prevent the interference of line impedance uncertainty could enhance current sharing among ESSs and system dynamic stability. An energy management system combined with hierarchical control based on smart communication for droop gain optimization also can be used to improve the quality of voltage/frequency with secondary and even tertiary control. However, the dependence on communication will lead to another problem, such as increased cost and decreased reliability [63].

DC MGs have recently drawn great attention for applications such as building electrical systems, data centers, and plug-in hybrid electric vehicles, due to their higher efficiency than AC MGs, their flexible control capability, and the convenience of integrating DC resources and loads. A schematic of a DC MG with the integration of RESs, battery energy storage systems (BESSs), and loads is shown in Figure 2.10. During autonomous operation, an ESS unit is also utilized in a DC entity to compensate for the power fluctuation between power generation and consumption. Bidirectional DC/DC converters are used to control the output of battery banks. RESs, including solar PV and wind turbine generators, are integrated through DC/DC and AC/DC converters, respectively. RES converters normally operate in a maximum power point tracking (MPPT) mode to harvest maximum renewable sources. A bidirectional DC/AC converter as a link converter is used to interlink the utility with the DC bus. A contactor at the DC side can be installed between the link converter and the DC entity to control their connection. A contactor is an electrically controlled switch used for switching an electrical power circuit, similar to a relay except with higher current ratings. The functionality and control method of the contactor is similar to that of an SSTS at the AC side in conventional AC entities. The contactor is closed in the grid-connected state and opened during islanded operation in case of a utility grid fault. The linked DC/AC converter monitors the AC-side power quality (voltage magnitude, frequency, phase unbalance) to enhance the system's response speed.

In an islanded DC entity, a coordinated energy management strategy, such as hierarchical control, should be used for power balance to prevent the ESS from overcharging and over-discharging. The state of charge (SOC) of an ESS is therefore monitored. Depending on different SOC scenarios, the coordinated operation of a DC islanded entity is achieved by managing all power flow from RESs, ESSs, and loads. The hierarchical structure is responsible for this coordinated control based on a reliable communication link. Under hierarchical control, the lower control level receives commands from the higher control level to take action. The secondary controller regulates the bus voltage at the nominal value. The central controller makes decisions based on the SOC condition of the ESS units collected from the primary level and then sends control mode signals to the other units. When one ESS is not fully charged, it is operated at the maximum power point (MPP) to utilize renewable energy effectively. On the other hands, the controller limits the input power of an ESS unit when it is fully charged. Simultaneously, RES units reduce their power output. When an ESS discharges during high power consumption, RES units should operate at MPP. In cases where it is unavoidable, noncritical load shedding can be conducted when power consumption is too high [30].

In the islanded mode, ESS units operate in voltage regulation mode and a linked DC/AC converter operates in the idle mode. In term of the return-to-utility state, the voltage quality of the utility is first checked at the central controller to ensure the disturbance has been cleared. When it has met the criteria, the signal for disturbance clearance is sent to the central controller through the SCADA. The link converter is activated to regulate the DC-side output voltage. It is checked again until the parameters are satisfactory. The voltage difference across the contactor should be minimized before the contactor is closed.

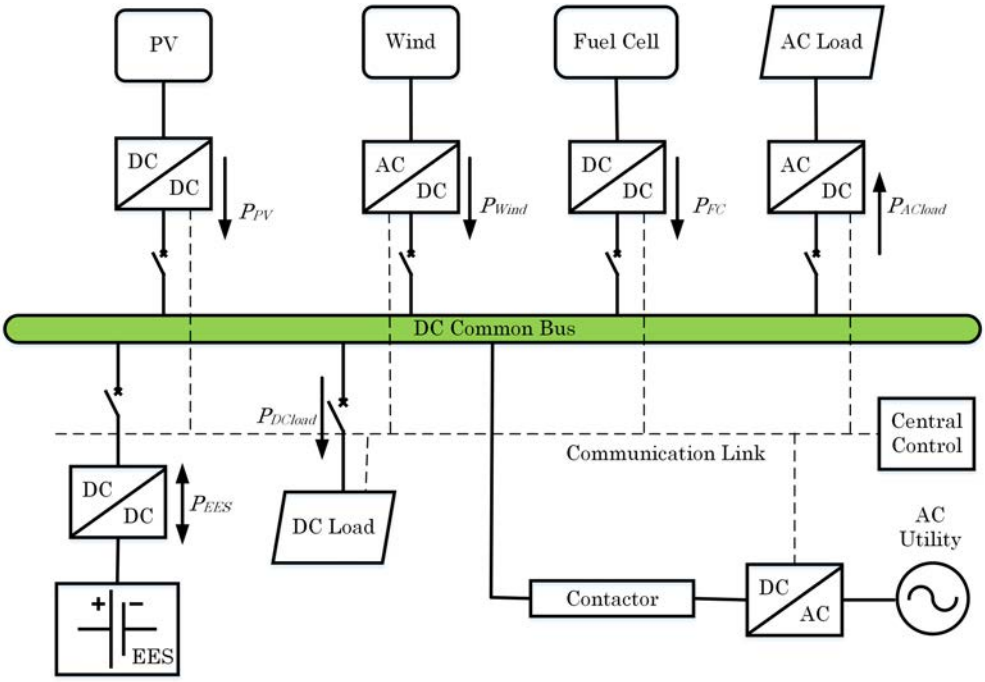


Figure 2.10: Schematic of a DC MG.

## 2.2 Future Perspective of Power Systems with High DG Penetration

Recent smart MGs are run based on small WT and PV sources, ESSs, and distributed loads which are connected to the PCC of the utility through the intelligent bypass switch (IBS) or the conventional SSTS. The overall system consists of a number of REs that require power electronic inverters. Because of the high penetration of REs, the integrated power system with a complicated physical connection and multi-layer cyber-link might easily suffer cascading outages. Faults may have conventional causes, such as a short circuit, lightning, or huge load changes; faults may also have unconventional causes, such as a natural disaster or terrorist attack. Some recent research efforts with advanced technologies are trying the address these problems: load forecasts to adjust the power balance during the day is a key power-saving solution which enables smart power communities [16]; a distribution network with residential DG units should be actively

made more flexible and dynamic where bidirectional power flow occurs, as new reconfigurations could be frequently observed [17]; a networked communication, computation, and sensing system facilitates all robust controllers to make the grid more secure, efficient, and reliable by quickly responding to any abnormal phenomenon based on adaptive self-healing and self-organizing mechanisms [13].

To build a robust power system with high RE penetration, the main idea is to connect many reliable MGs to the main grid or interconnect them through tie lines, thus forming MG clusters. This can make the control bulk system simpler, similar to the scheme in Figure 2.9. Each cluster is defined clearly, and the data of that cluster are sufficient and compensated whenever any new components, such as DGs or loads, are installed. The maximum number of elements within one cluster should be determined for easily handling tasks. In the distribution grid, to guarantee that the voltage of terminal loads is within limits, the number of elements from the substation cannot be too high. The conventional power system will be divided into many clusters. If a DC tie link cannot be made, the substation can be considered the common coupling point of one cluster. In the future grid, with more smart elements and sensitive load increases, cyber-attacks will increase, and the switch of elements will frequently occur. Also, the current configuration of the power distribution system can lead to a cascade fault and blackout. A fundamental MG can be defined as a part of the grid consisting of prime energy movers, power electronics converters, distributed energy storage systems, and local loads. MGs should be able to operate autonomously but also interact with the main grid. The seamless transfer from the grid-connected mode to islanded mode is also a desirable feature. A sequence for the seamless transfer has been described and implemented [31, 32]. These tie DC lines will act as interchange energy channels to balance the energy required by each MG; thus, the power flow of these lines will be further reduced. The clear operation of all elements of all grids could facilitate the flexible and reliable operation of the power system. Moreover, MGs represents a new paradigm of low-voltage distribution systems, since the generation is not only based on small generation machines but also on small prime movers, such as PVs, small wind turbines, or fuel cells, that require power electronic interfaces, such as AC/AC or DC/AC

inverters. These power electronic devices act very quickly and have full control of the transient response. However, in contrast with the generation machines, power electronics do not have inherent inertia that ensures the stability of the system and the steady-state synchronization of each unit. To compensate for this disadvantage, virtual inertias are often implemented through a control loop—the droop method. This method consists of reducing the frequency and the amplitude of the inverter output voltage proportionally to the active and reactive power. Voltage and frequency droop control has become disseminated and is regarded as a potential method [33, 34, 35] Thus, MGs will be able to maintain an active and reactive power balance, as well as avoid voltage collapses.

Advancing toward a secured power system since the integration of renewable energies, reconfigured power systems require future research on: (i) resilient controllers for a stronger and smarter grid by means of complex dynamical systems, forecasting uncertainty, and consideration of the environment, markets, policy [16]; (ii) technologies for sensing and monitoring, leading to improved data management, reliable communications, data analysis, state estimation, and visualization, eventually leading to systems with faster automation and self-healing through an accurate time response. Even in the case of faults leading to the islanding phenomenon, in order to improve power supply continuity, the authors in [2] studied a suitable island management system by allowing active or passive islanding transition with intelligent control: island detection, identification, fragmentation to operate simultaneously, synchronous merging, and return-to-mains, as seen in Figure 2.11. This well-equipped smart grid (by costly investigation) is a requisite to realizing this excellent performance.

**(.) Island Detection/Identification**: The fault should be detected immediately, i.e., within 2 s according to the IEEE 1547 standard, to facilitate islanded operation to allow, for example, sufficient time to acquire data from the power system to make a decision before returning to DGs. The system management, therefore, should understand completely all components which identify the DGs in each intentionally islanded entity and then initiate an appropriate coordinated control strategy, resulting in load sharing within these island entities.

**(.) Island Fragmentation and DG Isolation**: In order to ensure power supply continuity, some smaller island entities could be established after the fault. Since there are different configurations for each DG type, islanding protection may isolate the DG from entities, and the unbalanced power in such a case can cause frequency and phase deviations. The other DGs which stay connected should perform full frequency and phase control to compensate for power losses and any load disturbances.

**(.) Return-to-Utility and Island Merging**: The smaller islanding entities might be merged to become a bigger one, and then the whole islanded area could reconnect to the utility. To identify a suitable moment to take this action, the energy management system should monitor all the circuit breakers inside the entities and the SSTS status based on the phase angles of the voltages of individual DGs. This task is important to recover the normal operation of the power system, although the islanded operation can last for a long time.

Normally, strategies for identifying and splitting the network into stable and maintainable islanded entities largely rely on prior knowledge of the systems status, such as the matched load and generation in each entity, whether coherency is tight or slow among DGs, and the level of intelligence and flexibility of the MGs. In such a black start operation, frequency and voltage stability, active and reactive power flow control, active power filter capabilities, and storage energy management are the functionalities expected for eligible islanded entities [12].

Because of the high penetration of RE with intermittent fundamental input energy and variable power outputs, consideration must be given to the ability of controllers to maintain frequency and voltage within limits; this is especially important for frequency variation, which is particularly restricted in the synchronous islanded operation mode. In Figure 2.12, after the island fragmentation transient, the gas-wind island can be held within. When island merging occurs with the faster-responding diesel engine, control is improved and phase can be moderated. Therefore, faster-responding DG is beneficial. Additional phase control support for the island could be provided by other types of renewable technology, such as doubly-fed induction generators (DFIGs) for the fast response of storage in the

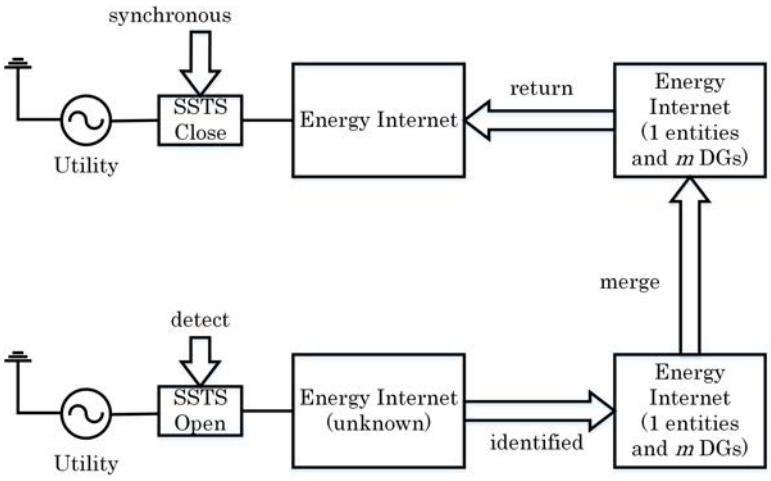


Figure 2.11: Islanding state transitions.

converter, energy storage with high-performance batteries, or a flywheel which can quickly balance a load–generation mismatch, and a load management system.

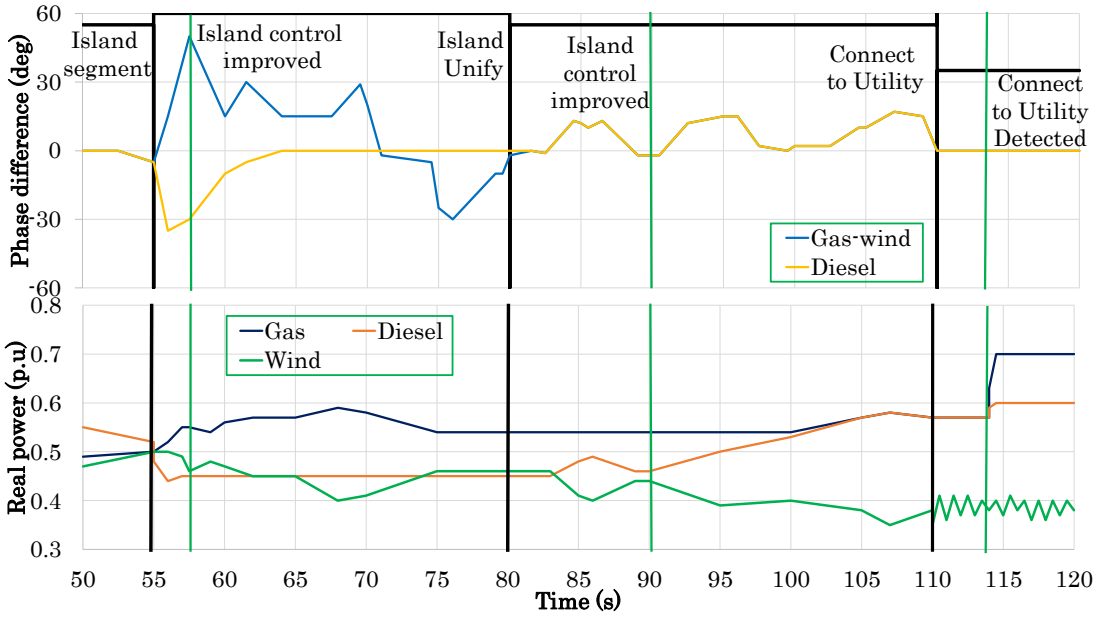


Figure 2.12: Mechanism of Island segmentation, unifying, and connect to utility.

### 2.2.1 Improved Functions to Flexible Grids

In order to adapt to high-penetration RE power system, the following improvements to the conventional MG are fundamental:

(.) Reliable islanding detection; (.) Accurate grid impedance estimation to facilitate droop control; (.) Improvement in the transient response of each component itself as well as the entire collaborative controller of MG; (.) Effective utilization of virtual impedance to share active/reactive power and harmonic components; (.) Improvement in adaptive droop control laws to increase the interactivity of the system; (.) Hierarchical controls applied smoothly to improve self-healing ability; (.) Enhanced voltage ride-through and power quality in the PCC regulated by DG units; (.) Consider black start operation of each islanded entity to facilitate synchronous multi-islanded operation; (.) More high-performance energy management support of ESSs.

These features will impart MGs with more intelligence and flexibility to integrate RE resources into the future smart grid.

### 2.2.2 Communication System

The modern communication network is more critical to the power system operation. It is expected to be secure, robust, scalable, and reliable, making it resilient to failures. The reconfigured grid has a two-way flow, not only of electricity but also information, leading to an automated power network. The messages exchanged through the communication networks consist of either information about the status of the grid or commands that enable status changes in the configuration of the network. Information and communication technology (ICT), Internet of Things (IoT), and Artificial Intelligence (AI) will thus play a major role in realizing modern power grids [17]. The communication mechanism can use power line signaling, smart meter technologies, or other commercial infrastructures (e.g., satellite, telephone, wireless, power line carrier, fiber optics, or microwaves based on LAN or WAN) [19]. Sensors need to be deployed in large numbers among

MGs in order to efficiently monitor MG conditions, such as faults at the transformers, the status of the breakers, power flow magnitude, and flow directions in distribution lines.

In the multi-islanded operation, all entities are connected physically by interconnecting tie links and communicatively based on the high-bandwidth communication link. New communication protocols provide new functionalities, such as data routing, broadcasting, multicasting, and so on. In the paper by [14], reliability communication is stated to have several facets: (i) probability that a given message will be lost entirely; (ii) use of redundant communication paths; (iii) automatic failure to protect against message loss; (iv) the expected time delay in delivering a message and the expected variability of that time delay; and (v) how competing messages may (or may not) be given priority when communication channels are saturated, known as quality of service.

When all information of the power system is stored online by IoT, protecting personal information related to utility customers and information about the utility itself is important. Since customer-level information is typically not very time-critical, slower and more computationally intensive mechanisms can typically be used to secure this information. A relatively critical protection requirement is placed on confidential information and the commands used to monitor and control the power system. To implement the best security, all the details of the security system should be published and well known, but the keys should be kept a secret, where only the owner or another authorized party has the key. Applying a layered protection approach, with multiple levels of firewalls and "demilitarized zones", requires more secure corporative firewall data.

## 2.3 Hierarchical Control and Seamless Mode Transfer

### 2.3.1 Seamless Mode Transfer

As mentioned previously, the hierarchical control which has long been applied to the AC power system can now be applied to energy management systems effectively operating in PEI-based MGs to facilitate seamless transfer between the grid-connected mode and islanded mode [1]. The hierarchical control structure of a current-controlled DG interface employs a power-sharing control loop, voltage control loop, and current control loop, as shown in Figure 2.13 [22]. In the grid-connected mode, the reference voltage vector is generated to control the DG interface as a PQ bus or a PV bus. In the islanding transition and isolated modes, the autonomous power-sharing controller generates a reference current vector. In each mode, a robust voltage controller with internal model dynamics against random, harmonic, and unbalanced voltage disturbances is designed to reject a wide range of voltage disturbances associated with these modes (e.g., harmonic, unbalanced, and random voltage disturbances). These controllers can be designed to either adapt to any mode based on sensors or are switched when detecting a transfer between modes.

(.) In grid-connected mode, the MG operates according to a standard, such as IEEE 1547-2003, UL 1541, or P1547.4.

(.) The transition to the islanded mode occurs intentionally (e.g., maintenance) or unintentionally (e.g., faults). This mode is facilitated by fault monitoring, predictive maintenance, and protection.

(.) In the islanded mode, entities must supply the required active and reactive powers, as well as provide frequency stability and operate within the specified voltage ranges.

(.) Reconnection of the islanded entities to the utility will proceed as soon as the synchronization operation is made (matching the voltage, frequency, and phase angle between islanded entities and utility).

During the transient-to-islanded mode, the switching effect will impose voltage disturbances and a power angle on the output voltage of DG units, leading to the instability of power-sharing dynamics. This happens in conventional power controllers due to their lack of transient damping to react to large swings and is a large-signal stability problem. For a smooth transition, a possible countermeasure is adaptive transient droop control, which simultaneously facilitates a stable and reliable DG operation in both the grid-connected mode and autonomous operation.

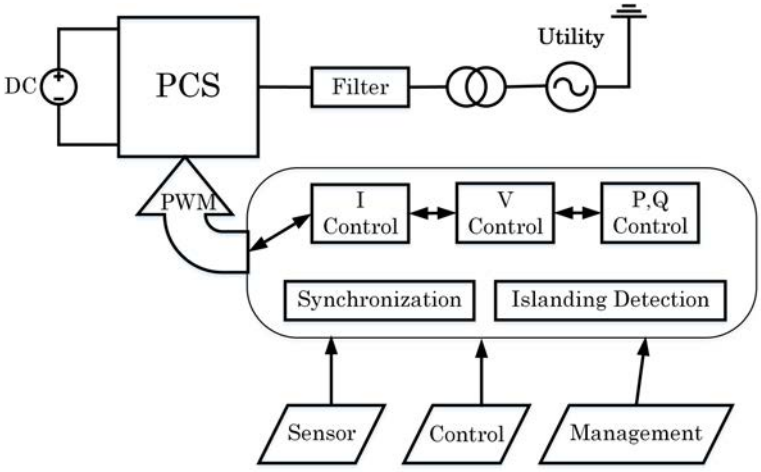


Figure 2.13: A hierarchical control structure of a current-controlled DG interface.

Two categories can be distinguished to achieve seamless transitions. (i) The first category employs primary control loops implemented in the inverters, which make use of complex inverter topologies or control algorithms to complete the transitions. (ii) The second category uses a hierarchical architecture, as explained for MGs.

(.) A study by [36] combined a single-phase MG composed of voltage-controlled voltage source inverters (VC-VSIs) (for batteries and other energy storage technologies) and current-controlled voltage source inverters (CC-VSIs) (for renewable energy sources, such as PVs and micro wind turbines, to maximize power output), which worked together in both operation modes. The primary control structures for VC-VSIs and CC-VSIs were considered together with secondary control loops, which are used to synchronize the MG, as a single unit

to the utility, rather than considering each unit separately. The integration of CC-VSIs into the MGs enables fault ride-through capabilities for these inverters which can continue to generate power for the MG, even during islanded operation; this MG can then seamlessly disconnect from the grid and operate autonomously, forming an island entity.

(.) If the energy sources are RE, one of the VC-VSIs should also ideally include an ESS due to the intermittency of the power input. In such cases, an additional loop integrated into the primary control loops of the inverters monitors the state of charge for the ESS, MPPT for the PV and micro-WTs, etc. The primary control implemented in the VC-VSIs enables operation in the islanded mode or grid-connected mode through the use of the droop control technique and islanding detection algorithms. Secondary control loops optimizing MG operation are used to minimize the reactive power flows between these inverters and achieve reactive power-sharing between the inverters in the islanded mode while also providing voltage and frequency restoration. The tertiary control layer considers the interaction between multiple MGs universally and the regulation of power flows across these MGs.

After faults, the aim is to transition from the islanded mode to the grid-connected mode, which requires a synchronous operation.

(.) Because of the appearance of different DGs and ESSs with power electronic components, the synchronization operation of an islanded entity is a rapid dynamic response with small inertia and low overload capability [65]. It is different from the quasi-synchronism control in power systems based on a regular rotating machine. In most existing work, MGs and utilities under ideal conditions (balance and no harmonics) are always considered when applying synchronization techniques and seamless reconnection to the utility. The controllers thus relates only to the synchronization control topology of basic positive series components. To achieve this control (control action), some methods enforce voltage at the link-feeder to directly track the utility voltage, which is rarely realizable due to the geographical location of DGs because they need to send a rapid communications signal in the time-domain, such as phase angles. Alternatively, a unified controller, which includes amplitude and phase compensators that control the local

controllers of DG units, can be used. Thus, the droop curves can shift up/down at the same time in order to synchronize the islanded entities' voltage with the utility.

(.) Due to the low short-circuit ratio and limited capacity, in the islanded mode, PEI-based entities with no support from the stiff utility are sensitive to the problems of voltage, frequency, and harmonic. In conventional power systems, the voltage distortion (e.g., total harmonic distortion (THD) $< 5\%$ and unbalance factor (UF) $< 2\%$) [38] is hard to emphasize in the synchronization process enough to make the reconnection process destabilized. Therefore, under non-ideal voltages, this process should also account for the synchronization of negative-sequence and low-order harmonic ingredients. The secondary control level of the hierarchical control composition of islanded entities executes algorithms of both positive and negative components. As discussed above, to operate VSCs, two types of control strategies can be used. With CCVSC units, CC-VSCs will be synchronized with the utility by the local PLL. Therefore, the transition from island to grid-connected modes is not a significant issue. Besides, in islanded mode, DGs usually use VCVSC units to support voltage and supply power balance.

(.) A distributed active synchronization algorithm can be applied for a smooth reconnection despite non-ideal voltages. All the DGs, ESSs, and loads decide the frequency and voltage of the islanded entities. Hence, synchronization control by using the secondary control level in the hierarchical control of controllable DGs is necessary to guarantee the stabilization of voltage/frequency and harmonics suppression of both islanded entities and the utility in the allowable range, according to any standard, before closing the SSTS. For example, for the voltage harmonics limitation in IEEE Standard 519-2014, individual harmonic distortion (IHD) $< 3\%$, THD $< 5\%$, and UF $< 2\%$. Different harmonic components should be considered according to the specific application. For instance, all odd harmonic ingredients (1–13) should be considered in general cases (linear/nonlinear balanced/unbalanced loads). To achieve a smooth reconnection, the minimization of basic and harmonic voltage differences between islanded entities and the utility is a potential and effective solution.

### 2.3.2 Hierarchical Coordination of AC and DC MGs

Due to the increase of DC sources in terms of renewable energy, DC ESSs, supercapacitor modules, or hydrolyzers and DC loads by means of PEIs among AC power systems, interest is rapidly growing in hybrid AC/DC MGs that combine both AC and DC systems coordinately to control the power flow between DC and AC parts. In this MG, the bidirectional interlinking converter that interfaces the DC subgrid to the AC subgrid plays a critical role. This converter links neighbor entities to form multi-MGs for power, supporting or enhancing the economic performance of the whole grid. Each cluster can manage its own frequency and voltage as an autonomous entity[39]. The overall control of a DC MG needs more research attention [1]. Studies on the topologies, architectures, planning, and configurations of MGs integrating different technologies—power electronics, telecommunications, generation, and ESSs—are necessary for ensuring a smooth transition between grid-connected and islanded modes. Compared with hierarchical control for large power systems with high inertia and inductive networks, in PEI-based MGs, there is no inertia, and the nature of the networks is mainly resistive. Contrary to that previously mentioned, in the control of a DC MG, a zero-layer of a zero-to-three level hierarchical controller has been adopted and organized, according to the literature, as follows.

(.) Level 0 (inner control loops): current and voltage, feedback and feedforward, and linear and nonlinear control loops of each module can be performed to regulate the output voltage and to control the current while keeping the system stable.

(.) Level 1 (primary control): the droop control method is used to emulate physical behaviors that make the system stable and more damped. A resistive virtual output impedance loop is included that integrates the soft-start approach.

(.) Level 2 (secondary control): maintains the normal values of frequency and voltage amplitude inside the DC entity by the virtual inertia and output virtual impedance, which is related to the other control loops, such as inner current, voltage loops, and the droop control, in order to run a synchronization operation for seamlessly reconnecting to the utility.

(.) Level 3 (tertiary control): controls the power flow among DC or AC entities and utilities.

Figure 2.14 shows the primary, secondary, and tertiary controls of a DC MG. Once the DC MG is connected to the DC source, the power flow can be controlled by changing the voltage inside the DC MG. By measuring the current iG (or the power) through the SSTS, it can be compared with the desired positive or negative current $(i * G)$ (or power), depending on whether energy is imported or exported.

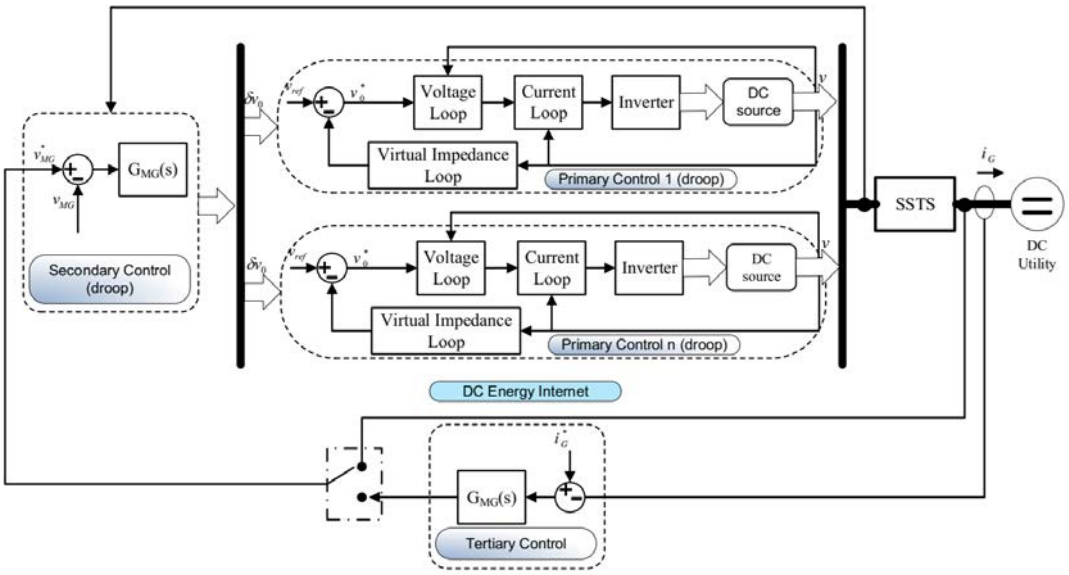


Figure 2.14: Primary and secondary controls of a DC MG.

In Figure 2.15 is a multi-MG cluster which, in a universal view, constitutes a proactive DG grid regardless of whether it is a DC or AC configuration. Each MG has its own hierarchical controller. Communication among MGs uses hierarchical controllers. The tertiary control of a cluster can provide high-level inertia to interconnect more MGs and fix the active and reactive power to be provided by this cluster, or it can act as the primary control to interconnect more clusters. The secondary control sends all references to each cluster of MGs to restore the frequency and amplitude. As a result, we can scale the control hierarchy as necessary. Using this approach, the system becomes more flexible and expandable, and, consequently, it can integrate increasingly more MGs, without changing the local hierarchical control system associated with each MG.

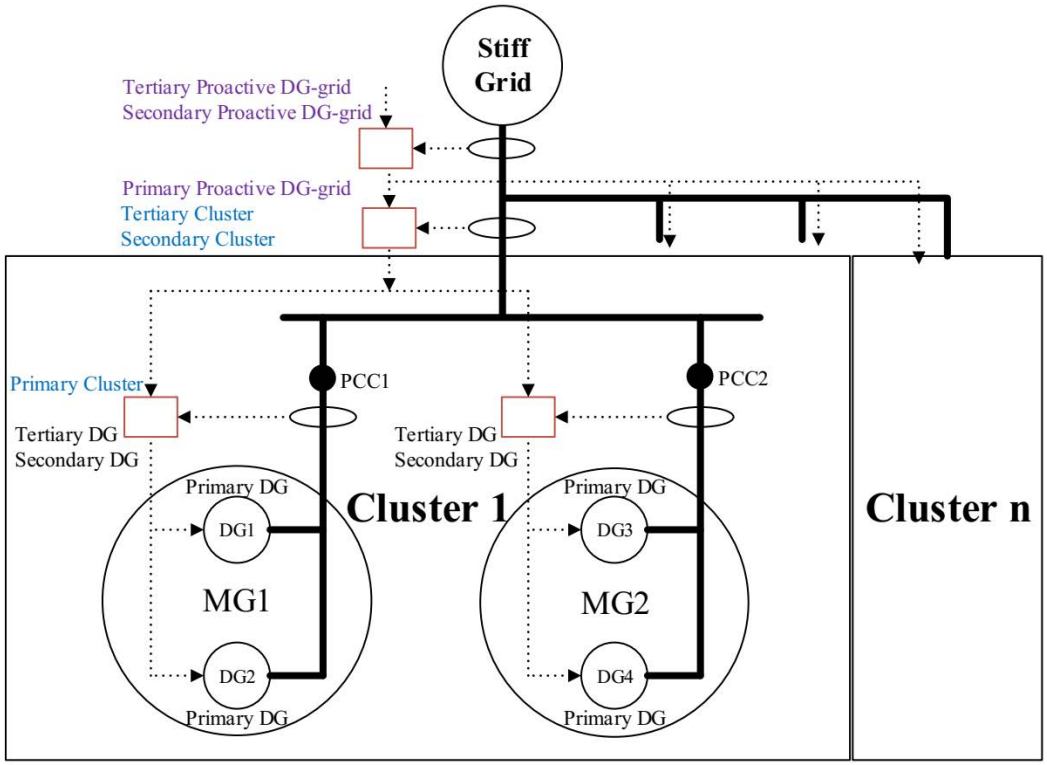


Figure 2.15: Clusters of multiple MGs forming a smart grid (SG) configuration.

### 2.3.3 Synchronous Operation for Reconnection

After a fault is cleared, an islanded entity is normally required to change its operational mode to grid-connected by reconnecting to the utility after synchronizing its operation. Contrary to a single machine using a synchronizer (phase angle, slip frequency, and voltage difference), the synchronization of islanded entities operating with many active components (such as REs, ESSs, and conventional generators) needs to be controlled in a coordinated way. This complicated scheme utilizes various PEI-based DGs, as well as the collaboration of alternator-based generators, which determines the frequency and voltage of entities. The common synchronization method, which waits for the fulfillment of synchronizing criteria while maintaining the entitys frequency and voltage at fixed values, does not always yield consistent results. For example, it takes a very long time until the phase difference matches the criteria. Also, an important factor in measuring

the synchronizing criteria is the estimation of the phase and frequency during non-ideal conditions. During synchronous operation, since the entity operates as an independent system, fast and robust voltage and frequency control must be provided even under harmonics, unbalanced loads, and noise [40]. Recently, most control strategies have been droop-based methods and/or master/slave control methods. DG units can be classified in power-controlled and voltage-controlled units. In the islanded mode, to maintain the voltage and frequency within the acceptable limits, at least one of the DG units is required to operate by a voltage-controlled mechanism. In droop-based methods, all DG units are involved in regulating the voltage and frequency of islanded entities. In the master/slave method, a DG unit with the highest power rating is responsible for regulating the voltage and frequency, as the master unit and the other slave units produce pre-specified amounts of active and reactive power. Master/slave control schemes are found to be both costly and unreliable [41].

In islanded entities, controllable energy sources consider the battery energy storage system (BESS) and diesel generators while REs, including PV, WTs, fuel cell, etc., are regarded as uncontrollable due to intermittent input energy. If an islanded entity has no rotational DG, the smart PCS of a PV or WT system will manage the frequency and voltage. The fuel cell generator, which needs a long time to change its output, is responsible for the lowest frequency band using a low-pass filter. The diesel generator takes charge of the middle-frequency band using a bandpass filter. The BESS, which has the fastest response, should control the higher frequency band. In another scheme, diesel generators with a larger capacity (50 kW) are used for the lowest band, and smaller diesel generators (20 kW) take charge of the middle frequency bands.

To facilitate a synchronous operation, the SSTS connecting the utility and an islanded entity normally use an intelligent electronic device (IED). The IED compares the criteria parameters of two sides for synchronizing criteria and switching the SSTS. It senses and compares the magnitude, frequency, and phase of the voltage of both sides during parallel operation to determine the synchronizing criteria. Signals can be measured by using a reference frame (fixed or rotating) transformation-based method under balanced or even unbalanced conditions [21].

In the islanded mode, the BESS acts as one of several controllers for frequency and voltage control. Unlike the grid-connected mode, the BESS does not strictly follow the reference values but uses the droop strategy [20]. A number of feedback signals, such as the voltage, current, frequency, and power, must be measured or calculated to support the BESS controller. During autonomous operation, many inverter-based DGs adopt the droop strategy for stable power-sharing. Determining precisely the components of unintentional entities in this mode is important for a central controller. That controller is used for active synchronizing control through the communication network. At first, it decides on the system's operational mode according to the SSTS connection status sensed by the IED. Then, it sends the operational command to every controllable DG to control the frequency and voltage of the synchronized entity. In this mode, the REs operate with MPP tracking to maximize generation efficiency. Not only is it uncontrollable, but it also acts as a disturbance in the maintenance of the stable voltage and frequency of the islanded entity.

The primary objective of active synchronizing control is to minimize the difference between these signals to satisfy the synchronizing criteria by manipulating output set-points of controllable DGs (weighted with the weight factors). The reclosing decision is made within a predetermined limit, which is irrespective of the exact moment of zero-crossing difference, as seen in Figure 2.16 Reclosing outside of the limit results in a big bump between two voltages.

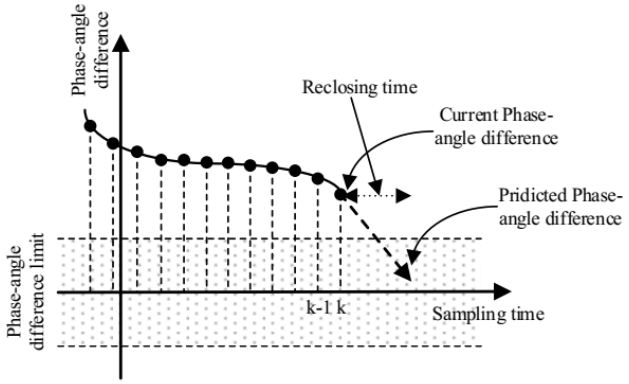


Figure 2.16: Phase angle difference estimation.

## 2.4 Voltage and Frequency Quality during Islanded Operation

### 2.4.1 Enhancing Voltage/Frequency Quality in Various Modes Using ESS

In the grid-connected operation, all DGs and ESSs are in the PQ control mode, where the MMS provides the output active and reactive power set-point via the $d$-and $q$-axis current commands. MGs have been typically regarded as a resistive or inductive systems in previous studies [1, 42, 43, 44, 45, 46, 47]. The different droop control strategies are applied depending on different system types. In islanded operation, the upper grid controller regulates the frequency and the voltage of the entity and also outputs the $d$-and $q$-axis current commands. During this mode, the power balance between supply and demand does not match, leading to voltage/frequency fluctuation. Then, the power balance is ensured by decreasing the generation or by load shedding to avoid a blackout. The frequency/voltage control of the islanded entity is not straightforward. For an entity which is composed only of RE units and conventional power units (the diesel generator, gas engine, and micro-turbine), it is hard to ensure good dynamic performance: due to relatively slow response time and intermittent power outputs, it is not possible to guarantee the power demands. Meanwhile, conventional systems are limited by their insufficient dynamic performance for load tracking. In particular, the local frequency of the islanded entities may change rapidly due to the low inertia of the entire system. To overcome these limitations, the introduction of an ESS is considered an effective solution to ensure power balance since this device is based on a power electronic device and has a very fast response time (in ms). The storage system in the entity is analogous to the spinning reserve of large generators in the conventional grid. The intermediate ESS is an inverter-interfaced battery ESS bank (BESS), compressed air energy storage (CAES), superconducting magnetic energy storage (SMES), electrochemical capacitor energy storage (ECES), supercapacitor, or flywheel energy storage (FES) [48].

A properly designed ESS can allow a system to stabilize by absorbing and

injecting instantaneous power. In previous studies, some ESS models have been proposed [49, 50, 51, 52, 53]. A cooperative control scheme between the ESS and other DGs is needed to effectively achieve the goal in islanded operation. A two-level control concept, which consists of primary and secondary control, has been proposed to stabilize the frequency of islanded entity: the primary control action in the ESS and the second control action in the entity management system (EMS). Fast-acting ESSs can effectively damp electromechanical oscillations because they provide storage capacity in addition to the kinetic energy of the generator rotors, which can share sudden changes in power requirements [9]. Additionally, the EMS of the central controller of islanded entities deals with management functions, such as disconnection during faults, switching to other controllers of all components of the entity, resynchronization after fault clearance, and the load-shedding process. This central controller is also responsible for the supervisory control of DGs and the ESS units by universal communication. By using collected local information, the controller generates a power output set-point and provides it to the primary controller of each DG unit and ESS unit to ultimately control the power output according to the given values. Fundamentally, the control capability of the ESS for balancing between generation and consumption may be limited by its available capacity. Therefore, the power output of the ESS should be brought back to zero as soon as possible by the secondary control in order to secure the maximum spinning reserve.

The secondary control algorithm of the central controller compares the measured power output of ESS ($P_{ESS}$ and $Q_{ESS}$) and the reference value ($P_{ESS}^{ref}$ and $Q_{ESS}^{ref}$) to obtain the error. This error generates the total required power and sends the commands to dispatch power output set-points for each individual controllable DG unit based on its participant/weighted factor, which normally depends on its capacity. During islanded operation, the power output of diesel generators is also changed from an initial constant value to a new power set-point calculated by the secondary control, as shown in Figure 2.17 at t = 5 s. In this figure, the BESS is specifically tested to represent the ESS system. In the second event, 10 kW of active load change at t = 15 s, the ESS can afford to inject the necessary active power into the entity to ensure power balance because the power output

of the ESS is bringing it back to zero; thus, it has sufficient spinning reserve margin. The power outputs of the diesel generators are changed from the initial constant values to new set points by the central controller. Facilitated by this cooperative control, the frequency and the voltage can be regulated at nominal values successfully, as shown in Figure 2.18. Like a BESS, the PEI-DG can respond quickly enough to implement droop control during the islanded operation. PEI-DG, however, depends on primary resources and a BESS depends on the SOC. Therefore, both BESS and PEI-DG need to depend on slow-response DG units, such as a diesel or gas generator, for secondary control.

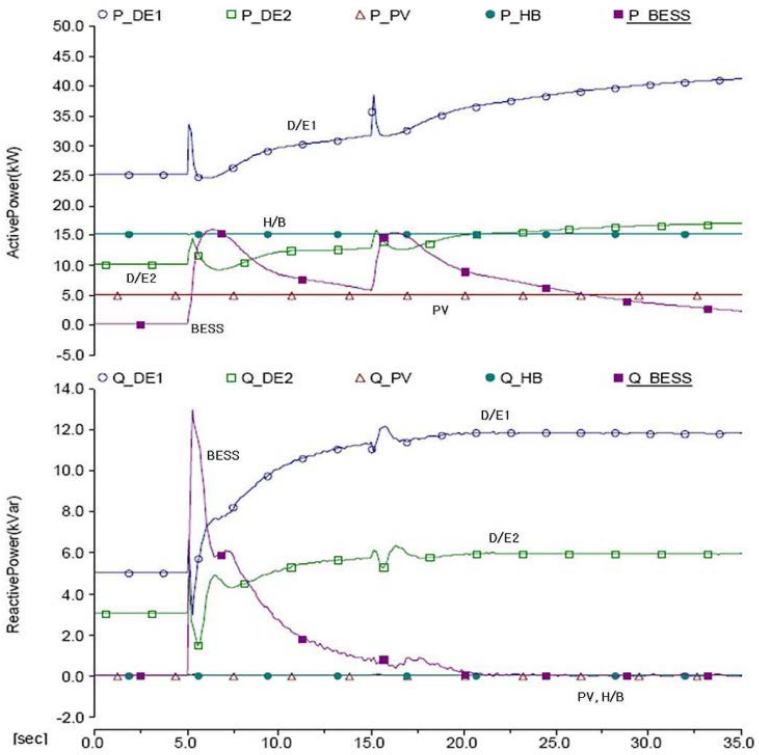


Figure 2.17: Power outputs of an energy storage system (ESS) and microsources [9].

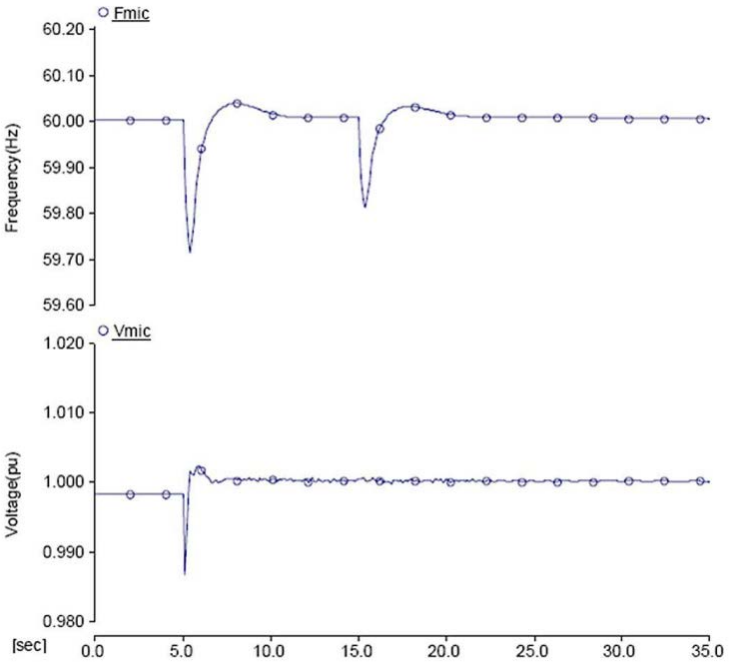


Figure 2.18: Frequency and voltage of an MG [9].

### 2.4.2 Load-Sharing Operation of Distributed MGs

Generally speaking, in an islanded entity, unbalanced and/or nonlinear loads such as motors might exist. Normally, the impedance load can absorb a sudden change in instantaneous real and reactive power, such as an infinite sink. However, with motor loads, a sudden change in the terminal voltage leads to a large oscillation in the real and reactive power level. Furthermore, the line impedances are not purely resistive or inductive, and the control of active and reactive power is not totally decoupled in nature. Therefore, in terms of total harmonic distortion and voltage imbalance indexes, the islanded entity should share the common loads entirely to ensure that quality within the islanding entity is maintained as it is in the grid-connected mode.

The conventional method for local load sharing is the droop characteristic using feedback local signals. The droop coefficients are chosen to meet the voltage requirements at PCC points and based on the rating of DGs. With non-ideal loads, both active and reactive power have double the frequency and distorted

components over the average components. Thus, DG units should supply double the frequency and distorted components to compensate for the unbalance and harmonics. The central controller is informed clearly of the status of all loads, DG units, and other parts among islanded entities by using a reliable communication system [10].

Calculating the output impedance of DG units, the feeder, and local loads can affect power-sharing, especially in $Q$-$V$ droop control. However, due to the complex structure of an islanded entity, the system impedance cannot be straightforwardly estimated. Communication-based solutions are utilized to improve sharing accuracy. Although the diverged locations of DG units challenge this method now, it is expected to be solved soon by improved communication technology at low costs, such as wireless solutions. In another approaches, the whole MG system is proposed to be composed of a certain physical network and several DG units in order to have most islanded entities in a clear configuration. Each DG unit can be equivalent to a droop-controlled voltage source (DVS) in series with a DG feeder. The DG feeder can be either a coupling inductor or a virtual feeder if the virtual impedance method is applied. By separating DVS units from the system, the equivalent network of an MG is obtained. For example, the equivalent network in its entirety contains $s$ DG feeders, $n$ network feeders, $s$ DVS nodes and $m$ network nodes, where s is the number of DG units. Finally, the system impedance can be estimated in any islanding case [54].

### 2.4.3 Voltage Quality

The droop control used to share loads during the islanded mode was conventionally designed for large synchronous generators in the balanced condition. Therefore, while applying it to a system with unbalanced loads, the unbalanced load currents flow through the line and converter impedances, giving rise to unbalanced terminal voltages which can trip off sensitive loads. When the voltage unbalanced factor (VUF) thresholds of local buses are exceeded, to eliminate any tripping, one costly solution is to install additional equipment, such as active power filters (APFs), static synchronous compensators (STATCOMs), dynamic

voltage restorers (DVRs), or unified power quality conditioners (UPQCs). A less costly but complicated alternative is to slightly enhance the capacity of existing converters of DG units and to modify their control algorithms to include some compensation functions. Through proper control, unbalanced voltage is mitigated by injecting negative-sequence currents through the current-controlled DG converters. Unbalanced voltage can also be compensated for by using multiple DGs.

In order to achieve negative-sequence reactive power-sharing, each DG is controlled as a negative-sequence conductor with its conductance drooping, along with the negative-sequence reactive power flow. However, the negative-sequence current sharing performance is affected by line impedance and droop coefficient mismatches. In this case, a droop controller can insert negative- and zero-sequence tunable virtual impedances, in addition to the usual positive-sequence impedance, allowing the DGs to perform selective voltage compensation. Normally, the enabled DG units maintain VUFs of the buses of interest at their thresholds, which can help to limit the currents passing through the enabled DGs while protecting their local sensitive loads.

In the case of a three-phase four-wire system, where four-leg converters are used for supplying single- and three-phase loads with an additional zero-sequence current return path, sharing an unbalanced load current among those four-leg converters also needs to take the zero-sequence component into account. It is necessary that the critical loads are placed close to converters with the compensation ability whenever their VUF exceeds certain thresholds. A three-phase four-wire islanded entity with $n$ DG units is shown in Figure 2.19. Each DG is tied to its local bus by a three-phase four-leg converter. The four-leg converters must regulate their respective bus voltages and share the loads by applying droop control. The positive-sequence current component and negative-, zero-sequence current components under unbalanced loads need to be addressed separately. All DGs are set to have the same p.u. power ratings and the control scheme is implemented in the $dq0$ synchronous reference frame. The central controller facilitated by communication links measures the voltage of the common bus, makes the management decision, and then transmits the compensation references to the DG units [26].

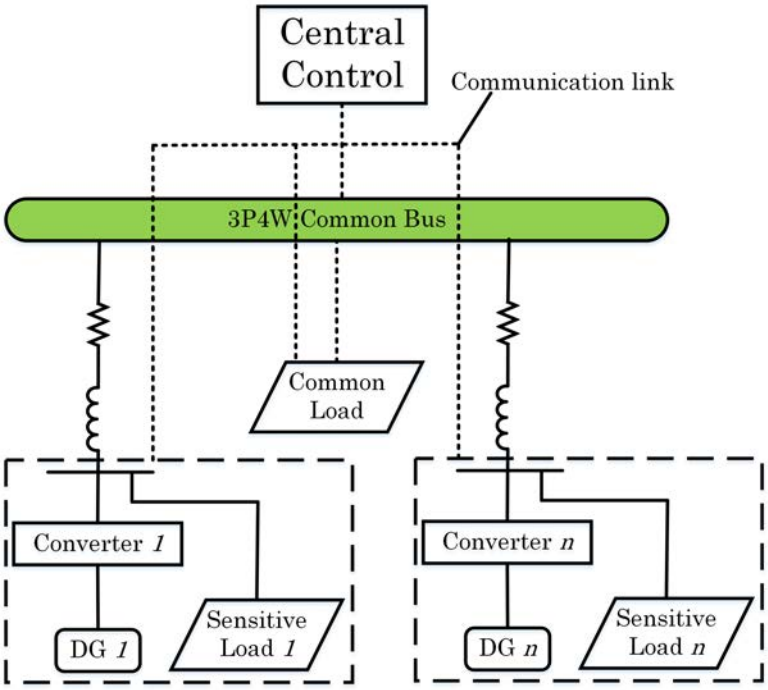


Figure 2.19: Illustrative three-phase four-wire islanded entity.

The configuration of a multi-functional inverter (MFI) with an ancillary service of voltage/frequency quality enhancement is depicted in Figure 2.20. With this system, extra voltage/frequency quality conditioners may no longer be essential in an inverter-dominated entity, avoiding additional investment and operational cost. Since it is the auxiliary function of an MFI, its capacity for voltage/frequency quality enhancement is limited and related to its working condition. Optimally utilizing the limited capacity of an MFI for harmonic and reactive power issues should be assigned with independent weights to enhance the voltage/frequency quality of the islanded entity as much as possible [55].

To integrate multiple MFIs into one powerful entity, a universal controller (UC) needs to be deployed. This controller utilizes a multi-objective optimal compensation model to assign the optimal compensation coefficients to each MFI based on the given initial information of the optimal model. In general, this control might use a hierarchical mechanism, and the optimal compensation may be embedded in the tertiary control to provide optimal voltage/frequency quality

services. With the guide of the UC, each MFI partly compensates for these issues in the MG according to the multi-objective optimal model in the tertiary control. Each MFI can autonomously work as an individual module without needing information from the other ones. In secondary control, the power output of MFIs is exchanged and modified by the UC to ensure the safe and economic operation of the islanded entity. In the local primary controller of the MFI, an output current-tracking controller is embedded so that the MFI generates the desired active, reactive, and harmonic current that fulfill the functions required by the DERs interfacing with the utility and enhances the quality of voltage/frequency of the entity.

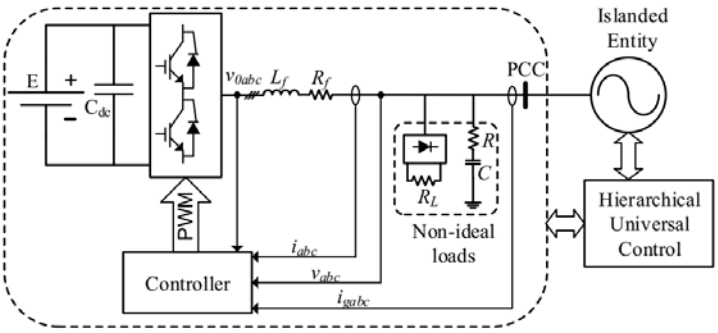


Figure 2.20: Microgrid feeder with a multi-functional inverter (MFI).

### 2.4.4 Summary

This chapter discusses the islanding phenomenon and subsequent actions to maintain the power supply with a high penetration of RE. The self-controlling for DG unit and central controlling using a hierarchical scheme are explained explicitly. The capability to operate in conventional grid-connected mode or islanded mode and the smoothy transient between two based on the advanced controller is pointed out. In order to make the smart and resilient operation of the coming power system, many research directions need to be investigated such as robust hierarchical controller, advanced droop control, active/reactive power-sharing, harmonic mitigation inside the islanded entity, high-performance ESS and its proper controller, reliable communication system, etc.

# Chapter 3

# Active islanding detection method in DC grid-connected photovoltaic system.

## 3.1 Literature reviews

Many islanding detection strategies in AC networks have been proposed in the literature. In recent years, several studies about islanding detection methods in the DC system has been conducted.

Among those methods, a very promising IDM was proposed in [63]. This method based on the reflection of frequency and voltage deflections of the AC side on the DC side through the DC-AC converter. That method was tested under various load conditions, load switching, multiple DGs operation, and different load quality factors. However, that IDM was for islanding detection of AC system, not for the DC system. Moreover, due to the disturbances of frequency and voltage at the AC side affect the DC voltage insignificantly. So that the effectiveness of the method is limited. Also, maximum power point tracking (MPPT) is not discussed in the paper.

The active detection technique, positive feedback islanding methods were proposed in [64]. The technique was introduced to reduce the non-detection zone

(NDZ) in the worst case when the power of the load is matched with the power of the DG. The idea of this method is to inject the disturbance signal by using an inner loop or outer loop feedback signal in islanded condition. That signal will make the system unstable by using the Routh-Hurwitz stability criterion. The main challenge in this method is how to select again that guarantees the DG instability while islanding occurs and keep the DG stability in normal condition. The paper proposed four different methods to realize this technique, comparing and evaluating the performance of this method. Nevertheless, the system under analysis in this paper has only one DG source. In the case of multi-DG sources, the challenge of that method becomes more and more difficult.

The active method in [65] based on the insertion of a controllable load, connected in parallel with the DC microgrid central switch. The parameters of the controllable load depend on the characteristics of the measuring component. The IDM was simple and easy to implement. However, that method only applies in case of constant DG source and loads.

In [66], the harmonic injection capability is incorporated into the interleaved flyback inverter to detect islanding condition. This technique is proposed that bypasses the unfolding H-bridge, without affecting the active power generation of the inverter and without requiring any hardware modification. In addition, the anti-islanding technique based on the harmonic injection technique is presented and implemented into the flyback micro-inverter. However, this anti-islanding technique uses in the AC grid.

The passive islanding technique in [67] was proposed. The method based on autocorrelation function (ACF) of a modal current envelope to extract the transient content. After that, the variation of the ACF is calculated, called criterion variance in the autocorrelation of the modal current envelope to define between islanding and normal conditions. By using the method, the islanding condition can detect effectively. However, this technique uses in the AC grid.

In [68], the active technique is used to detect islanding phenomenon in DC grid. In the paper, a current perturbation was injected to make current imbalance for a certain period at a scheduled frequency and observing the response. In

normal condition, the fluctuation of DC voltage is small when the injected current changed. When islanding occurs, the DC voltage will change much more than the normal one. After that, the injected current continuously decreases to increase the DC voltage drop speed. So, it has a shorter detection time than other IDMs. However, the system under analysis is relatively simple.

Due to the limitation of those previous researches, this chapter proposes method depends on injecting perturbation signal and rate of change of output power is used to detect islanding issue in a DC grid-connected photovoltaic system. According to the proposed method, the islanding problem can detect faster than the other methods. Moreover, this method can cover both hardest and another islanding condition. In addition, this method is testing not only in single but also in multi-PV operation scenarios. The rest of this paper is organized as follows. In Section 1.5, the islanding detection methods for AC grid are investigated and the difference between islanding detection in AC and DC grid is described. Section 3.2 explains the DC testing grid and the inject perturbation signal method. In Section 3.3, the simulation results are described and analyzed. The chapter is concluded in the final section.

In the next section, the system description and scheme explanation are illustrated.

## 3.2 System description and active Islanding Detection Method (IDM)

### 3.2.1 System Description

Figure 3.1 shows the diagram of the system under analysis. Because the role of renewable energy sources is the same. Assume that the renewable energy source in the system under analysis is only a photovoltaic source. This system consists of a 50 kW PV array, output capacitor $C$, DC/DC converter with maximum power point tracking (MPPT) and islanding detection program. The DC load is shown as an equivalent resistance and the DC bus is modeled as a constant

voltage source. The specifications of the PV module are introduced in Table 3.1. The inverter is used to connect the AC grid and the DC grid. In Figure 3.2, VSC controller is modeled as a voltage source converter (VSC) average model to regulate DC bus voltage (keep DC bus voltage stable at 500 V).

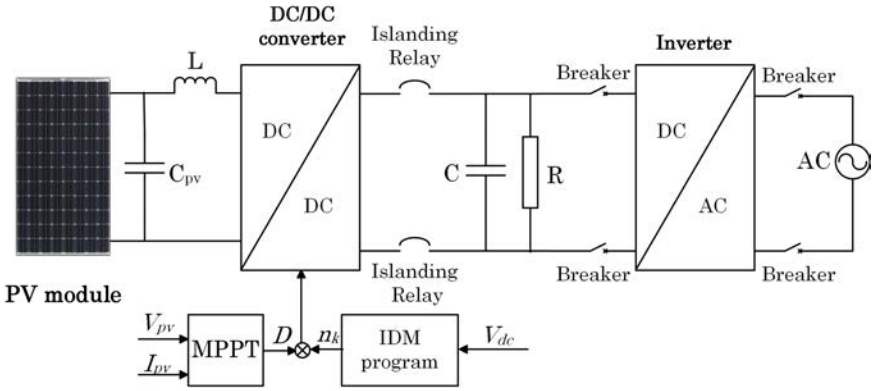


Figure 3.1: System model under analysis.

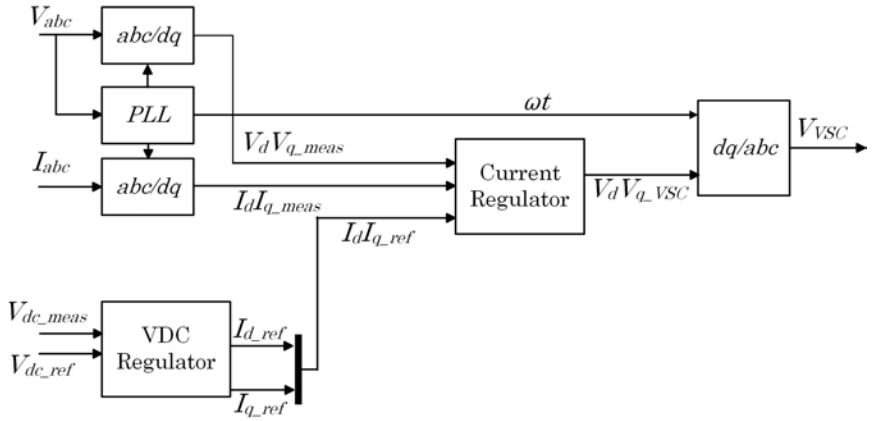


Figure 3.2: Diagram of voltage source converter (VSC) controller.

Table 3.1: Specifications of SunPower SPR-305E-WHT-D (SunPower, San Jose, California, USA) PV module.

| Information | Value |
|---|---|
| Open circuit voltage | 64.2 V |
| Short circuit current | 5.96 A |
| Voltage at maximum power point | 54.7 V |
| Current at maximum power point | 5.58 A |
| Maximum power | 305.226 W |
| Parallel strings | 66 |
| Series-connected modules per string | 5 |
| Active PV power at 1000 ($W/m^2$) and 25 °C | 100 kW |
| Active PV power at 500 ($W/m^2$) and 25 °C | 50 kW |
| Active PV power at 250 ($W/m^2$) and 25 °C | 25 kW |
| Active PV power at 100 ($W/m^2$) and 25 °C | 10 kW |

### 3.2.2 Active islanding detection method using perturbation signal.

Because only DC voltage signal can be used to detect islanding condition in the DC grid when islanding occurs. So, the idea for IDM in the DC grid focus on how to make the change of DC voltage is large enough and faster than without IDM. Based on this idea, the IDM injects the perturbation signal to the output of the MPPT to change the value of the duty cycle before supply to boost converter is proposed. By using this IDM, the islanding condition can detect easier and faster than without IDM. Figure 3.3 describes in detail how to inject the perturbation signal.

The IDM program receives DC voltage value from the measurement device to decide the value of the perturbation signal generated by the IDM program. The perturbation signal makes the duty cycle of a boost converter fluctuate according to the fluctuation of the perturbation signal. In normal condition, the DC load is supplied by both PV through DC/DC converter and AC grid through the inverter. Due to the dc-link regulation of the inverter, the dc voltage is almost not

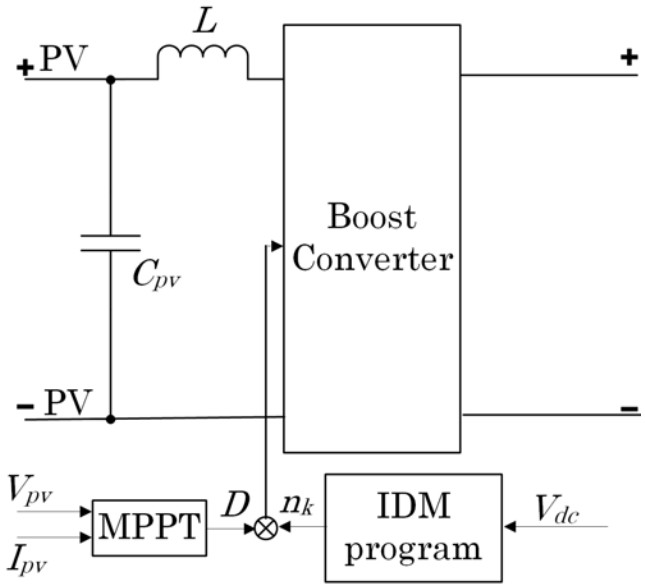


Figure 3.3: Controller perturbation signal circuit ($V_{dc}$ is the measurement DC bus voltage, $V_{pv}$ is the PV voltage and $I_{pv}$ is the PV current, $n_k$ is the perturbation factor, $D$ is the duty cycle).

affected by the perturbation signal. However, when the AC grid is disconnected, without the dc-link regulation, the dc voltage is affected by the perturbation signal. If the dc voltage fluctuation caused by the perturbation signal exceeds a set threshold value, the islanding detection method decreases the perturbation signal's value (increases the amount of perturbation). If the dc voltage drops enough, it will make the rate of change of output power exceeds a set threshold value (islanding detection threshold value). The dc voltage change and the rate of output power change caused by the perturbation signal are accelerated and the islanding phenomenon is faster detected than without the islanding detection method.

The flowchart in Figure 3.4 explains the detailed procedure of the proposed method.

The IDM is verified step by step simulation. The simulation is executed in two main cases: single PV operation and multi-PV operation. In both cases, the proposed IDM is tested in two conditions: hardest islanding condition (the

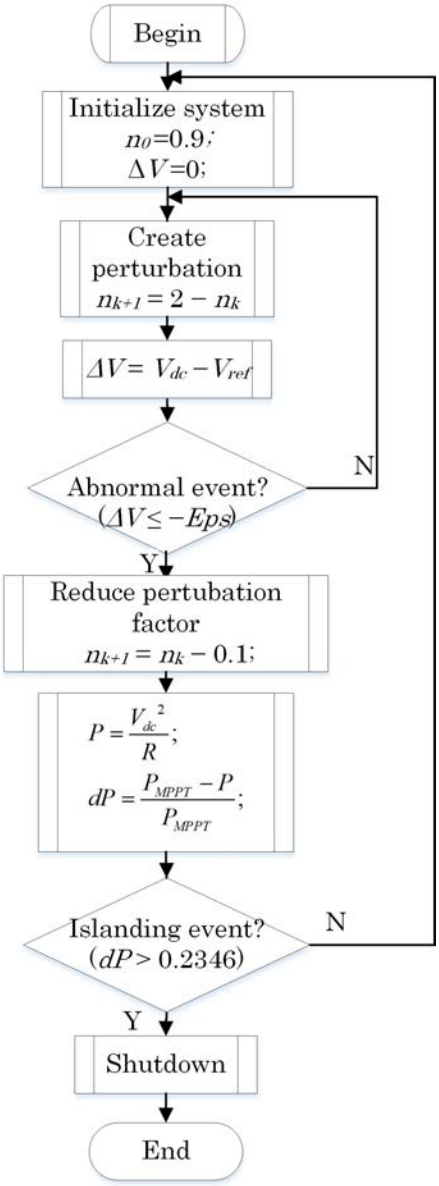


Figure 3.4: Flow chart of the IDM program ($n_0$ is perturbation factor at the beginning, $\Delta V$ is voltage deviation, $Eps$ is abnormal event value, $dP$ is the rate of change of output power).

power of load and PV are equal) and another islanding condition (the power of the load is greater than the power of PV). The sampling time is $T_s = 5\times\ 10^{-5}$. The simulation time of each specific condition is 3 (s) and is performed with two

following steps:

- Step 1: Start the inject perturbation signal at 0.4 (s) from the system startup.
- Step 2: The islanding event is activated at 1.5 (s) from the system startup by disconnect the AC grid.

The simulation results show that proposed IDM is able to detect the islanding event in all conditions.

The equivalent circuit in normal and islanding condition is illustrated in Figure 3.5. The main idea of this method is to inject a perturbation signal into boost converter to make the fluctuation of $V_{dc}$ and the DC/DC input current as well. In normal condition, with the $V_{dc}$ compensated by the inverter, the fluctuation of $V_{dc}$ is small. However, when the AC grid disconnected, without the DC bus regulation by the inverter, the $V_{dc}$ fluctuation is affected by $n$. If the $V_{dc}$ fluctuation exceeds the abnormal threshold value, the $n$ value will decrease to make the rate of change of output power reach the threshold value faster than without IDM.

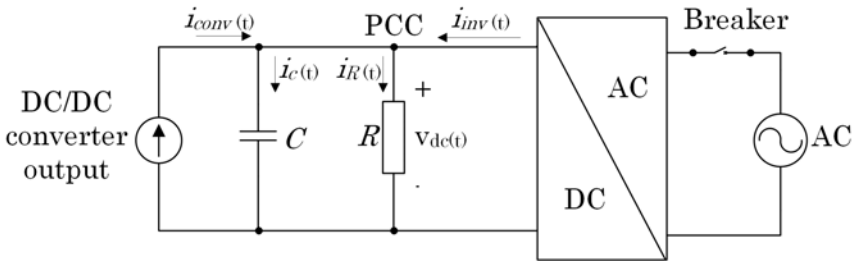


Figure 3.5: Equivalent circuit in normal and islanding conditions.

For the analysis of the hardest islanding condition, the DC load power is perfectly matched with the power generated by PV. The assumptions are constant DC load and PV power. The explanation of the inject perturbation signal method is presented in Equations (3.1)–(3.16).

Based on the equivalent circuit, the Kirchhoffs law for the capacitor node after islanding:

$$i_c(t) = i_{conv}(t) - i_R(t) \tag{3.1}$$

where

- $i_R(t)$ is the current of DC load.
- $i_C(t)$ is the current of DC/DC converter output capacitance.
- $i_{conv}(t)$ is the DC/DC converter output current.

Equation (3.1) can be rewritten

$$C\frac{dv_{dc}(t)}{d_t} = i_{conv}(t) - \frac{v_{dc}(t)}{R} \tag{3.2}$$

$$\frac{dv_{dc}(t)}{dt} + \frac{1}{RC}v_{dc}(t) = \frac{1}{C}i_{conv}(t) \tag{3.3}$$

where

- $v_{dc}(t)$ is the DC bus voltage in islanding condition.
- $R$ is the DC load resistance.
- $C$ is the DC/DC converter output capacitance.

Because $i_{conv}(t)$ is unit step function

$$i_{conv}(t) = \begin{cases} i_{conv}(-t_0) & t \leq t_0 \\ i_{conv}(+t_0) & t > t_0 \end{cases} \tag{3.4}$$

where

- $i_{conv}(-t_0)$ is the DC/DC converter output current before time $t_0$.
- $i_{conv}(+t_0)$ is the DC/DC converter output current after time $t_0$.

Take the Laplace transforms of both sides of Equation (3.3)

$$sv_{dc}(s) - v(0) + \frac{1}{RC}v_{dc}(s) = \frac{1}{C} \cdot \frac{i_{conv}(s)}{s} \tag{3.5}$$

$$v_{dc}(s) = \frac{v(0)}{(s + \frac{1}{RC})} + R\left[\frac{1}{s} - \frac{1}{s + \frac{1}{RC}}\right] i_{conv}(s) \tag{3.6}$$

where

- $v(0)$ is the initial DC voltage before islanding condition.
- $s$ is the Laplace operator.

From Equation (3.6), we can find the inverse transformation

$$v_{dc}(t) = v(0)e^{-\frac{1}{RC}t} + Ri_{conv}(t) - Ri_{conv}(t)e^{-\frac{1}{RC}t} \tag{3.7}$$

The DC/DC converter output current can be rewritten

$$i_{conv}(t) = (1 - n_k D)i_{pv}(t) \tag{3.8}$$

$$= N_k i_{pv}(t) \tag{3.9}$$

where

- $n_k$ is the injected perturbation factor at step k.
- $i_{pv}(t)$ is the current of the PV module.
- $D$ is the duty cycle.
- $N_k$ is the DC/DC output current perturbation factor at step k.

Therefore, Equation (3.9) becomes

$$v_{dc}(t) = [v(0) - N_k R i_{pv}(t)]e^{-\frac{1}{RC}t} + N_k R i_{pv}(t) \tag{3.10}$$

According to Equation (3.10), when islanding occurs, the decrease of output current perturbation factor $N_k$ makes DC bus voltage drop. In general, the result is correct in the time domain.

In this paper, the rate of change of output power is used to decide whether islanding has occurred or not. This threshold value is explained in Equations (3.11)–(3.18).

Before islanding, the DC load power is

$$P_{pv} + \Delta P = \frac{{V_{dc}}^2}{R} \tag{3.11}$$

- $P_{pv}$ is the PV maximum power.
- $\Delta P$ is the change of active power.
- $V_{dc}$ is the DC bus voltage in normal condition ($V_{dc} = V_{ref}$).
- $V_{ref}$ is the DC bus voltage reference (500 V).

After islanding occurs, the DC load power is

$$P_{pv} = \frac{(V_{dc} + \Delta V)^2}{R} \tag{3.12}$$

where

- $\Delta V$ is the change of DC bus voltage in islanding condition.

Assuming PV is in constant power control, so, the active power supplied by AC grid is

$$\Delta P = \frac{V_{dc}^2}{R} - \frac{(V_{dc} + \Delta V)^2}{R} \tag{3.13}$$

Normalizing $\Delta P$

$$\frac{\Delta P}{P_{pv}} = \frac{\frac{V_{dc}^2}{R} - \frac{(V_{dc}+\Delta V)^2}{R}}{\frac{(V_{dc}+\Delta V)^2}{R}} \tag{3.14}$$

$$\frac{\Delta P}{P_{pv}} = \left(\frac{V_{dc}}{V_{dc} + \Delta V}\right)^2 - 1 \tag{3.15}$$

$$\left(\frac{V_{ref}}{V_{max}}\right)^2 - 1 \leq \frac{\Delta P}{P_{pv}} \leq \left(\frac{V_{ref}}{V_{min}}\right)^2 - 1 \tag{3.16}$$

where

- $V_{max} = (V_{dc} + \Delta V)$ is the over voltage threshold.
- $V_{min} = (V_{dc} - \Delta V)$ is the under voltage threshold.

The voltage threshold of islanding is selected according to EN50160 standard

$$0.9V_{ref} < V_{dc} < 1.1V_{ref} \tag{3.17}$$

Therefore, the rate of change of output power threshold is given by

$$-0.1736 \leq \frac{\Delta P}{P_{pv}} \leq 0.2346 \tag{3.18}$$

All results are shown and discussed in the next section.

## 3.3 Simulation Results

The testing proceduce is following:

- The perturbation signal injected to PV converter at $t = 0.4$ s from the system startup.
- The islanding condition occurs at $t = 1.5$ s from the system startup.

The model parameters are shown as below:

- DC bus voltage is $V_{dc} = 500$ V.
- Under voltage threshold is $V_{dcmin} = 450$ V.
- Rate of change of output power threshold is 0.2346.

- The perturbation duration $T = 8$ ms is determined from the dc-link voltage variation and MPPT efficiency.
- The perturbation factor at normal condition is $n = 0.9$ to 1.1 (The factor $n$ starts from 0.9, changes to 1.1 and reset to 0.9 once it is detemined that the dc-link voltage is regulated. It continuously decreases by 0.1 until IDM detects the islanding condition).

In this test, the result gives the difference of detection time between the original inject perturbation method in [68] and the improvement method.

### 3.3.1 Single PV Operation

In the single PV operation scenario, PV module power is 50 kW and the diagram is shown in Figure 3.6.

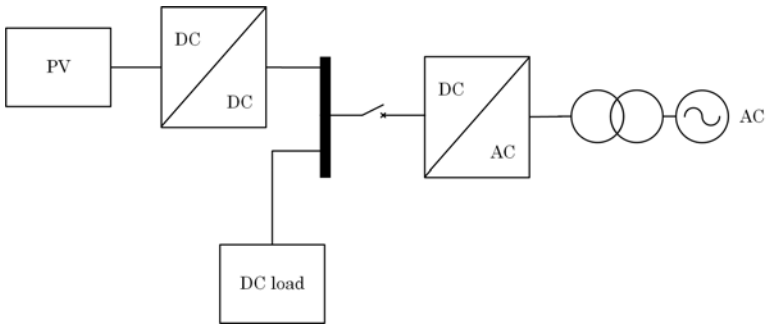


Figure 3.6: Single PV operation.

In single PV operation scenarios, the IDM is tested in two cases are displayed in Table 3.2.

Table 3.2: Single PV operation scenario.

| Cases | Total PV (kW) | Total Load (kW) | Vdc (V) |
|---|---|---|---|
| 1 | 50 | 50 | 500 |
| 2 | 50 | 62.5 | 500 |

The result in the first case is shown in Figure 3.7, and in the second case is shown in Figure 3.8. Figure 3.7 shows the islanding detection times of original and improved IDM in the worst case are same $t = 44$ ms. Meanwhile, the islanding condition cannot be detected by the OV/UV passive method because the DC voltage does not exceed UV threshold in the worst case. In another case, without IDM, Figure 3.8 shows that islanding condition can detect when the DC voltage reaches UV threshold in $t = 33$ ms, slower than the detection time $t = 28$ ms when applied both original and improved IDM. In the single PV operation scenario, there is no difference between the original method and the proposed method. Besides, there is significantly different between with and without IDM.

In addition, the proposed IDM almost neither affect the power quality nor MPPT efficiency. This conclusion based on the following explanation.

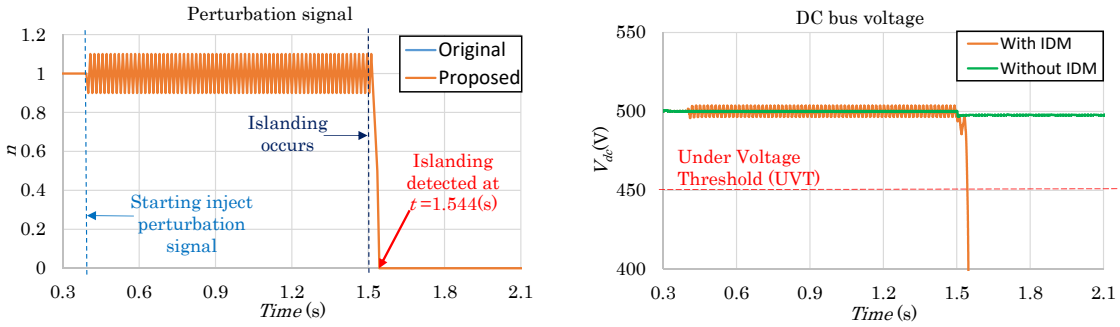


(**a**) (**b**)

Figure 3.7: Result in case of single PV operation, 50 kW PV, hardest islanding condition: (**a**) Perturbation signal and (**b**) DC bus voltage (with and without IDM).

First, for power quality. Due to the system under analysis is DC grid, the power quality degradation depends on the fluctuation of DC voltage ($V_{dc}$) when proposed IDM is applied. The DC voltage is regulated by DC/AC inverter to stabilize at 500 V in normal condition. Meanwhile, the measurement value fluctuation is 496.5 V$\leq V_{dc} \leq$ 503.6 V or 99.3% $\leq V_{dc} \leq$ 100.7% while the normal

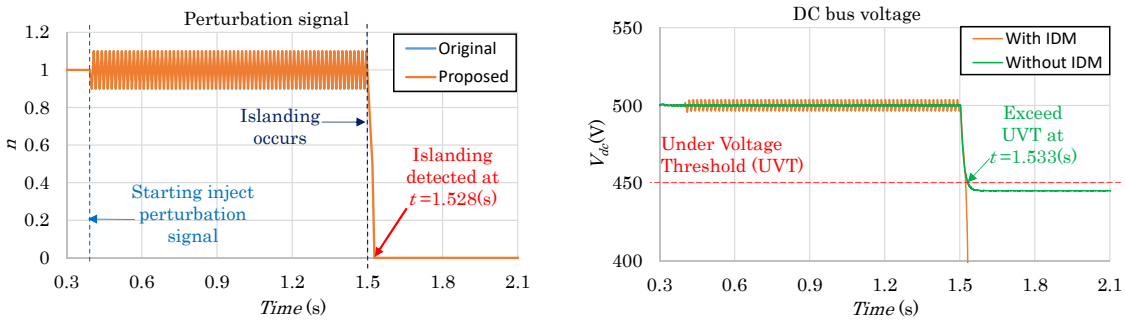


(**a**) (**b**)

Figure 3.8: Result in case of single PV operation, 50 kW PV, another islanding condition: (**a**) Perturbation signal and (**b**) DC bus voltage (with and without IDM).

voltage threshold is $90\% \leq V_{dc} \leq 110\%$. Therefore, our proposed method does not significantly affect power quality.

Furthermore, for the issue of MPPT affection raised by the proposed method. The MPPT affection can represent by MPPT efficiency and its calculation based on the equation below:

$$\eta = \frac{V_{mpm}}{V_{mpref}} 100 \tag{3.19}$$

where

- $\eta$ is the MPPT efficiency.
- $V_{mpm} = 270.5$ V is the PV array voltage measurement at maximum power point.
- $V_{mpref}$ is the PV array voltage reference at maximum power point (manufacturer value).

The PV array voltage reference at maximum power point calculation based on the under equation:

$$V_{mpref} = V_{mpref\_module} \cdot m \tag{3.20}$$

where

- $V_{mpref\_module}$ = 54.7 V is the PV module voltage reference at maximum power point.
- $m = 5$ is the series-connected modules per string.

Consequently, the MPPT efficiency when the proposed IDM is applied is:

$$\eta = \frac{270.5}{54.7 \cdot 5} 100 = 98.9\% \tag{3.21}$$

For that reason, the proposed IDM does not significantly affect the MPPT efficiency.

### 3.3.2 Multi-PV Operation

The multi-PV operation scenario diagram is displayed in Figure 3.9.

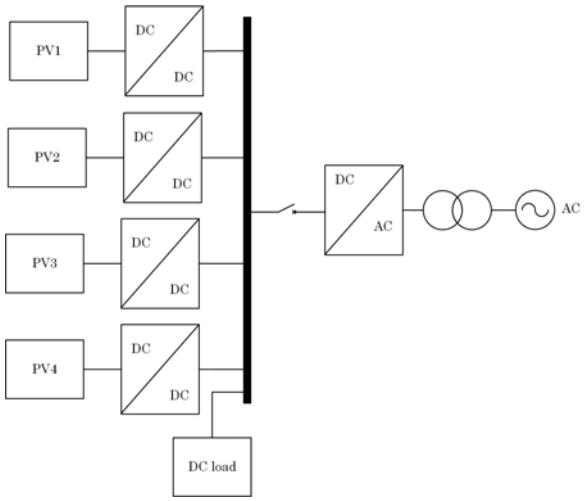


Figure 3.9: Multi-PV operation.

In this scenario, IDM is tested in both the worst-case and another case with different total PV power in Table 3.3.

In this scenario, there is a considerable difference not only between with and without IDM but also between original and proposed methods. The results of six cases are discussed as follows.

Table 3.3: Multi-PV operation scenario (kW).

| Cases | PV1 | PV2 | PV3 | PV4 | Total PV | Load | Vdc(V) |
|---|---|---|---|---|---|---|---|
| 1 | 50 | 50 | 50 | 50 | 200 | 200 | 500 |
| 2 | 50 | 50 | 50 | 50 | 200 | 250 | 500 |
| 3 | 25 | 25 | 25 | 25 | 100 | 100 | 500 |
| 4 | 25 | 25 | 25 | 25 | 100 | 125 | 500 |
| 5 | 10 | 10 | 10 | 10 | 40 | 40 | 500 |
| 6 | 10 | 10 | 10 | 10 | 40 | 50 | 500 |

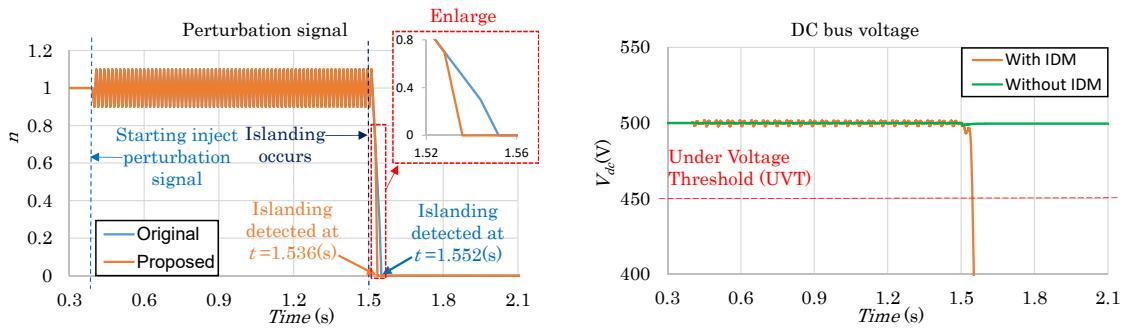


(**a**) (**b**)

Figure 3.10: Result in case of multi-PV operation, 200 kW PV, hardest islanding condition (case 1): (**a**) Perturbation signal and (**b**) DC bus voltage (with and without IDM).

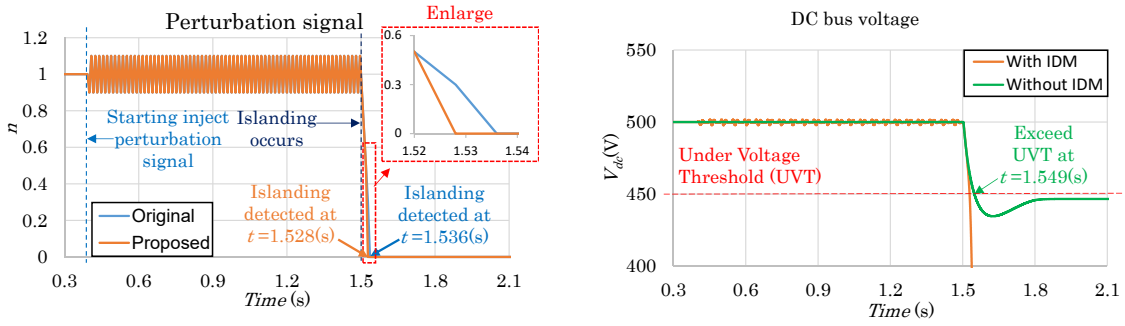


(**a**) (**b**)

Figure 3.11: Result in case of multi-PV operation, 200 kW PV, another islanding condition (case 2): (**a**) Perturbation signal and (**b**) DC bus voltage (with and without IDM).

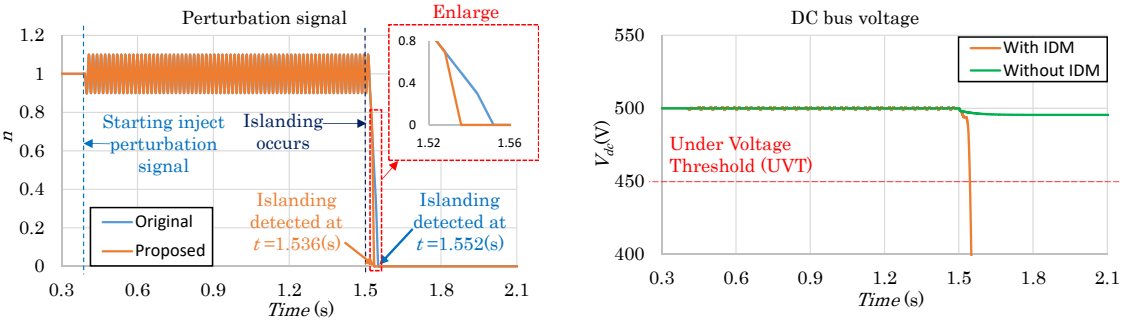


(**a**) (**b**)

Figure 3.12: Result in case of multi-PV operation, 100 kW PV, hardest islanding condition (case 3): (**a**) Perturbation signal and (**b**) DC bus voltage (with and without IDM).

In the first and second cases, the total PV power is 200kW, the results are shown in Figure 3.10 to Figure 3.11. In Figure 3.10, the original method can detect islanding condition in the worst case after $t = 52$ ms. Meanwhile, after $t = 36$ ms, the proposed method can detect the same condition. The detection

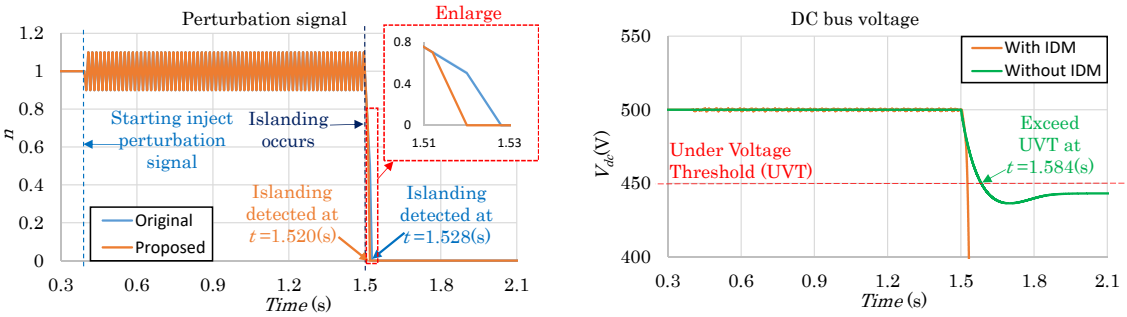


(**a**) (**b**)

Figure 3.13: Result in case of multi-PV operation, 100 kW PV, another islanding condition (case 4): (**a**) Perturbation signal and (**b**) DC bus voltage (with and without IDM).

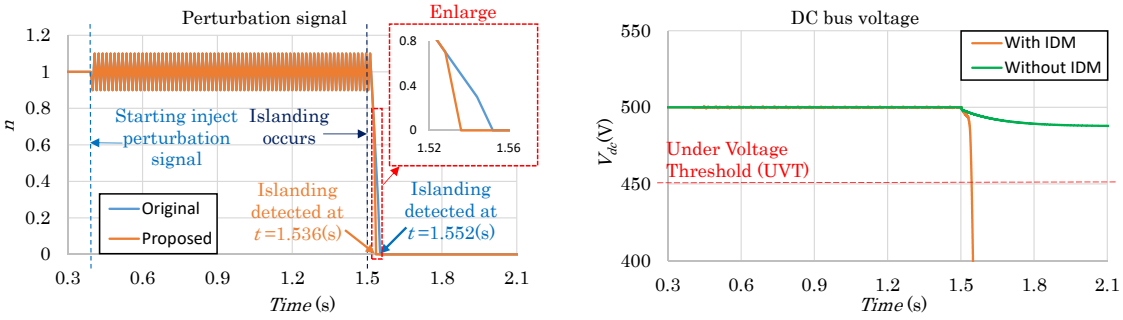


(**a**) (**b**)

Figure 3.14: Result in case of multi-PV operation, 40 kW PV, hardest islanding condition (case 5): (**a**) Perturbation signal and (**b**) DC bus voltage (with and without IDM).

time decreases more than 30%. Of course, if IDM is not applied, the islanding problem cannot be detected.

With different DC load condition, the results are shown in Figure 3.11. By applying the proposed method, the detection time is $t = 28$ ms, 22% faster than

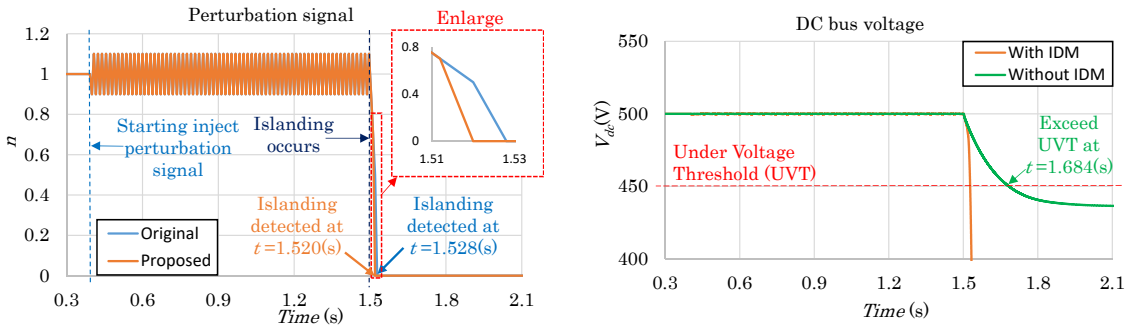


(**a**) (**b**)

Figure 3.15: Result in case of multi-PV operation, 40 kW PV, another islanding condition (case 6): (**a**) Perturbation signal and (**b**) DC bus voltage (with and without IDM).

the original method and 43% faster than without IDM.

Similarly, in the next two cases, the total PV power is 100 kW. In the hardest islanding condition case, the difference of detection time is still more than 30% between original IDM and proposed IDM. Without IDM, the islanding issue cannot be detected because the DC bus voltage does not reach the threshold value.

When the unbalance between DC load and PV source occurs (the unbalance case), the disparity is different from the previous two cases. The detection time of proposed method is $t = 28$ ms, 28% faster than the original method. Without IDM, the detection time is 76% slower than the proposed method. The results are shown in Figures 3.12 and 3.13.

In the last two cases, the total PV power is 40 kW, the results are the same as the previous one in the worst case are illustrated in Figure 3.14. In the unbalanced case, with proposed IDM, the time detection is 89% faster than without IDM, the results are displayed in Figure 3.15. Based on the above discussion, the proposed method can detect faster at least 22% than the original one and minimum 43% faster than without IDM.

## 3.4 Summary

The main contribution of this chapter is proposed IDM can detect islanding phenomenon faster than the others IDMs and without IDM. In addition, it is capable of detecting not only in hardest but also another islanding condition. Furthermore, the proposed method can detect in both single and multi-PV operation cases. In case the power of PV is greater than the power of load, this IDM cannot be applied. Changing the perturbation factor can decrease but cannot increase PV power, because the power of PV is limited. This unsolved case will research in future work.

However, the problem when applied the proposed IDM to the large-scale PV system needs to be discussed. Can the perturbation signal make the high voltage fluctuate in a large-scale PV system? The answer is YES due to the explanation below.

The idea of the proposed method is to inject the perturbation signal to make duty cycle fluctuate. The fluctuation of the duty cycle is proportionate with the rate of input and output voltage of the DC/DC converter is shown in equation

$$D = 1 - \frac{V_{in}}{V_{out}} \tag{3.22}$$

Therefore, the affection of the perturbation signal on the fluctuation of the dc-link voltage does not depend on the high or low level of the dc-link voltage.

Theoretically, the proposed IDM can be applied to both small-scale and large-scale photovoltaic system.

In fact, many converters are connected in parallel because of the converter's capacity limitation in the large-scale solar system. Therefore, the main problem with a multi-PV operation is the cancellation effect on the injected perturbation signal of the proposed IDM. This problem will be analyzed and the solution will be proposed in the next chapter.

# Chapter 4

# Injected Signals Cancellation Analysis and Solution in Multi-PV System.

## 4.1 Literature reviews

Islanding phenomenon is one of the consequences of the emergence and development of microgrids in the power system. Injected signal cancellation is a common problem in a multi-distributed generation that has a significant influence on active islanding detection method.

In [74], a new islanding detection strategy for low-voltage inverter-interfaced microgrids was presented. This strategy was based on adaptive neuro-fuzzy inference system (ANFIS). The ANFIS method monitors seven inputs measured at the point of common coupling (PCC) such as a root-mean-square of voltage and current (RMSU and RMSI), total harmonic distortion of voltage and current (THDU and THDI), frequency, and active and reactive powers based on practical measurement in a real microgrid. The ANFIS method detects islanding condition by using its pattern recognition capability and nonlinear mapping of the relation between input signals.

A novel hybrid islanding detection method for grid-connected microgrids in

the case of multiple inverter-based distributed generators was proposed in [75]. This method was based on the slope of linear reactive power disturbance (RPD) and four passive criteria, namely, voltage variation, voltage unbalance, rate of change of frequency and correlation factor between the RPD and frequency variation. Islanding is detected when the frequency exceeds its thresholds. However, the cancellation issue in the case of multiple inverter-based distributed generators was ignored in this study.

In [76], a new method used the transient response of voltage waveform to detect the islanding condition. This method was based on two new criteria, namely, the peak of the transient index value (TIV) and the positive sequence superimposed phase angle at the point of common coupling.

In [77], a method based on Kalman filter (KF) was proposed to extract and filter the harmonic components of the measured voltage signal at distributed generation terminals. The islanding detected by the selected harmonic distortion (SHD) was calculated by the KF after the different changes in the power system. This change were detected by a residual signal.

An unintentional islanding detection method based on the combination of the main criterion of switch status and the auxiliary criterion based on the no-current and difference-voltage criteria was proposed for "hand-in-hand" DC distribution network in [78]. However, the power supply reliability of the DC distribution network must be considered.

A novel islanding detection approach based on the relationship between the angular frequency and the derivative of the equivalent resistance observed from the small-scale synchronous generators in microgrids, including small-scale synchronous generators, was proposed in [79]. The derivative of the equivalent resistance observed from the small-scale synchronous generators approaches to zero when the islanding occurs in small-scale synchronous generator side.

In the previous chapter, we proposed an active islanding detection method by injecting the perturbation signal to make the power imbalance and voltage fluctuation exceed the thresholds faster and easier in the islanding condition. This method can rapidly and efficiently detect the islanding condition. However,

the cancellation problem when using this method in multi-PV operation has not been considered.

Many converters are connected in parallel because of their capacity limitation in a large-scale solar system. Therefore, the cancellation issue can occur in a multi-PV operation.

On the basis of the literature, no research has been conducted on the cancellation issue in multi-DG operation when using active islanding detection method. In this study, the cancellation issue when using the active IDM in the previous chapter is analyzed. Moreover, the solution improves the islanding detection method in the previous chapter to eliminate the injected signal cancellation is proposed and verified by Matlab/Simulink.

## 4.2 System description and injected signal cancellation.

The injected signal cancellation in the DC grid-connected photovoltaic system is analyzed in this section.

### 4.2.1 System description

As mentioned in the previous chapter, the cancellation signal occurs in multi-PV operation and the number of the PV module must be even. To simplify, the two PVs operation system is used to analysis as shown in Figure 4.1.

Figure 4.2 shows the diagram of the system under analysis. This system consists of a 100 kW PV array, output capacitor $C$, DC/DC converter with maximum power point tracking (MPPT) and islanding detection program. The DC load is shown as an equivalent resistance and the DC bus is modeled as a constant voltage source. The specifications of the PV module are introduced in Table 4.1. The inverter is used to connect the AC grid and the DC grid. VSC

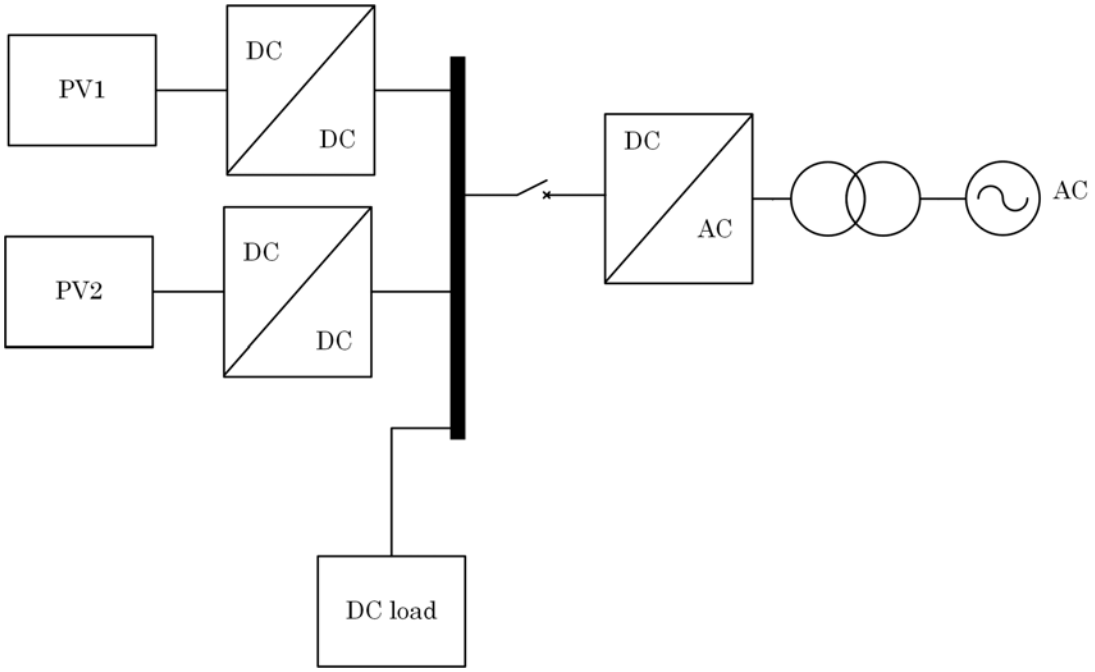


Figure 4.1: Cancellation testing system.

controller is modeled as a voltage source converter (VSC-detail model) to regulate DC bus voltage (keep stable at 500 V).

Table 4.1: Specifications of SunPower SPR-305E-WHT-D (SunPower, San Jose, California, USA) PV module.

| **Information** | **Value** |
|---|---|
| Open circuit voltage | 64.2 V |
| Short circuit current | 5.96 A |
| Voltage at maximum power point | 54.7 V |
| Current at maximum power point | 5.58 A |
| Maximum power | 305.226 W |
| Parallel strings | 66 |
| Series-connected modules per string | 5 |

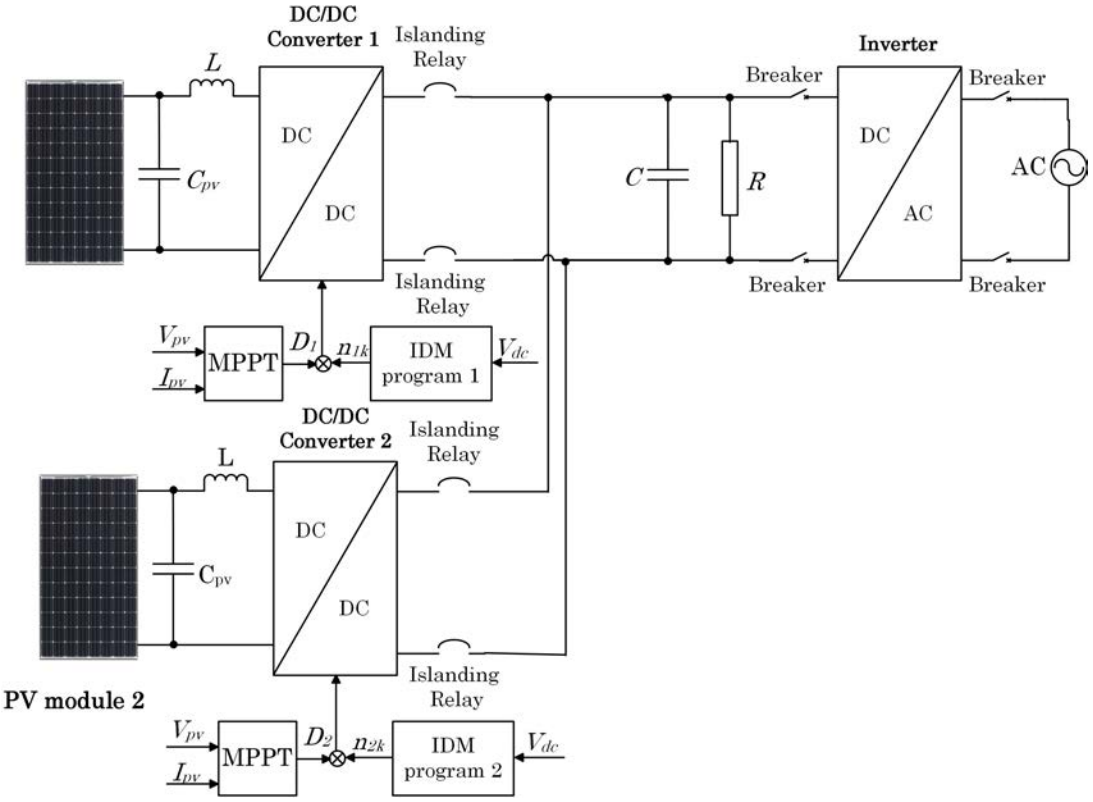


Figure 4.2: System model under analysis.

The sampling time is $T_s = 5\times\ 10^{-5}$. The simulation time is 2 (s) and is performed with two following steps:

- Step 1: Start the injection of perturbation signal at 0.4 s after system startup.
- Step 2: The islanding event is activated at 1.2 s after system startup by disconnecting the AC grid.

### 4.2.2 Injected signal cancellation.

By using the proposed IDM in the multi-PV system, the cancellation can occur when the perturbation signals of PV1 and PV2 are in the opposite positions, as shown in Figure 4.3.

- The perturbation signal factors at normal condition in normal case are $n =$ 0.9 to 1.1.
- The perturbation signal factors at normal condition in cancellation case are $n = 1.1$ to 0.9 for PV1 and $n = 0.9$ to 1.1 for PV2.

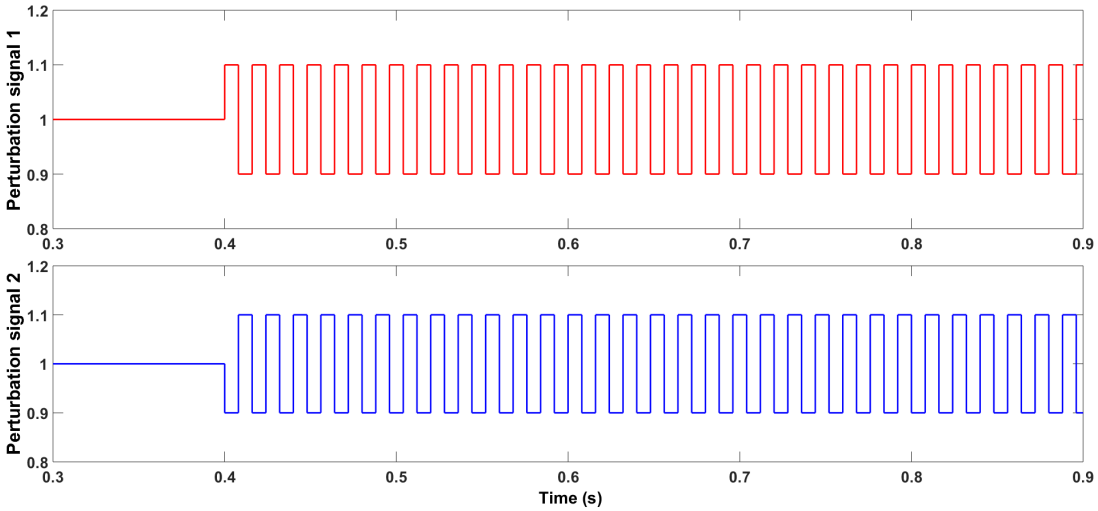


Figure 4.3: Perturbation signals in cancellation signal scenario.

Figure 4.4 describes in detail how the injected signal cancellation can occur.

The cancellation problem is explained below: Based on the Equation (3.10), the dc-link voltage at perturbation $N_1$ from PV1 is shown in Equation (4.1)

$$v_{dc1}(t) = N_1 R i_{pv}(t) + [v(0) - N_1 R i_{pv}(t)] e^{-\frac{1}{RC}t} \tag{4.1}$$

where: $v_{dc1}(t)$ is the DC-link voltage at time $t$ when perturbation signal 1 is injected and, $N_1$ is the perturbation signal of PV1.

The DC-link voltage at perturbation $N_2$ from PV2 is shown in Equation (4.2):

$$v_{dc2}(t) = N_2 R i_{pv}(t) + [v(0) - N_2 R i_{pv}(t)] e^{-\frac{1}{RC}t} \tag{4.2}$$

where: $v_{dc2}(t)$ is the DC-link voltage at time $t$ when perturbation signal 2 is injected.

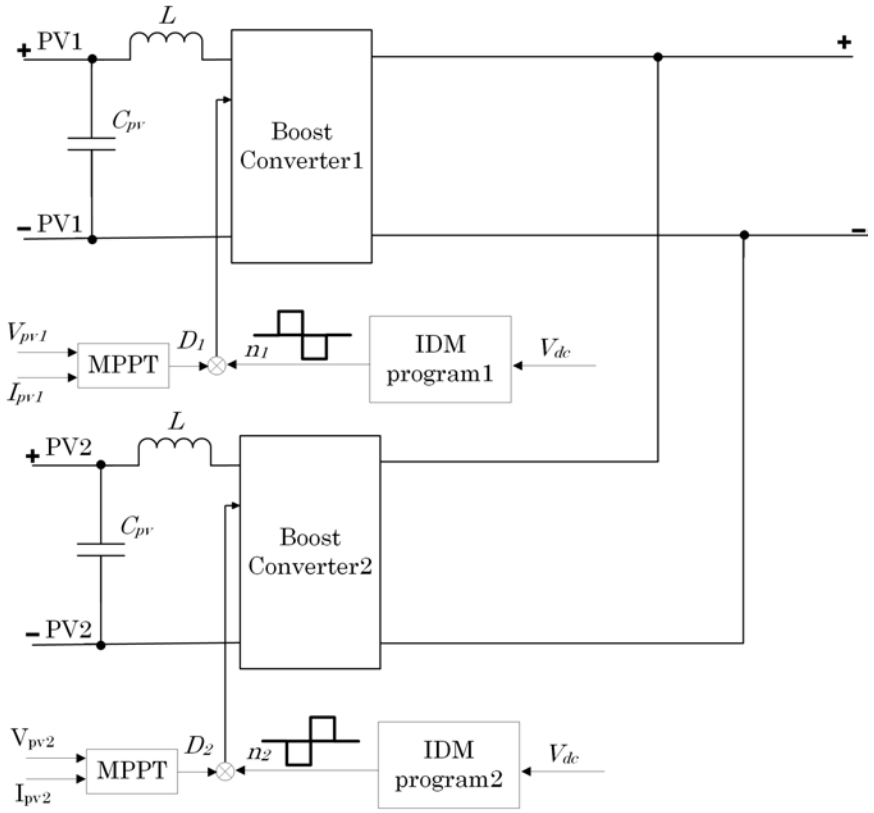


Figure 4.4: Controller perturbation signal circuit ($V_{dc}$ is the measurement DC bus voltage; $V_{pv1}$ and $V_{pv2}$ are the PV1 and PV2 voltages, respectively; $I_{pv1}$ and $I_{pv2}$ are the PV1 and PV2 currents, respectively; $n_1$ and $n_2$ are the perturbation factors of IDM programs 1 and 2, respectively; $D_1$ and $D_2$ are the duty cycles of boost converter 1 and 2, respectively).

The DC-link voltage without injecting the perturbation signal is as follows:

$$v_{dc0}(t) = N_0 R i_{pv}(t) + [v(0) - N_0 R i_{pv}(t)] e^{-\frac{1}{RC}t} \tag{4.3}$$

where: $v_{dc0}(t)$ is the DC-link voltage without perturbation signal at time $t$ after islanding occurs.

The fluctuation of DC-link voltage caused by the perturbation signal from

PV1 is shown in Equation (4.4):

$$v_{dc1}(t)-v_{dc0}(t) = \{N_1 Ri_{pv}(t)+[v(0)-N_1 Ri_{pv}(t)]e^{-\frac{1}{RC}t}\}-\{N_0 Ri_{pv}(t)+[v(0)-N_0 Ri_{pv}(t)]e^{-\frac{1}{RC}t}\} \tag{4.4}$$

The Equation (4.4) is simplified

$$v_{dc1}(t) - v_{dc0}(t) = (N_1 - N_0)Ri_{pv}(t)(1 - e^{-\frac{1}{RC}t}) \tag{4.5}$$

Equation (1.7) becomes

$$v_{dc1}(t) - v_{dc0}(t) = (n_0 - n_1)DRi_{pv}(t)(1 - e^{-\frac{1}{RC}t}) \tag{4.6}$$

or

$$\Delta v_{1dc}(t) = (n_0 - n_1)DRi_{pv}(t)(1 - e^{-\frac{1}{RC}t}) \tag{4.7}$$

The fluctuation of DC-link voltage caused by the perturbation signal from PV2 is shown in Equation (4.8):

$$v_{dc2}(t)-v_{dc0}(t) = \{N_2 Ri_{pv}(t)+[v(0)-N_2 Ri_{pv}(t)]e^{-\frac{1}{RC}t}\}-\{N_0 Ri_{pv}(t)+[v(0)-N_0 Ri_{pv}(t)]e^{-\frac{1}{RC}t}\} \tag{4.8}$$

The Equation (4.8) is simplified

$$v_{dc2}(t) - v_{dc0}(t) = (N_2 - N_0)Ri_{pv}(t)(1 - e^{-\frac{1}{RC}t}) \tag{4.9}$$

Equation (4.9) becomes

$$v_{dc2}(t) - v_{dc0}(t) = (n_0 - n_2)DRi_{pv}(t)(1 - e^{-\frac{1}{RC}t}) \tag{4.10}$$

or

$$\Delta v_{2dc}(t) = (n_0 - n_2)DRi_{pv}(t)(1 - e^{-\frac{1}{RC}t}) \tag{4.11}$$

Based on Equations (4.7) and (4.11), the injected signal cancellation occurs when:

$$\Delta v_{1dc}(t) + \Delta v_{2dc}(t) = 0 \tag{4.12}$$

$$2n_0 = n_1 + n_2 \tag{4.13}$$

If $n_0 = 1$ (without perturbation signal), $n_1 = 1.1$, and $n_2 = 0.9$, then Equation (4.13) is satisfied. Consequently, the fluctuation of DC-link voltage is canceled because the perturbation signals from PV1 and PV2 have the same value but opposite directions. Thus, the DC-link voltage fluctuations have been canceled.

The simulation result verifies the problem.

## 4.3 Simulation testing scenarios and results

The system is tested under the balance case between the DC load and PV in Table 4.2, and the procedure is as follows:

- The perturbation signal is injected at $t = 0.4$ s after the system startup.
- The islanding condition occurs at $t = 1.2$ s after the system startup.

The model parameters are shown as below:

- Maximum power (each PV) is $P_{\max} = 50$ kW.
- Switching frequency of converter is $f_s = 10$ kHz.
- DC bus voltage is $V_{dc} = 500$ V.
- Under voltage threshold is $V_{dcmin} = 450$ V.
- The islanding threshold is 0.2346.
- The perturbation duration is $T = 8$ ms.
- The perturbation signal factors at normal condition in normal case are $n =$ 0.9 to 1.1.
- The perturbation signal factors at normal condition in cancellation case are $n = 1.1$ to 0.9 for PV1 and $n = 0.9$ to 1.1 for PV2.

Table 4.2: Normal and cancellation scenarios.

| Cases | PV1 (kW) | PV2 (kW) | Total PV (kW) | Load (kW) | Vdc(V) |
|---|---|---|---|---|---|
| Normal | 50 | 50 | 100 | 100 | 500 |
| Cancellation | 50 | 50 | 100 | 100 | 500 |

For the first test, the IDM will test in 2 scenarios: normal and cancellation. The results are shown in the Figure 4.5 and Figure 4.6.

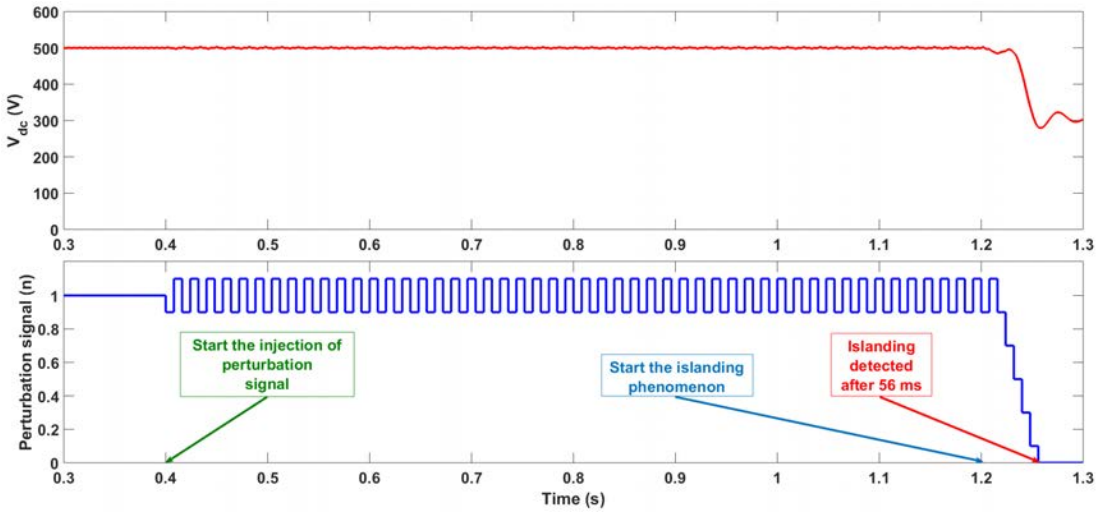


Figure 4.5: Normal scenario.

The result in the normal scenario is shown in Figure 4.5, and the cancellation scenario result is shown in Figure 4.6. Figure 4.5 shows that the islanding condition is detected after 56(ms).The IDM cannot detect the islanding condition when the cancellation problem occurs. In closing, injecting two perturbation signals in the opposite directions can make the cancellation occur completely.

The impact of the injected signal cancellation on the islanding detection method is significantly based on the results. The islanding detection method cannot detect the islanding phenomenon in the cancellation scenario.

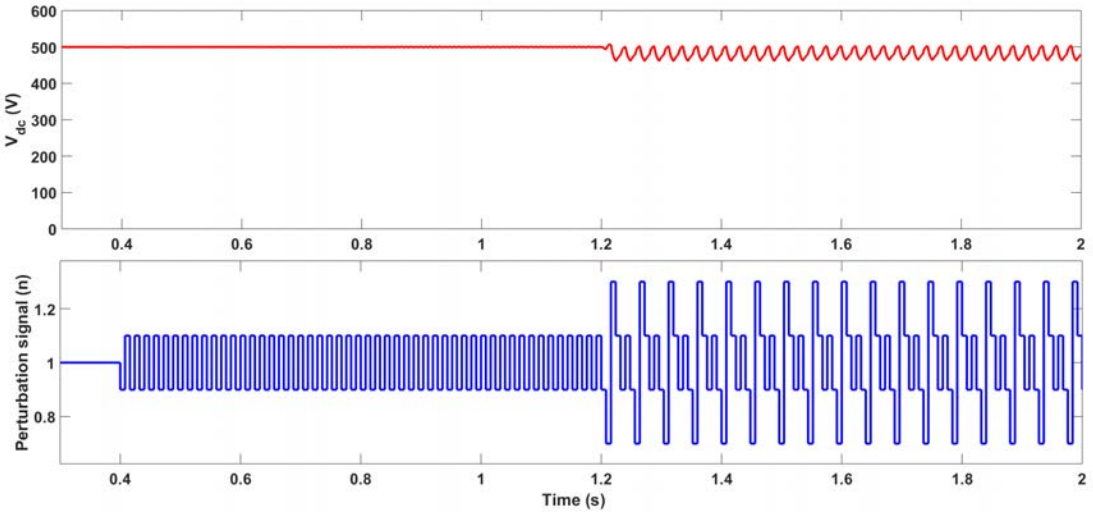


Figure 4.6: Cancellation scenario.

## 4.4 Improved islanding detection method based on the proposed solution.

According to the previous section, the cancellation problem occurs by using two perturbations in opposite directions. The main meaning of the solution is how to prevent the occurrence of cancellation.

First, the beginning of the proposed IDM uses the perturbation signal in the range $n$ =0-1.1. As the range of perturbation signal includes values over and below the normal value ($n$ =1), the injected signal cancellation caused by the perturbation signals in opposite directions can occur.

Second, to prevent the occurrence of cancellation, the perturbation signal value is changed so that the opposite signals cannot occur.

Therefore, the solution for the cancellation problem is to change the perturbation signal values in the range $n$ = 0-1.1 to $n$ = 0-1, and in the normal condition from $n$ = 0.9-1.1 to $n$ = 0.9-1. By changing this value, the injected signal cancellation is eliminated. Similar to the Equations (4.1)-(4.13), the solution is explained below:

The injected signal cancellation occurs when:

$$2n_0 = n_1 + n_2 \tag{4.14}$$

By using the new perturbation signal ($n_0 = 1$, $n_1 = 1$, and $n_2 = 0.9$), Equation (4.14) becomes

$$2 \neq 1.9 \tag{4.15}$$

Based on Equation (4.15), the fluctuation of DC-link voltage caused by the perturbation signals from PV1 and PV2 cannot cancel each other. Thus, the proposed solution can solve the injected signal cancellation.

By generalizing this solution with $n_k$ perturbation signals ($k = 1 \div \infty$), the injected signal cancellation occurs when:

$$\Delta v_{1dc}(t) + \Delta v_{2dc}(t) + ... + \Delta v_{kdc}(t) = 0 \tag{4.16}$$

or

$$n_0 - n_1 + n_0 - n_2 + ... + n_0 - n_k = 0 \tag{4.17}$$

Finally,

$$kn_0 = \sum_{k=1}^{\infty} n_k \tag{4.18}$$

As $n_0 = 1$ (without perturbation signal) and $n_k \leq 1$, Equation (4.18) is correct when all perturbation signal values are 1 (without perturbation signal case).

With other values of the perturbation signals (with perturbation signal), Equation (4.18) becomes

$$kn_0 > \sum_{k=1}^{\infty} n_k \tag{4.19}$$

For this reason, the injected signal cancellation is eliminated by using the proposed solution.

The flowchart in Figure 4.7 explains the detailed procedure of the proposed solution. The solution is verified by a step-by-step simulation.

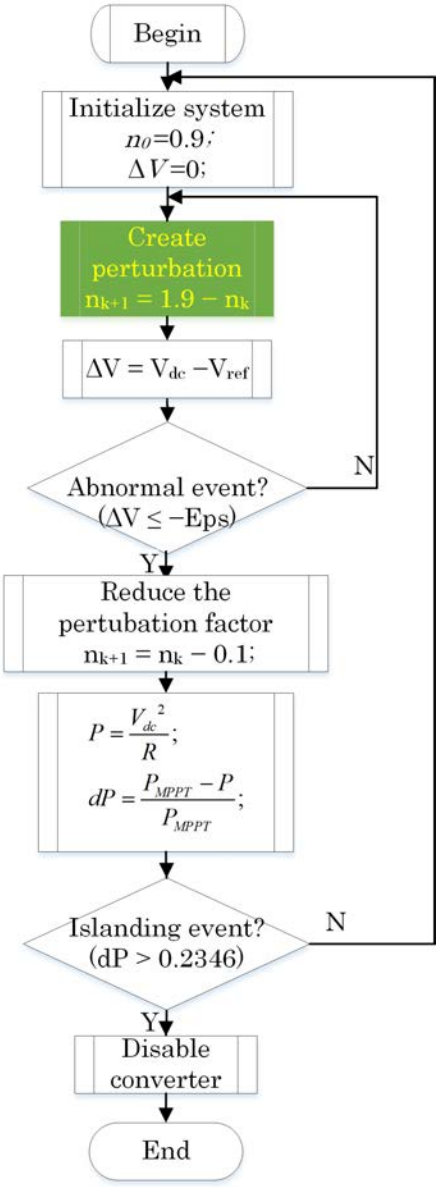


Figure 4.7: Flow chart of the improved IDM program ($n_0$ is perturbation factor at the beginning, $\Delta V$ is voltage deviation, $Eps$ is abnormal event value, $dP$ is the rate of change of output power).

The testing scenario is the hardest case (the power of DGs and load are

balance) in Table 4.2, and the procedure as following:

- The perturbation signal injected at $t = 0.4$ s after the system startup.
- The islanding condition occurs at $t = 1.2$ s after the system startup.

The testing scenarios in Table 4.3 are the worst case (the power of DGs and the load are balance), and the procedure is similar to the previous testing procedure. The model parameters are almost similar to the previous testing, only the new perturbation factors are different. The perturbation factors at normal condition in cancellation case are $n$ = 1-0.9 for PV1 and $n$ = 0.9-1 for PV2.

Table 4.3: Multi-PV operation scenario.

| **Cases** | **PV1(kW)** | **PV2(kW)** | **PV3(kW)** | **PV4(kW)** | **Total PV(kW)** | **Load(kW)** |
|---|---|---|---|---|---|---|
| 2-PV | 50 | 50 | 0 | 0 | 100 | 100 |
| 3-PV | 50 | 50 | 50 | 0 | 150 | 150 |
| 4-PV | 50 | 50 | 50 | 50 | 200 | 200 |

Also, the eight-PV scenario tests to verify the effect of the improved IDM. The parameters of the eight-PV scenario are as below:

- Each PV module power is 50 kW.
- Total PV power is 400 kW.
- Load power is 400 kW.
- DC bus voltage is 500 V.

As shown in the results in Figure 4.8, the injected signal cancellation occurs in the two-PV scenario. With the improved islanding detection method based on the proposed solution, the islanding condition is detected after 40 ms when the islanding occurs. The solution is effective in the two-PV scenario.

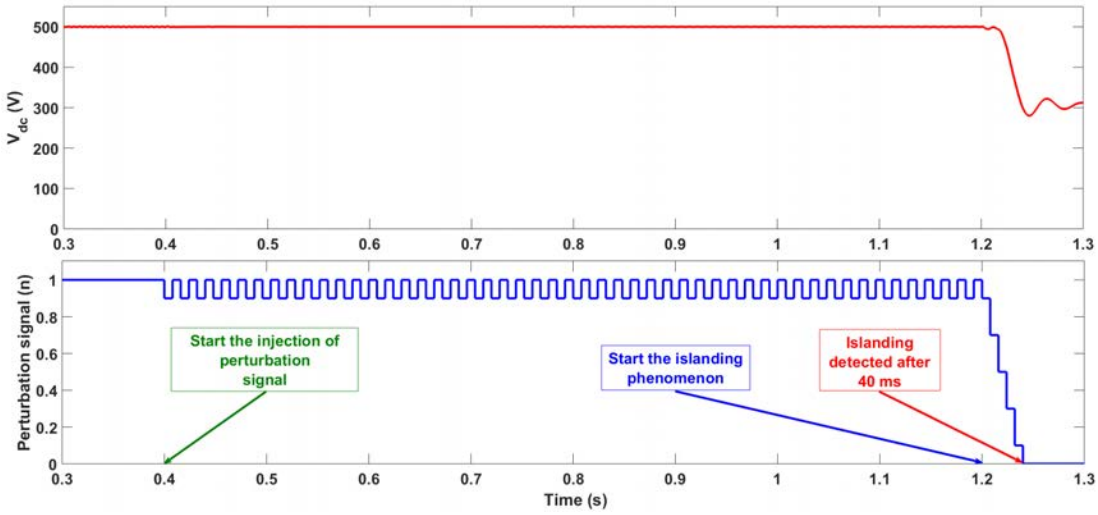


Figure 4.8: Solution result in to-PV scenario.

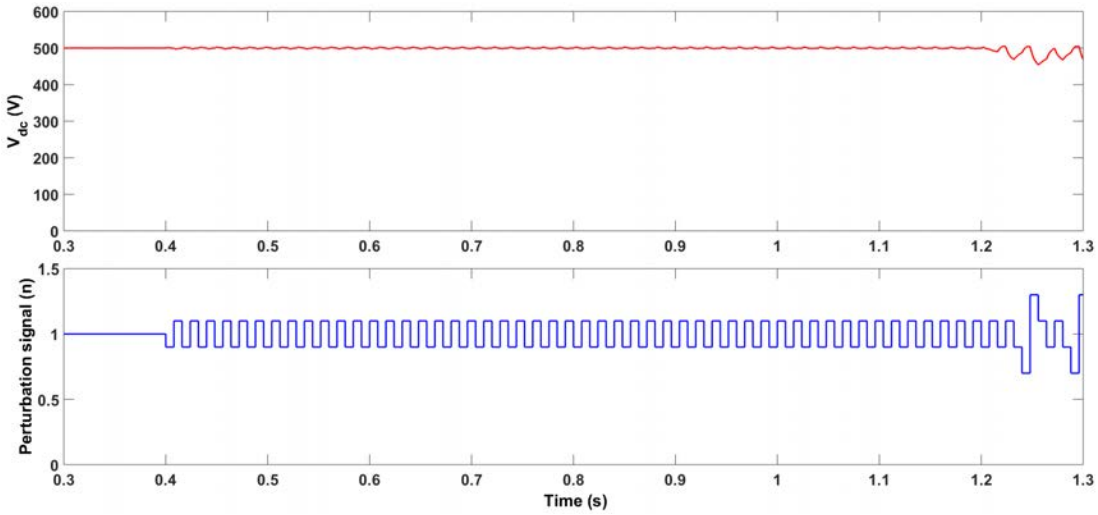


Figure 4.9: Cancellation result in three-PV scenario.

The results in Figures 4.9 show that the islanding condition is detected after 64 ms when the islanding occurs by applying the proposed solution to the improved islanding detection method in the injected signal cancellation case.

With the same result in the four-PV scenario, the islanding condition can be detected after 48 ms when the islanding occurs by using the improved islanding detection method, but it cannot be detected by using the original one. The results

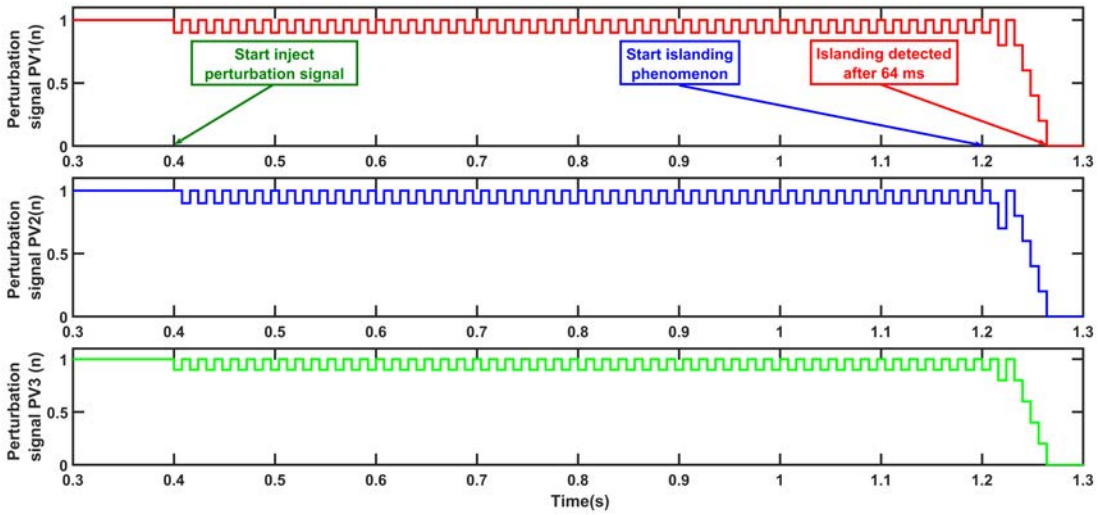


Figure 4.10: Solution result in three-PV scenario.

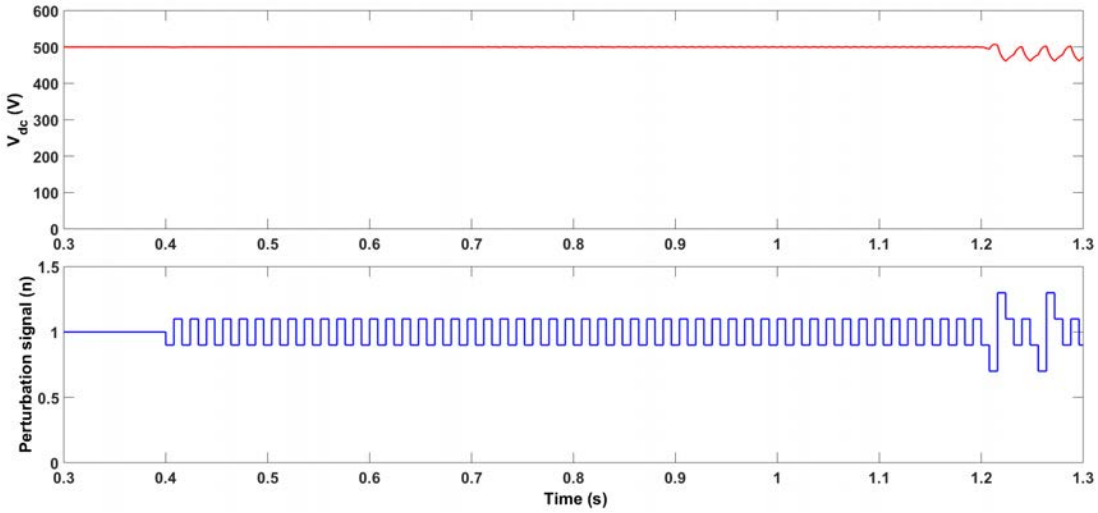


Figure 4.11: Cancellation result in four-PV scenario.

are shown in Figures 4.11 and 4.12.

In eight-PV scenario result in Figure 4.13 has a similar result, the improved islanding detection method by applying the proposed solution can detect the islanding condition after 48 ms.

Based on the simulation results and mathematical explanations, the proposed solution eliminates the injected signal cancellation by using the improved island-

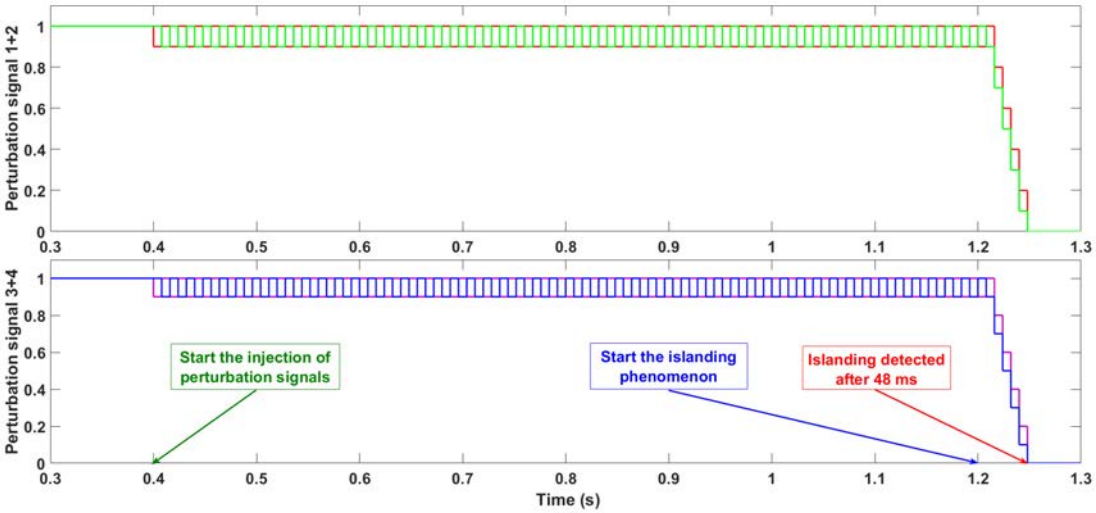


Figure 4.12: Solution result in four-PV scenario.

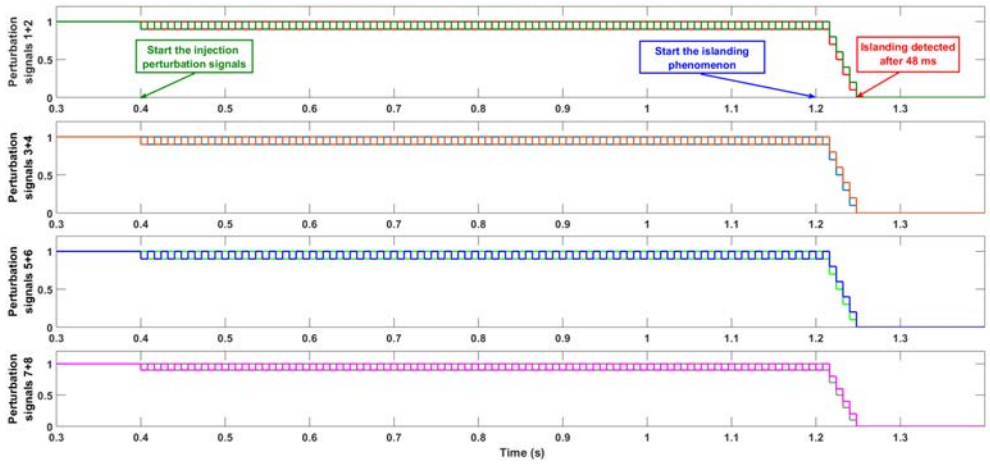


Figure 4.13: Solution result in eight-PV scenario.

ing detection method based on the proposed solution in two-PV, three-PV, four-PV, and eight-PV scenarios.

Moreover, the injected signal cancellation is eliminated not only in the specified cases but also in the general case by using the improved islanding detection method. This result shows the achievement and efficiency of the proposed solution

## 4.5 Summary

In this chapter, the islanding detection method based on perturbation signal injection and the rate of change of output power in DC grid-connected photovoltaic system is investigated.

The impact of injected signal cancellation on the islanding detection method in the previous chapter is significant. The islanding detection method in the previous chapter cannot detect the islanding phenomenon but works well without injected signal cancellation (detection time is 56 ms).

The solution of using the new perturbation factors ($n = 0.9$-$1$ in normal condition) is proposed. With this solution, the islanding detection method in [13] can detect the islanding phenomenon after 40 ms (two-PV scenario), 64 ms (three-PV scenario), and 48 ms (four-PV and eight-PV scenarios) when the injected signal cancellation appears.

Through the mathematical explanations and simulation results, the injected signal cancellation is eliminated. Moreover, the improved islanding detection method by applying the proposed solution is correct not only in specified cases but also in the general case.

# Chapter 5

# Conclusions and Future Works

## 5.1 Conclusions

*Chapter 2* discusses the islanding phenomenon and the subsequent required actions to maintain the power supply with a high penetration of RE. The self-control of a DG unit and central control using a hierarchical scheme are explained in detail. The ability to operate in the conventional grid-connected mode or islanded mode and the smooth transition between the two based on an advanced controller is highlighted.

Many objects are discussed in this paper, including multi-agent systems for the Energy Internet, flexible operation in the flexible islanded operation of proactive DG grids, hierarchical control of islanded entities, droop control (both conventional and advanced) for load sharing without communication, the intelligently controlled islanding scheme, and the role of the ESS in islanded entities, all of which show the flexible operation of the future power system.

Future perspectives of the power system with high DG penetration are also presented on the basis of discussions about improved functions for flexible grids and communication systems.

Moreover, knowledge surrounding hierarchical control and seamless mode transfer, such as seamless mode transfer, hierarchical coordination of AC and

DC MGs, and synchronous operation for reconnection, is also considered to be an important part of this chapter.

Furthermore, discussions regarding power quality (voltage, frequency, and harmonic) during islanded operation are given to cover some important aspects of power generation.

Finally, for the smart and resilient operation of the emerging power system, many research directions which need investigation are presented, such as robust hierarchical controllers, advanced droop control, active/reactive power-sharing, harmonic mitigation within an islanded entity, high-performance ESS and its controller, and reliable communication systems.

Besides, in *Chapter 3*, the proposed islanding detection method can detect in both single and multi-PV operation cases. In case the power of PV is greater than the power of load, this IDM cannot be applied. Changing the perturbation factor can decrease but cannot increase PV power, because the power of PV is limited.

However, the main problem with the multi-PV operation is the cancellation effect on the injected perturbation signal of the proposed IDM. In *Chapter 4*, the cancellation issue was analyzed and the potential solution has been proposed. Due to the mathematical explanation and the simulation results, the solution makes the injected signal cancellation is eliminated in the general case.

## 5.2 Future works

Throughout this study, this IDM was tested in single and multi-PV operation. It was not applied in the multi-converter system. Besides, the islanding detection method has implemented an run on a personal computer (PC). It is better if this method can verify in the experimental system or real system. Finally, due to the concern about fault-right-through characteristic, the IDM must cooperate to prevent the wrong disconnection. Hence, the following issues are going to be considered soon:

*a.* To consider the proposed active IDM in multi-converter operation.

*b.* To implement the developed islanding detection methods on a real system such that fair comparative experiments can be conducted.

*c.* Apply the IDM in the system included fault-right-through characteristic.

*d.* To research on islanding operation: seamless mode transfer, power quality during islanding condition.

# References


[1] Guerrero, J.M.; Vasquez, J.C.; Matas, J.; de Vicuna, L.G.; Castilla, M. Hierarchical control of droop-controlled AC and DC microgrids—A general approach toward standardization. *IEEE Trans. Ind. Electron.* **2011**, *58*, 158172.

[2] Best, R.J.; Morrow, D.J.; Laverty, D.M.; Crossley, P.A. Techniques for multiple-set synchronous islanding control. *IEEE Trans. Smart Grid* **2011**, *2*, 6067.

[3] IEEE Standards Coordinating Committee 21 (SCC21). IEEE Guide for Design, Operation, and Integration of Distributed Resource Island Systems with Electric Power Systems; IEEE Std 1547.4; IEEE: New York, NY, USA, 2011; pp. 154.

[4] Sun, Q.; Han, R.; Zhang, H.; Zhou, J.; Guerrero, J.M. A multiagent-based consensus algorithm for distributed coordinated control of distributed generators in the energy internet. *IEEE Trans. Smart Grid* **2015**, *6*, 30063019.

[5] Eddy, Y.S.F.; Gooi, H.B.; Chen, S.X. Multi-agent system for distributed management of microgrids. *IEEE Trans. Power Syst.* **2015**, *30*, 2434.

[6] Pipattanasomporn, M.; Feroze, H.; Rahman, S. Multi-agent systems in a distributed smart grid: Design and implementation. In Proceedings of the 2009 IEEE/PES Power Systems Conference and Exposition, Seattle, WA, USA, 1518 March 2009; pp. 18.

[7] Dou, C.; Lv, M.; Zhao, T.; Ji, Y.; Li, H. Decentralised coordinated control of microgrid based on multi-agent system. *IET Gener. Transm. Distrib.* **2015**, *9*, 24742484.

[8] Dou, C.; Yue, D.; Han, Qi.; Guerrero, J.M. Multi-Agent System-Based Event-Triggered Hybrid Control Scheme for Energy Internet. *IEEE Access* **2017**, *5*, 32633272.

[9] Kim, J.Y.; Jeon, J.H.; Kim, S.K.; Cho, C.; Park, J.H.; Kim, H.M.; Nam, K.Y. Cooperative control strategy of energy storage system and microsources for stabilizing the microgrid during islanded operation. *IEEE Trans. Power Electron.* **2010**, *25*, 30373048.

[10] Majumder, R.; Ghosh, A.; Ledwich, G.; Zare, F. Load sharing and power quality enhanced operation of a distributed microgrid. *Renew. Power Gener. IET* **2009**, *3*, 109119.

[11] Blaabjerg, F.; Teodorescu, R.; Liserre, M.; Timbus, A.V. Overview of control and grid synchronization for distributed power generation systems. *IEEE Trans. Ind. Electron.* **2006**, *53*, 13981409.

[12] Vasquez, J.C.; Guerrero, J.M.; Miret, J.; Castilla, M.; de Vicuna, L.G. Hierarchical control of intelligent microgrids. *IEEE Ind. Electron. Mag.* **2010**, *4*, 2329.

[13] Anderson, D.; Zhao, C.; Hauser, C.H.; Venkatasubramanian, V.; Bakken, D.E.; Bose, A. A vitural smart grid. *IEEE Power Energy Mag.* **2012**, 33–40. Available online: `http://magazine.ieee-pes.org/files/2011/12/jan2012_anderson.pdf`.

[14] Nordell, D.E. Terms of protection: The many faces of smart grid security. *IEEE Power Energy Mag.* **2012**, *10*, 1823.

[15] Hull, J.; Khurana, H.; Markham, T.; Staggs, K. Staying in control. *IEEE Power Energy Mag.* **2012**, *10*, 4148.

[16] Amin, S.M.; Giacomoni, A.M. Smart grid-safe, secure, self-healing. *IEEE Power Energy Mag.* **2012**, *10*, 3340.

[17] Bouhafs, F.; Mackay, M.; Merabti, M. Links to the future. *IEEE Power Energy Mag.* **2012**, *10*, 2432.

[18] Hua, M.; Hu, H.; Xing, Y.; Guerrero, J.M. Multilayer control for inverters in parallel operation without intercommunications. *IEEE Trans. Power Electron.* **2012**, *27*, 36513663.

[19] He, J.; Li, Y.W. An enhanced microgrid load demand sharing strategy. *IEEE Trans. Power Electron.* **2012**, *27*, 39843995.

[20] Cho, C.; Jeon, J.H.; Kim, J.Y.; Kwon, S.; Park, K.; Kim, S. Active synchronizing control of a microgrid. *IEEE Trans. Power Electron.* **2011**, *26*, 37073719.

[21] Cho, C.; Kim, S.K.; Jeon, J.H.; Kim, S. New ideas for a soft synchronizer applied to CHP cogeneration. *IEEE Trans. Power Deliv.* **2011**, *26*, 1121.

[22] Mohamed, Y.A.R.I.; Radwan, A.A. Hierarchical control system for robust microgrid operation and seamless mode transfer in active distribution systems. *IEEE Trans. Smart Grid* **2011**, *2*, 352362.

[23] Agundis-Tinajeroa, G.; Segundo-Ramreza, J.; Visairo-Cruza, N.; Savaghebib, M.; Guerrerob, J.M.; Barocio, E. Power flow modeling of islanded AC microgrids with hierarchical control. *Electr. Power Energy Syst.* **2019**, *105*, 2836.

[24] Mahmood, H.; Michaelson, D.; Jiang, J. Reactive power sharing in islanded microgrids using adaptive voltage droop control. *IEEE Trans. Smart Grid* **2015**, *6*, 30523060.

[25] Sun, Y.; Shi, G.; Li, X.; Yuan, W.; Su, M.; Han, H.; Hou, X. An f-P/Q Droop Control in Cascaded-Type Microgrid. *IEEE Trans. Power Syst.* **2017**, *33*, 11361138.

[26] Zhou, X.; Tang, F.; Loh, P.C.; Jin, X.; Cao, W. Four-leg converters with improved common current sharing and selective voltage-quality enhancement for islanded microgrids. *IEEE Trans. Power Deliv.* **2016**, *31*, 522531.

[27] Isazadeh, G.; Khodabakhshian, A.; Gholipour, E. New intelligent controlled islanding scheme in large interconnected power systems. *IET Gener. Transm. Distrib.* **2015**, *9*, 26862696.

[28] Wang, Z.; Chen, B.; Wang, J.; Chen, C. Networked microgrids for self-healing power systems. *IEEE Trans. Smart Grid* **2016**, *7*, 310319.

[29] Tang, X.; Hu, X.; Li, N.; Deng, W.; Zhang, G. A novel frequency and voltage control method for islanded microgrid based on multienergy storages. *IEEE Trans. Smart Grid* **2016**, *7*, 410419.

[30] Wu, D.; Tang, F.; Dragicevic, T.; Guerrero, J.M.; Vasquez, J.C. Coordinated control based on bus-signaling and virtual inertia for islanded DC microgrids. *IEEE Trans. Smart Grid* **2015**, *6*, 26272638.

[31] Tirumala, R.; Mohan, N.; Henze, C. Seamless transfer of grid-connected PWM inverters between utility-interactive and stand-alone modes. In Proceedings of the Seventeenth Annual IEEE Applied Power Electronics Conference and Exposition, Dallas, TX, USA, 1014 March 2002; pp. 10811086.

[32] Jung, S.; Bae, Y.; Choi, S.; Kim, H. A low cost utility interactive inverter for residential fuel cell generation. *IEEE Trans. Power Electron.* **2007**, *22*, 22932298.

[33] Borup, U.; Blaabjerg, F.; Enjeti, P.N. Sharing of nonlinear load in parallel-connected three-phase converters. *IEEE Trans. Ind. Appl.* **2001**, *37*, 18171823.

[34] Reza, M.; Sudarmadi, D.; Viawan, F.A.; Kling, W.L.; van der Sluis, L. Dynamic stability of power systems with power electronic interfaced DG. In Proceedings of the 2006 IEEE PES Power Systems Conference and Exposition, Atlanta, GA, USA, 29 October1 November 2006; pp. 14231428.

[35] Slootweg, J.G.; Kling, W.L. Impacts of distributed generation on power system transient stability. In Proceedings of the Power Engineering Society Summer Meeting, Chicago, IL, USA, 2125 July 2002; Volume 2, pp. 862867.

[36] Micallef, A.; Apap, M.; Spiteri-Staines, C.; Guerrero, J.M. Single-phase microgrid with seamless transition capabilities between modes of operation. *IEEE Trans. Smart Grid* **2015**, *6*, 27362745.

[37] Tang, F.; Guerrero, J.M.; Vasquez, J.C.; Wu, D.; Meng, L. Distributed active synchronization strategy for microgrid seamless reconnection to the grid under unbalance and harmonic distortion. *IEEE Trans. Smart Grid* **2015**, *6*, 27572769.

[38] *519-2014—IEEE Recommended Practice and Requirements for Harmonic Control in Electric Power Systems*; IEEE: New York, NY, USA, 11 June 2014; ISBN 978-0-7381-9005-1.

[39] Che, L.; Shahidehpour, M.; Alabdulwahab, A.; Al-Turki, Y. Hierarchical coordination of a community microgrid with AC and DC microgrids. *IEEE Trans. Smart Grid* **2015**, *6*, 30423051.

[40] Rezaei, M.M.; Soltani, J. Robust control of an islanded multi-bus microgrid based on input-output feedback linearisation and sliding mode control. *IET Gener. Transm. Distrib.* **2015**, *9*, 24472454.

[41] Abdelaziz, M.M.A.; Farag, H.E.; El-Saadany, E.F. Optimum reconfiguration of droop-controlled islanded microgrids. *IEEE Trans. Power Syst.* **2016**, *31*, 21442153.

[42] Lopes, J.A.P.; Moreira, C.; Madureira, A. Defining control strategies for microgrids islanded operation. *IEEE Trans. Power Syst.* **2006**, *21*, 916924.

[43] Vandoorn, T.L.; Renders, B.; Degroote, L.; Meersman, B.; Vandevelde, L. Active load control in islanded microgrids based on the grid voltage. *IEEE Trans. Smart Grid* **2011**, *2*, 139151.

[44] Barklund, E.; Pogaku, N.; Prodanovic, M.; Hernandez-Aramburo, C.; Green, T.C. Energy management in autonomous microgrid using stability-constrained droop control of inverters. *IEEE Trans. Power Electron.* **2008**, *23*, 23462352.

[45] Diaz, G.A.; Gonzalez-Moran, C.; Gomez-Aleixandre, J.; Diez, A. Scheduling of droop coefficients for frequency and voltage regulation in isolated microgrids. *IEEE Trans. Power Syst.* **2010**, *25*, 489496.

[46] Delghavi, M.B.; Yazdani, A. A unified control strategy for electronically interfaced distributed energy resources. *IEEE Trans. Power Deliv.* **2012**, *27*, 803812.

[47] Delghavi, M.B.; Yazdani, A. An adaptive feedforward compensation for stability enhancement in droop-controlled inverter-based microgrids. *IEEE Trans. Power Deliv.* **2011**, *26*, 17641773.

[48] Ortega, .; Milano, F. Generalized Model of VSC-Based Energy Storage Systems for Transient Stability Analysis. *IEEE Trans. Power Syst.* **2015**, *31*, 33693380.

[49] Pal, B.C.; Coonick, A.H.; Jaimoukha, I.M.; El-Zobaidi, H. A linear matrix inequality approach to robust damping control design in power systems with superconducting magnetic energy storage device. *IEEE Trans. Power Syst.* **2000**, *15*, 356362.

[50] Wu, J.; Wen, J.; Sun, H.; Cheng, S. Feasibility study of segmenting large power system interconnections with AC link using energy storage technology. *IEEE Trans. Power Syst.* **2012**, *27*, 12451252.

[51] Sui, X.; Tang, Y.; He, H.; Wen, J. Energy-storage-based low-frequency oscillation damping control using particle swarm optimization and heuristic dynamic programming. *IEEE Trans. Power Syst.* **2014**, *29*, 25392548.

[52] Singh, V.P.; Mohanty, S.R.; Kishor, N.; Ray, P.K. Robust H-infinity load frequency control in hybrid distributed generation system. *Electr. Power Energy Syst.* **2013**, *46*, 294305.

[53] Fang, J.; Yao, W.; Chen, Z.; Wen, J.; Cheng, S. Design of anti-windup compensator for energy storage-based damping controller to enhance power system stability. *IEEE Trans. Power Syst.* **2014**, *29*, 11751185.

[54] Zhu, Y.; Zhuo, F.; Wang, F.; Liu, B.; Gou, R.; Zhao, Y. A virtual impedance optimization method for reactive power sharing in networked microgrid. IEEE Trans. Power Electron. **2016**, *31*, 28902904.

[55] Zeng, Z.; Li, H.; Tang, S.; Yang, H.; Zhao, R. Multi-objective control of multi-functional grid-connected inverter for renewable energy integration and power quality service. *IET Power Electron.* **2016**, *9*, 761770.

[56] Jenkins, N.; Ekanayake, J.B.; Strbac, G. *Distributed Generation*; Institution of Engineering and Technology: London, UK, 2010; p. 272.

[57] Elsayed, A.T.; Mohamed, A.A.; Mohammed, O.A. Review DC microgrids and distribution systems: An overview. *Electr. Power Syst. Res.* **2015**, *119*, 407–417.

[58] Hammerstrom, D.J. AC Versus DC Distribution Systems: Did We Get it Right? In Proceedings of the IEEE Power Engineering Society General Meeting, Tampa, FL, USA, 24–28 June 2007; pp. 1–5.

[59] Seo, G.-S.; Baek, J.; Choi, K.; Bae, H.; Cho, B. Modeling and analysis of DC distribution systems. In Proceedings of the IEEE 8th International Conference on Power Electronics and ECCE Asia, Jeju, South Korea, May 30–June 3 2011; pp. 223–227.

[60] Starke, M.R.; Tolbert, L.M.; Ozpineci, B. AC vs. DC distribution: A loss comparison. In Proceedings of the IEEE PES Transmission and Distribution Conference and Exposition, Chicago, IL, USA, 21–24 April 2008; pp. 1–7.

[61] Sannino, A.; Postiglione, G.; Bollen, M. Feasibility of a DC Network for Commercial Facilities. *IEEE Trans. Ind. Appl.* **2003**, *39*, 1499–1507.

[62] *IEEE Application Guide for IEEE Std 1547TM, IEEE Standard for Interconnecting Distributed Resources with Electric Power Systems*; IEEE Standard 1547.2TM; IEEE Press: New York, NY, USA, 2008.

[63] Papadimitriou, C.N.; Kleftakis, V.A.; Hatziargyriou, N.D. A Novel Method for Islanding Detection in DC Networks. *IEEE Trans. Sustain. Energy* **2017**, *8*, 441–448.

[64] Mohamad, A.M.I.; Mohamed, A.-R.I. Assessment and Performance Comparison of Positive Feedback Islanding Detection Methods in DC Distribution Systems. *IEEE Trans. Power Electron.* **2016**, *32*, 6577–6594.

[65] Kleftakis, V.A.; Lagos, D.T.; Papadimitriou, C.N.; Hatziargyriou, N.D. Seamless transition between interconnected and islanded operation of DC Microgrids. *IEEE Trans. Smart Grid* **2017**, *PP*, doi:10.1109/TSG.2017.2737595.

[66] Voglitsis, D.; Papanikolaou, N.; Kyritsis, A.C. Incorporation of Harmonic Injection in an Interleaved Flyback Inverter for the Implementation of an Active Anti-Islanding Technique. *IEEE Trans. Power Electron.* **2016**, *32*, 8526–8543.

[67] Haider, R.; Kim, C.H.; Ghanbari, T.; Bukhari, S.B.A.; Zaman, M.S.U.; Baloch, S.; Oh, Y.S. Passive islanding detection scheme based on autocorrelation function of modal current envelope for photovoltaic units. *IET Gener. Transm. Distrib.* **2018**, *12*, 726–736.

[68] Seo, G.-S.; Lee, K.-C.; Cho, B.-H. A new DC anti-islanding technique of electrolytic capacitor-less photovoltaic interface in DC distribution systems. *IEEE Trans. Power Electron.* **2013**, *28*, 1632–1641.

[69] Mahat, P.; Chen, Z.; Bak-Jensen, B. Review of Islanding Detection Methods for Distributed Generation. In Proceedings of the Third International Conference on Electric Utility Deregulation and Restructuring and Power Technologies, Nanjing, China, 6–9 April 2008.

[70] Funabashi, T.; Koyanagi, K.; Yokoyama, R. A review of islanding detection methods for distributed resources. In Proceedings of the IEEE Power Tech Conference, Bologna, Italy, 23–26 June 2003.

[71] Mulhausen, J.; Schaefer, J.; Mynam, M.; Guzmn, A.; Donolo, M. Anti-Islanding Today, Successful Islanding in the Future. In Proceedings of the 2010 63rd Annual Conference for Protective Relay Engineers, College Station, TX, USA, 29 March–1 April 2010.

[72] Samuelsson, O.; Strath, N. Islanding detection and connection requirements. In Proceedings of the IEEE Power Engineering Society General Meeting, Tampa, FL, USA, 24–28 June 2007; pp. 1–6.

[73] Kunte,R.S.; Gao, W. Comparison and Review of Islanding Detection Techniques for Distributed Energy Resources. In Proceedings of the 40th North American Power Symposium, Calgary, AB, Canada, 28–30 September 2008.

[74] D. Mlaki, H. R. Baghaee and S. Nikolovski, "A Novel ANFIS-Based Islanding Detection for Inverter-Interfaced Microgrids", in IEEE Transactions on Smart Grid, vol. 10, no. 4, pp. 4411-4424, July 2019. doi: 10.1109/TSG.2018.2859360

[75] X. Chen, Y. Li and P. Crossley, "A Novel Hybrid Islanding Detection Method for Grid-Connected Microgrids With Multiple Inverter-Based Distributed Generators Based on Adaptive Reactive Power Disturbance and Passive Criteria", in IEEE Transactions on Power Electronics, vol. 34, no. 9, pp. 9342-9356, Sept. 2019. doi: 10.1109/TPEL.2018.2886930.

[76] R. Nale, M. Biswal and N. Kishor, "A Transient Component Based Approach for Islanding Detection in Distributed Generation", in IEEE Transactions on Sustainable Energy, vol. 10, no. 3, pp. 1129-1138, July 2019. doi: 10.1109/TSTE.2018.2861883.

[77] R. Haider, C. H. Kim, T. Ghanbari and S. B. A. Bukhari, "Harmonic-signature-based islanding detection in grid-connected distributed generation systems using Kalman filter", in IET Renewable Power Generation, vol. 12, no. 15, pp. 1813-1822, 19 11 2018. doi: 10.1049/iet-rpg.2018.5381

[78] W. Song, Y. Chen, A. Wen, Y. Zhang and C. Wei, "Detection and switching control scheme of unintentional islanding for 'hand-in-hand' DC distribution network", in IET Generation, Transmission and Distribution, vol. 13, no. 8, pp. 1414-1422, 23 4 2019. doi: 10.1049/iet-gtd.2018.5942.

[79] R. Bekhradian, M. Davarpanah and M. Sanaye-Pasand, "Novel Approach for Secure Islanding Detection in Synchronous Generator Based Microgrids", in IEEE Transactions on Power Delivery, vol. 34, no. 2, pp. 457-466, April 2019. doi: 10.1109/TPWRD.2018.2869300

# Research Achievements

[P.1] T.T. Son, N.D. Tuyen and Goro FUJITA, "Islanding detection in DC networks",*2017 52th International Universities Power Engineering Conference (UPEC)*, Crete, Greece, 2017, pp. 279-283.

[P.2] T.T. Son, N.D. Tuyen and Goro FUJITA, "Cancellation Signal Issue by Using Islanding Detection Method based on Injecting Pertubation Signal and Rate of Change of Output Power in DC Network-Connected Photovoltaic System", *International Workshop on Power Engineering in Remote Islands (IWPI)*, Jeju, Korea, 2018.

[P.3] T.T. Son, N.D. Tuyen and Goro FUJITA, "Islanding Detection Method Based on Injecting Perturbation Signal and Rate of Change of Output Power in DC Grid-Connected Photovoltaic System, in *Energies 2018, 11, 1313, https://doi.org/10.3390/en11051313.*

[P.4] T.T. Son, N.D. Tuyen and Goro FUJITA, "The Analysis of Technical Trend in Islanding Operation, Harmonic Distortion, Stabilizing Frequency, and Voltage of Islanded Entities", in *Resources 2019, 8, 14*,

*https://doi.org/10.3390/resources8010014.*

[P.5] T.T. Son, N.D. Tuyen and Goro FUJITA, "Injected Signal Cancellation caused by Perturbation Signal in the Multi-PV System: Analysis and Solution.", submitting to Applied Sciences 2019.